(2)

OCEAN SYSTEMS RESEARCH TECHNICAL REPORT 91-04

submitted to:

DAVID TAYLOR RESEARCH CENTER
Code 1240: Mike Gallagher
Bethesda, MD 20084-5000

A Report Assessing the
Feasibility of a

SUBMERSIBLE MOTOR
AMPHIBIOUS THRUSTER

Submitted by:

Ocean Systems Research, Inc.
580 Bellerive Dr., Suite 5C
Annapolis, Maryland 21401

Approval: James W. White
James W. White
President

This material is based upon work supported by the Department of the Navy under contract number N00167-90-C-0067. Any opinions, findings, and conclusions or recommendations expressed in this publication are those of the authors and do not necessarily reflect the views of the Department of the Navy.

UNCLASSIFIED
URITY CLASSIFICATION OF THIS PAGE

REPORT DOCUMENTATION PAGE

REPORT SECURITY CLASSIFICATION NCLASSIFIED	1b RESTRICTIVE MARKINGS
SECURITY CLASSIFICATION AUTHORITY	3 DISTRIBUTION/AVAILABILITY OF REPORT Approved for public release; distribution is unlimited.
DECLASSIFICATION/DOWNGRADING SCHEDULE	
PERFORMING ORGANIZATION REPORT NUMBER(S) OSR - TR - 91-04	5 MONITORING ORGANIZATION REPORT NUMBER(S) DTRC-SD-CR-03/91
NAME OF PERFORMING ORGANIZATION)CEAN SYSTEMS RESEARCH, INC.	6b OFFICE SYMBOL (If applicable)
7a NAME OF MONITORING ORGANIZATION DAVID TAYLOR RESEARCH CENTER	
ADDRESS (City, State, and ZIP Code))80 BELLERIVE DR., SUITE 5C ANNAPOLIS, MARYLAND 21401	7b ADDRESS (City, State, and ZIP Code) CODE 1240, (MCPO) BETHESDA, MD. 20084-5000
NAME OF FUNDING/SPONSORING ORGANIZATION ICRDAC AWI	8b OFFICE SYMBOL (If applicable)
9 PROCUREMENT INSTRUMENT IDENTIFICATION NUMBER N00167 - 90 - C - 0067	
ADDRESS (City, State, and ZIP Code))UANTICO, VIRGINIA 22134-5080	10 SOURCE OF FUNDING NUMBERS

PROGRAM ELEMENT NO	PROJECT NO	TASK NO	WORK UNIT ACCESSION NO
65502N	C1824	N90-24	

TITLE (Include Security Classification)

A REPORT ASSESSING THE FEASIBILITY OF A SUBMERSIBLE MOTOR AMPHIBIOUS THRUSTER

PERSONAL AUTHOR(S)

13a TYPE OF REPORT	13b TIME COVERED	14 DATE OF REPORT (Year, Month, Day)	15 PAGE COUNT
FINAL	FROM 9/90 TO 4/91	1991 APRIL	111

SUPPLEMENTARY NOTATION

COSATI CODES			18 SUBJECT TERMS (Continue on reverse if necessary and identify by block number)
FIELD	GROUP	SUB GROUP	Amphibious Assault Vehicle Propulsion System Demonstrator Thrusters, contrarotation

ABSTRACT (Continue on reverse if necessary and identify by block number)

Ocean Systems Research, Inc. has completed a preliminary design of a novel thruster to be used as a propulsion system for the Marine Corp's Amphibious Assault Vehicle Propulsion System Demonstrator. The thruster would be used in an electric drive system.

The system uses contrarotating axial flow impellers to develop a hydraulic head against an exit nozzle. The contrarotation is more efficient than single stage impellers and the outer diameter of each of the two stages can be smaller. Instead of complex contrarotating shafts and gears, the impellers are driven at the tips by independent electric motors each of 200 hp capacity. The motors are submersible having coated rotor and encapsulated stator.

The bearings for the machine are on the outer diameter and they are water lubricated. They are of the deflection pad type.

Some advantages of this machine over other electric drive systems are that it is much less complex and that its overall length is reduced.

20 DISTRIBUTION/AVAILABILITY OF ABSTRACT	21 ABSTRACT SECURITY CLASSIFICATION
☐ UNCLASSIFIED/UNLIMITED ☒ SAME AS RPT ☐ DTIC USERS	

22a NAME OF RESPONSIBLE INDIVIDUAL	22b TELEPHONE (Include Area Code)	22c OFFICE SYMBOL
Michael Gallagher	(301) 227-1852	MCPO

D FORM 1473, 84 MAR 83 APR edition may be used until exhausted
All other editions are obsolete

SECURITY CLASSIFICATION OF THIS PAGE
UNCLASSIFIED

TABLE OF CONTENTS

ABSTRACT

Ocean Systems Research, Inc. has completed a preliminary design of a novel thruster to be used as a propulsion system for the Marine Corp's Amphibious Assault Vehicle Propulsion System Demonstrator. The thruster would be used in an electric drive system.

The system uses contrarotating axial flow impellers to develop a hydraulic head against an exit nozzle. The contrarotation is more efficient than single stage impellers and the outer diameter of each of the two stages can be smaller. Instead of complex contrarotating shafts and gears, the impellers are driven at the tips by independent electric motors each of 200 hp capacity. The motors are submersible having coated rotor and encapsulated stator.

The bearings for the machine are on the outer diameter and they are water lubricated. They are of the deflection pad type.

Some advantages of this machine over other electric drive systems are that it is much less complex and that its overall length is reduced.

EXECUTIVE SUMMARY

This report covers the preliminary design of a contrarotating axial flow thruster system. The thruster, designated Submersible Motor Amphibious Thruster (SMAT), uses two submersible induction motors to drive its impellers in a duct. The motors surround and drive the impellers at their tips, so that there is no complicated shafting or gears.

The objective of this effort was to demonstrate the feasibility of this novel thruster concept and to develop the design far enough so that evaluations could be made. The work included hydrodynamic design of the impellers and nozzle using both pump and propeller design methods. The induction motors were selected from among more than 50 point designs. They produce 200 horsepower and use 321 Hz power at a full speed of 2100 rpm.

The mechanical design and integration results in a unique housing configuration which has rectangular end sections and a circular waist. The bearings are of the deflection pad type, and they are located on the outside diameter of the machine. There is no shaft or shaft support struts. The bearing pads are nitrile coated, and they run against a hard chrome surface so they are water lubricated.

The SMAT is an improvement over the alternative which is a high speed motor driving a set of impellers through an epicyclic speed reducing gear. It has few moving parts. It is only 55 inches long, and it is more efficient.

This report is supplemented by drawings of the SMAT concept which show how the SMAT can be built. OSR recommends that we build a prototype unit to prove the technologies upon which the Submersible Motor Amphibious Thruster is based, and that we test it first in a stationary position and then finally on the Amphibious Assault Vehicle Propulsion System Demonstrator.

1.0 Introduction

Ocean Systems Research, Inc. has carried out this investigation in support of the United States Marine Corp's improvements to the Amphibious Assault Vehicle. Until recently, these vehicles could perform their mission successfully with a waterborne speed of about eight miles per hour. But recent advances in an enemy's ability to repel amphibious landings have made a much higher speed desirable.

Modern versions of advance amphibious assault vehicles have used a planing hull for improved speeds up to 25 miles per hour. These tracked vehicles would use waterjets mounted on a flapped transom for waterborne propulsion. The waterjet propellers are driven by a separate motor which is also mounted on the transom. A recently completed prototype propulsion system used hydraulic motors to drive the propellers. System tests were successful, but some major improvements are still necessary.

The vehicle could be improved if the overall length of the thruster system could be reduced. As shown in Figure 1., the thrusters protrude above the top of the vehicle when they are oriented vertically for land operation. This detracts from the overall profile of the vehicle and hinders gun and other operations.

Another important improvement would be the incorporation of electric drive in the vehicle. The hydraulic system now in use in an experimental vehicle requires high pressure hydraulic piping and hose, and a large volume of hydraulic oil. The dangers, especially in combat, of the hydraulic system are that it could rupture, injuring marines in the vehicle, or the spilled oil could hinder their egress from the vehicle once landed. The viscous losses in the hydraulics detract from the overall efficiency of the system.

In 1988, a study for David Taylor Research Center, reference 1, proposed an electric drive system which used four high speed electric motors to drive the waterjets. Figure 2. illustrates the configuration of the thrusters. The use of high speed motors reduced the size and weight of the system, but the motors were somewhat unreliable. The motors operated at 9000 rpm driving the jet through epicyclic reduction gears. A final report on the same subject, reference 2, indicates that the motors and gear system could provide only 161 of the required 400 horse power because of cooling difficulties. The addition of an external oil cooling system might alleviate the problem somewhat, but major design changes would be required.

OSR believes that the cooling requirements for the waterjet motors can be solved by using a direct drive, lower speed motor which would have a much larger surface area and generate lower losses. Moreover, OSR has devised a different configuration for

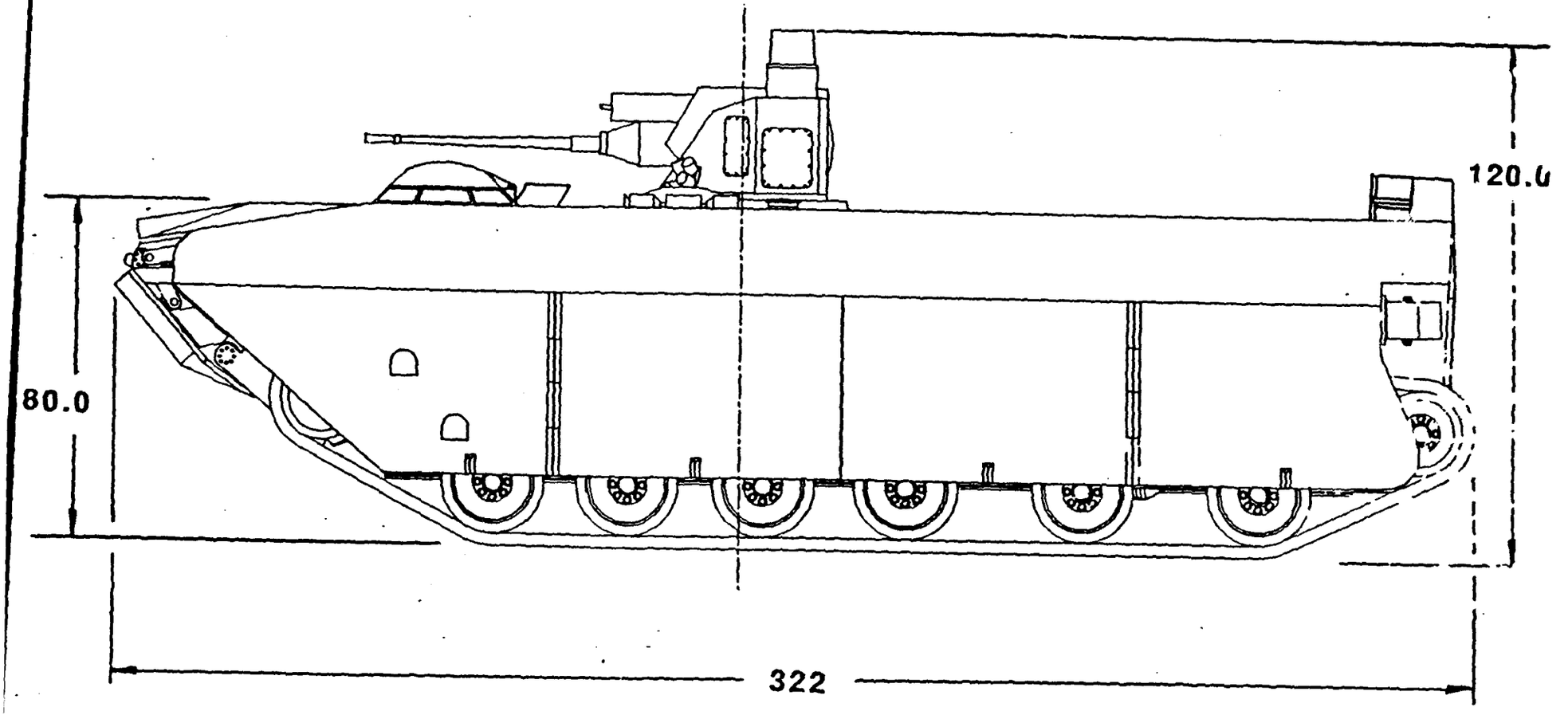

PSD - LAND MODE

Figure 1

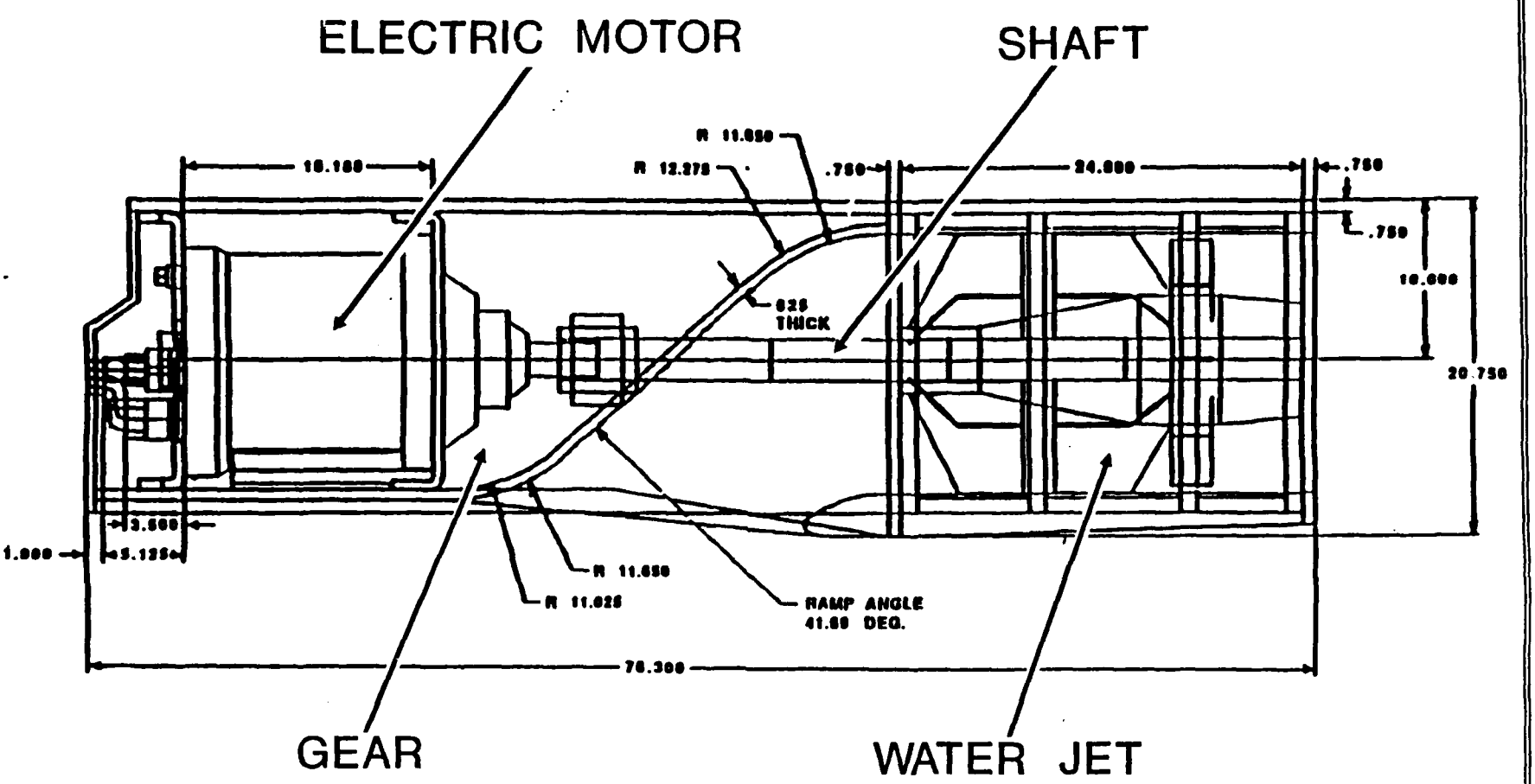

ALTERNATIVE ELECTRIC DRIVE

Figure 2

the motor thruster system which reduces the overall length to 72% of the length required for the system which uses a high speed motor and speed reducing gear.

The objectives of this work were to investigate the feasibility of the OSR approach and to design a system in enough detail so that an evaluation could be made. We have shown that large improvements in system configuration and performance are possible, and we have completed a conceptual design which shows how a thruster incorporating the OSR approach would be manufactured. We have called it the Submersible Motor Amphibious Thruster (SMAT).

2.0 Discussion

2.1 System Requirements

Table 1 lists the design assumptions and constraints to which the SMAT has been designed.

TABLE 1

Maximum Vehicle Speed	- 25 mph
Required Thrust	- 4000 lbs
Speed at Max Thrust	- 18 mph
Available Power	- 400 Hp
Power Supply	- 450 Hz max
Submergence	- 5 psi
Width	- 19.25 in
Length	- 64 in max

We have assumed that overall reductions in weight, volume and surface area are desirable since these can improve the hydrodynamic performance of both the thruster and the vehicle itself. We have further assumed that the inflow into the thruster face is of uniform velocity distribution. This latter assumption is made in the absence of better knowledge. A complete description of the wake profile of the vehicle could help in the final design of the impeller blades, but obtaining that description and using it is outside the scope of the present effort.

2.2 SMAT Description

The SMAT is a two stage, contrarotating axial flow thruster. It is rim driven by a pair of induction motors which are completely enclosed so that they can be submerged. The bearings for the SMAT are water cooled and lubricated, and they are located on the outer diameter of the machine rather than on a central shaft. Figure 3.[1] is a cross sectional layout of the thruster system.

There are several advantages to using the contrarotating

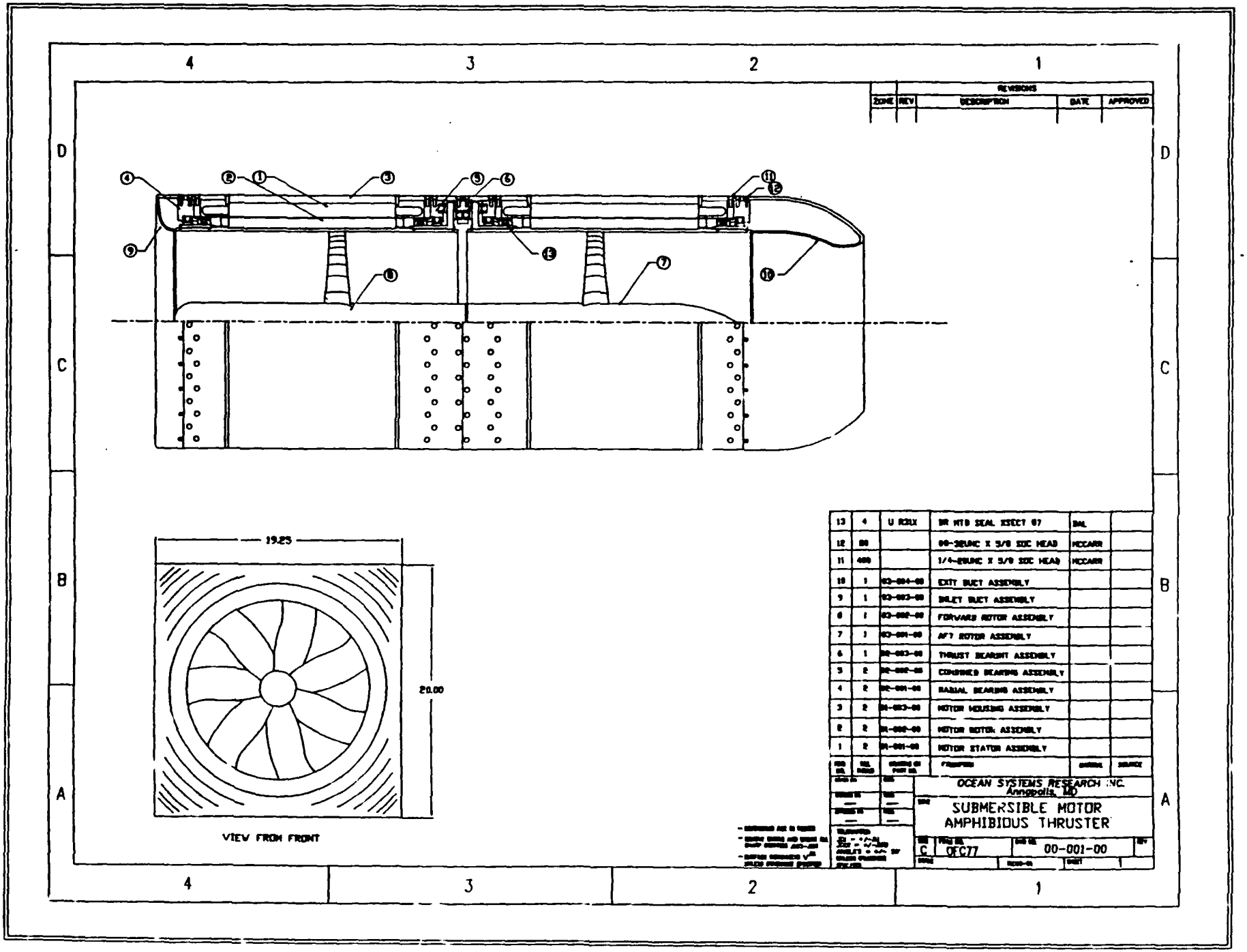
4
3
2
1
D
C
B
A
REVISIONS
ZONE
REV
DESCRIPTION
DATE
APPROVED
19.25
20.00
VIEW FROM FRONT
OCEAN SYSTEMS RESEARCH INC.
Annapolis, MD
SUBMERSIBLE MOTOR
AMPHIBIOUS THRUSTER
00-001-00

Figure 3

scheme. First, it is more efficient. When the inlet impeller imparts energy to the volume of water, much of it is rotational kinetic energy. A contrarotating second stage converts the rotational energy to axial. In studies with ship propellers, contrarotating propellers were nine to fifteen percent more efficient than single or tandem propellers.

Second, since there are two stages imparting energy to the volume of water passing through the thruster, each stage can have a smaller diameter. This is particularly important to the SMAT because it is restrained in overall outside diameter and because the volume outside the impeller tips must be occupied by the electric motor parts.

Contrarotation can reduce the overall length of the machine. In a machine with a single rotating row of impeller blades, a second row of stator blades removes the tangential component of the flow for maximum axial thrust. If there is a low suction pressure as is the case with the amphibious assault vehicle, then a second rotating impeller is required. The three separate rows of blades necessarily lengthen the overall machine.

Contrarotating machines are less popular because of one major drawback. The mechanical drives for them can be extremely complex. In most cases, a contrarotating set of coaxial shafts complete with bearings and seals is driven by a single prime mover through a contrarotating gearbox. By driving the impellers at the tips with surrounding electric motors, the complexities are mostly eliminated. In fact, the SMAT is a relatively simple machine. There are no gear systems, and no shafts. There is only one axis of rotation and all of the rotating parts are in two assemblies each of which rotates as one piece.

Another advantage of the tip (or rim) driven approach is that it reduces mechanical stresses at the roots of the impeller blades. In a hub driven propeller, the blades are cantilevers with high bending stresses at the hub connection. Most propeller blades are thicker at the root for this reason. Hydrodynamic optimization must give way to mechanical strength considerations. Since the SMAT is driven at the blade tips, these blades are stressed more like a beam with both ends fixed. Also, since the driving force is being applied at the largest diameter of the impeller, it is spread out over a larger area which further reduces the stress in the impeller material. Since the blade tips are attached to the driving rim, the blades can be loaded all the way to their ends, unlike other propellers which must be unloaded at the tips.

Because the electrical parts of the SMAT are at the outer diameter of the machine, they have a larger outside diameter than otherwise. In general, motors become more efficient as the diameter increases and the length decreases. This is especially true when a motor has many poles.

The larger surface area affords better heat transfer. Cooling problems, as demonstrated with previous electric drives for this vehicle, can be handled without external cooling systems. For example, the outside surface area of the SMAT motors is 2.5 times as great as that of the motor for the previous electric drive system.

Because the motor parts are surrounding the impellers there is no obstruction to the thrusters inflow. When the motor is connected by a shaft to the impellers, it is normally coaxial with them. This means that a curved inlet duct must be provided to avoid the motor's obstruction. Besides adding length to the thruster system, the curved duct changes the velocity distribution into the impeller and exacerbates any cavitation problems which might exist. The SMAT thruster has a clean inflow and, in fact, takes advantage of a complete ram inlet.

The SMAT motors are the induction type. Although permanent magnet motors are an attractive alternative, we chose induction motors because of their common usage, simple construction, and reliable operation. Induction motor technology is well understood as is their control.

The bearings for the SMAT are also on the outside diameter of the machine. There is no central shaft. Without the central shaft there is no need for struts to hold the shaft bearings. The elimination of the struts also helps to keep a clean inflow into the machine.

The bearings are water lubricated deflection pad bearings. They need no external lubrication system. Being located on the outer diameter, they tend to have higher losses than bearings on a central shaft which reduces the overall efficiency of the machine by approximately 1%. The choice to locate the bearings on the outside diameter was also influenced by the fact that water lubricated thrust bearings would have a larger diameter than could be accommodated by the central hub.

2.3 Design Approach

2.3.1 Hydrodynamic Design

The SMAT hydrodynamic problem is unique because the machine has the some characteristics of a ducted propeller and some of a waterjet. The approach to design is different for these two kinds of machine, but experience with contrarotating versions is limited for both. Designers of waterjet systems typically approach the problem in the same way as they would an axial flow pump. Propeller designers have modified their procedures to include the effects of the duct.

OSR approached the problem from both directions. For the

waterjet design we used axial flow pump methods to verify a single point design which incorporated the dimensions and parameters of the impellers which we proposed in our first iteration of the SMAT design. The design methods were strictly manual except for a small computer program which we wrote to do some of the more tedious calculations. The blade selection procedure was adapted from that contained in reference 3. Appendix A contains the complete design procedure.

The results of the manual design were encouraging. We found that we could use blades which would be easy to manufacture because they have zero camber and that we could use thick blade sections. Because we kept a constant solidity with increasing section radius, the blades sections increase in chord length as their radial position increases. This is only possible with a tip driven system because the blades do not need to be unloaded at the tip. The resultant blade appearance is somewhat strange when compared to propeller blades or even to axial flow pump blades. The blade sections are illustrated in Figure 4. Table 2 contains the results of the manual design.

TABLE 2

Flow Rate	- 57 cu-ft/sec
Jet Velocity	- 61.7 ft/sec
Tip Diameter	- 14.5 inch
Rotational Speed	- 2100 rpm

The manual design approach increased our confidence and highlighted some of the design issues which are involved. The result served as a benchmark for further more sophisticated studies.

For continued design studies we shifted to methods which propeller designers more typically use. Appendix B contains the results of the studies which use a two dimensional lifting line computer code to do parametric studies. The code, which is normally used for open propellers, was modified to include the effects of the contrarotating impellers and of the duct. The studies show the effects of changing diameters and rotational speeds. It was encouraging during this phase of the design to note that the parametric studies included the point design generated in the manual design.

Efforts in the hydrodynamic design ceased at this point in order for the electrical design to determine the largest possible tip diameter. The electrical design eventually determined that diameter to be 14.25 inches. A final design with that tip diameter has the characteristics listed in Table 3.

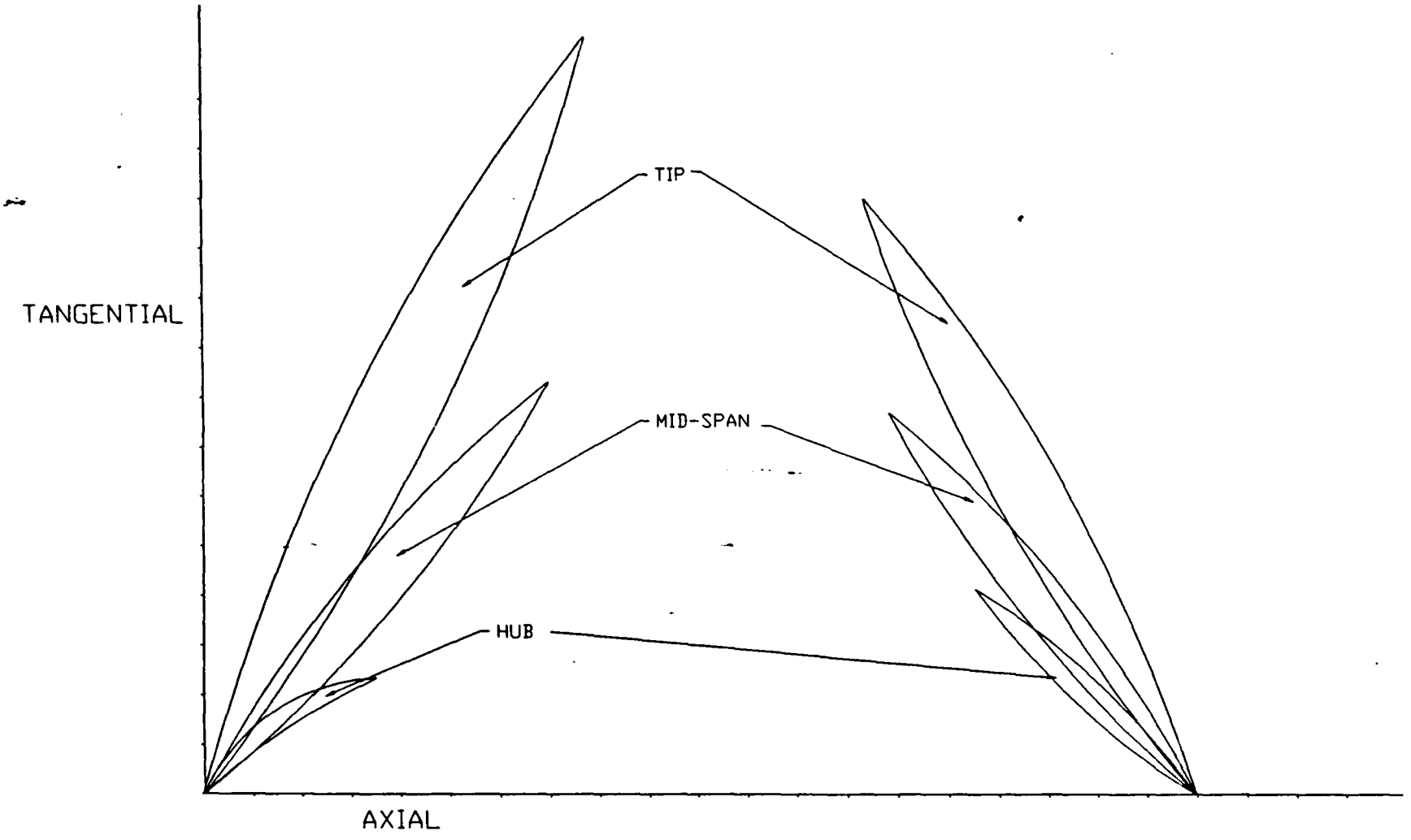

FIGURE 4
SMAT BLADE SECTIONS
(PUMP METHOD)

TABLE 3

Position	- Forward	- Aft
Number of Blades	- 7	- 9
Expanded Area Ratio	- 0.9	- 0.9
Hub Diameter Ratio	- 0.2	- 0.2
Rotation	- Right Hand	- Left Hand
Vehicle Speed	- 18 mph	- 18 mph
Rotative Speed	- 2100 rpm	- 2100 rpm
Thrust	- 1797 lbs	- 2044 lbs
Torque	- 500.2	- 500.2
Power	- 200 shp	- 200 shp

2.3.2 Electrical Design

Knowing the range of possibilities for the diameters and speeds, we were able to progress into the electrical design of the machine. Appendix C is a discussion of the various considerations which go into the selection of the electrical parameters. Figure 5 is a one page summary of all these parameters. The information on this sheet is sufficient to manufacture the electrical components once the housing and other parts are defined.

The discussions in Appendix C centers about attempts to design a motor which would accommodate a 14.5 inch impeller tip diameter. More than 50 point designs were conducted. The number of poles was varied from 10 to 22 and the input frequency was changed from 150-450 Hz. The electrical designers attempted to keep the core length below 12.5 inches, and they tried several different lengths for magnetic air gap. The initial study concludes that we would need to select a smaller propeller tip diameter and probably a longer core length.

Figure 6 is a speed/torque curve for the proposed SMAT motors. It is developed using information from another OSR project which uses a similar contrarotating configuration with water lubricated deflection pad bearings. The required starting torque is high because the bearings are on a large diameter and because the fluid film lubrication can not be established at zero speed. All of the initial electrical studies generated designs with at best marginal capability to overcome this high starting torque.

Other conclusions reached by the initial electrical designs were that the heat removal capabilities of the initial designs was suspect and that it would be difficult to make connections with the windings since there is little room between the housing and the outer diameter of the stator core.

Subsequent analysis using a 14.25 inch tip diameter and a 13 inch core length improved the overall design substantially. Starting torque is sufficient with an air gap dimension of 0.040

inches. The mechanical design of the housing would be adjusted to make room for the electrical connections.

2.3.3 Mechanical Design

The mechanical design of the SMAT can by studied by referring to the drawings which are supplied separately. The mechanical design of the SMAT is strongly influenced by the constraint on the overall width. A motor with an outer core diameter of 18.75 inches such as this one would normally be supported by a frame which is much larger in diameter and there would be much more room at the ends of the windings.

To compensate for the dimensional restrictions, the motor housing has taken an unusual shape. The interior of the housing must have a circular inner bore to accommodate the stator laminations. As shown in Figure 7, the outer ends of the cylinder transition to rectangles. The rectangles fill the entire space available for the SMAT thruster.

If a pure cylindrical tube were used for the outer stator housing, its thickness would be 0.25 inch which would be only marginally stiff enough for a motor this size. Instead, a cylindrical tube with an outer diameter of 20 inches contains the stator laminations. Once the laminations are installed, flats on opposite edges of the tube are milled so that the maximum width is 19.25 inches.

During manufacture of the electrical motor it is necessary to clamp the laminations together. To accomplish this in the SMAT motor, the manufacturer will first weld a transition piece to the end of the housing cylinder. Once the laminations are in place, a second transition piece, welded to the other end of the cylinder, will clamp them in place. The transition pieces are 1/2 inch plates with rectangular outer shape. A circle is removed from the center of the plate, and the circle diameter is 1/4 inch less than the outer diameter of the core. The resultant shoulder clamps the laminations.

The rectangular housing pieces are welded to the transition pieces. These parts of the housing hold the ends of the motor housing. The outer shape of the housing ends is rectangular, and the inner bore is circular. The inner bore of this piece must be concentric with the inner bore of the stator core because it positions the bearing pieces.

The radial bearing supports have rectangular outer shape and a circular ledge on the inner surface which fits into the inner bore of the housing ends.

The bearings, which are the deflection pad type, work on the principle that bearing pressure and drag will cause the effective

FORM 6

GENERAL DYNAMICS/ELECTRO DYNAMIC
A.C. INDUCTION MOTOR
DESIGN & ELEC. SPEC. SHEET

ENCL	HP	VOLTS	AMPS	SYN R.P.M.	FL R.P.M.	PH	CIQ	°C RISE	INS. CL.	DUTY	M/P # TYPE	DES.	CODE
	200.00	440		3140		3	021	70					

ROTOR VOLTS	ROTOR AMPS	BRUSHES PER SET & GRADE	ENGR.	APP'D	DATE	CUSTOMER	ORDER #
1.00 SF							2000CEAL

	BLANK #	O.D.	I.D.	# SLOTS	SLOT-DIE S&A	SLOT SETTING	GROSS CORE	VENTS 3/8	NET CORE	CARTER FACTOR	GRADE STL #24	AIR GAP
STATOR		18.750	16.500	108	1001 0		13.000	0	13.000	1.075	M-19	.0400
ROTOR		16.420	14.750	144	1028 25		13.000	0	13.000	1.040	M-19	

COIL WDG. DWG. #	TURNS PER COIL	WIRE SIZE	WIRE WT.	WIRE SIZE	WIRE WT.	WIRE AREA (IN²)	COILS PER GROUP	NET SLOT AREA	FULLNESS	PITCH	MLT	COIL DIMENSIONS ST	SPD	LOOP
STATOR	4	3 #13	65.7	0 # 0	0.0	.01221	2.0	0.179	78	6	33.1	15.0	2.3	17.5
ROTOR														

CONNECTION & CABLE

DIE. SPEC #	CONN.	INTERNAL CONN DWG.	EXTERNAL CONN DWG.	CABLES #	CABLES SIZE	LEADS #	LEADS VOLTS	R LINE @25°C
								0.0174

NO. OF CORE PLATES STATOR= 936 ROTOR= 936
ST CORE STL. WT= 132.8 LBS ROT CORE STL. WT= 118.2 LBS

REMARKS-
VTI=10.6 VCI= 42.3
BAR WT= 36.73 LB
ER(2)WT= 14.02 LB.

ROTOR CAGE	BAR SIZE AREA	LENGTH	MATERIAL	END RING THICK	RAD. HT.	MATERIAL	TRICKEY FACTOR	SKEW O.D.	ARBOR	FIXTURE	FABRICATED BAR DIMENSIONS (ACTUAL)	FAN #
	0.0585	13.00		0.625	0.710		1.17				x x	

REFERRAL FACTORS	CONN	CKT	Nt	Kp	Kd	K damp	B fy MEGALINES	BG fy KILOLINES/IN²	K1	K2	K3	R er μ ohms	R b μ ohms	Kr	Ks
	1	6	24	.966	.966	.92	0.80	33.4	0.053	0.653	42	8	154	2.41	.626

	λ OF ROT NECK OR BRIDGE	λ sL	λ sr	HARMONIC LEAKAGE FACTORS	λ b	λ e	B tg fy (KILOLINES/IN²)	B ts fy (KILOLINES/IN²)	B c fy (KILOLINES/IN²)	AMPS per in²	A COND. per in.	ELEC LOADING (x 10⁻⁶)	RING DENSITY
STATOR	—	—	1.156	.02050	0.745	0.296	110.7	110.5	101.5	3790	772	2.93	—
ROTOR	0.50	0.958	2.231	.01935	1.014	0.067	71.0	78.2	92.4	3505			1185

PERFORMANCE	R1 ph @25°C	R2'r @25°C	R2'L @25°C	X1	X2'r	X2'L	Xm	Io	FL SLIP	PO SLIP	FLT lb. ft	°C RISE FL THER	°C RISE FL RXR
CALCULATED	0.0087	0.007	0.016	0.117	0.116	0.071	1.6	144.43	.0076	.0391	495.0		
TEST													

	EFFICIENCY 1/2	3/4	FL	1 1/4	1 1/2	POWER FACTOR 1/2	3/4	FL	1 1/4	1 1/2	LRA	LRPF	LRT (pu)	POT (pu)	PUT
CALCULATED	0.930	.945	.950	.950	.881	.565	.692	.742	.764	.865	1958	.185	0.53	2.38	1.11
GUARANTEE															
TEST															

FULL LOAD LOSSES	V AIR GAP	F.L. AMPS	SEC. CU @ °C	PRI. CU @ °C	F & W	CORE	STRAY	TOTAL
CALCULATED	231.1	277.68	1153	2477	550	4082	879	8635
TEST								

TEST S.O. #
TEST
DATE

COMMERCIAL-

NO LOAD TEST

VOLTS	AMPS	WATTS

SURGE RING DWG-

ROTOR ASSEMBLY-
NAVY-
ROTOR PLATE- 98
STATOR PLATE- 99
RING & FAN ASSEMBLY

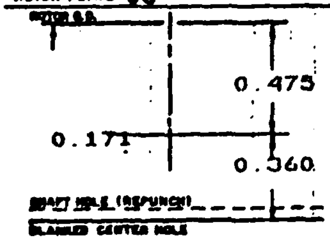

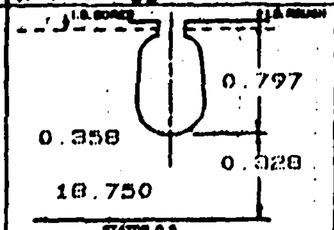

G.L.: 504
C.L.: 2000
T.L.: 1579

LRT-BAR= 14.0 ST= 30 ER= 272

FRAME	CORE	TYPE	WDG		POLES		REV.

SHEET OF

Figure 5

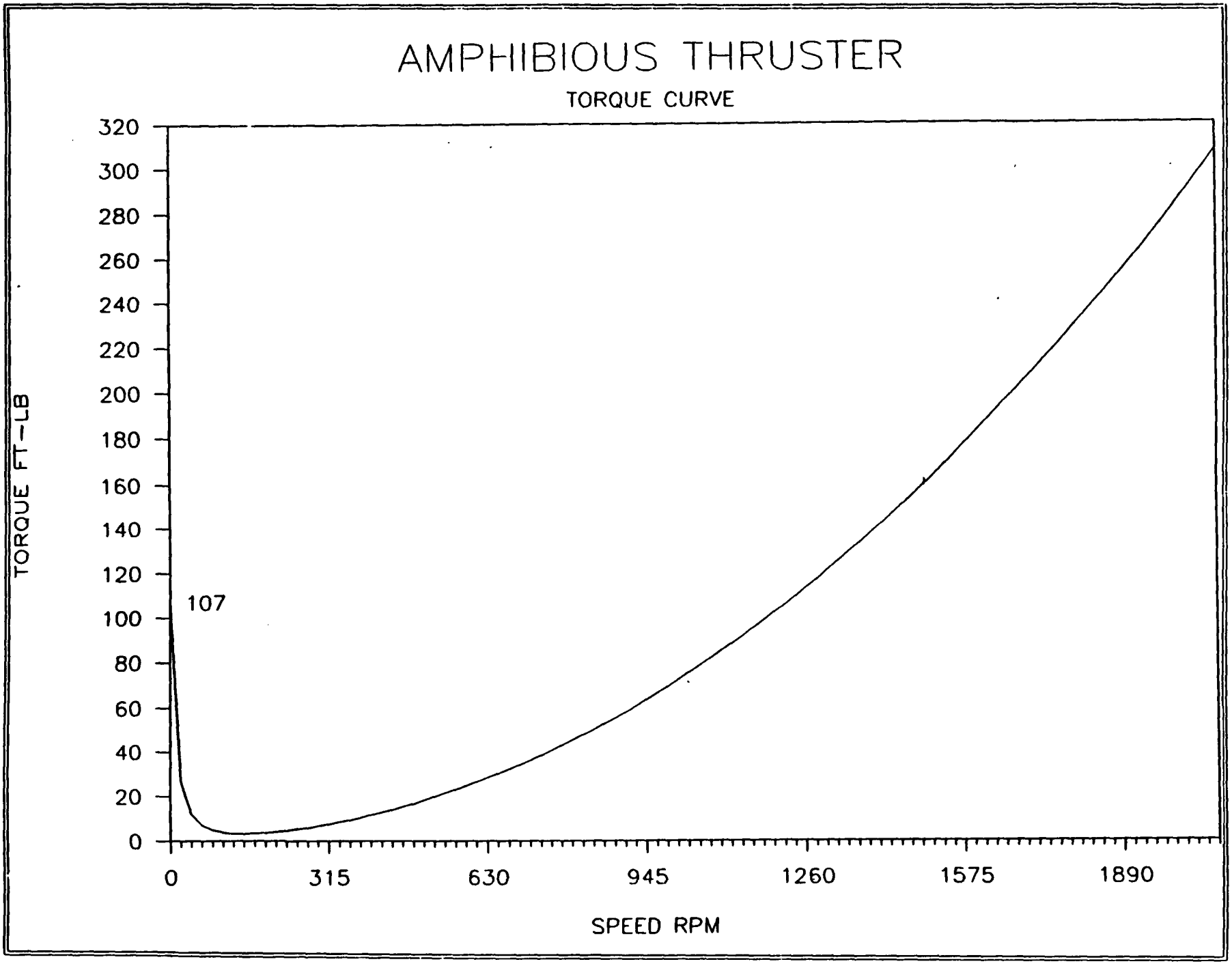
AMPHIBIOUS THRUSTER
TORQUE CURVE
TORQUE FT-LB
320
300
280
260
240
220
200
180
160
140
120
100
80
60
40
20
0
107
0
315
630
945
1260
1575
1890
SPEED RPM

Figure 6

bearing surface to deflect in such a way as to create a fluid lubricating wedge. Figure 8 illustrates schematically the general principal of the bearing being deflected by a drag force. A similar design uses a biased support system so that one side of the support is weaker in the upstream direction.

Ocean Systems Research, Inc has used deflection pad bearings in a previous project and they have worked well. See reference 4 for further discussion of the deflection pad bearings.

The SMAT motor runs totally submerged in sea water. It would be possible to run with water in the "air" gap between rotor and stator cores. Unfortunately, this would cause mechanical losses to increase by as much as 48 horse power. Using the techniques of reference 5:

$$\text{Loss} = \frac{0.078 \cdot \pi \cdot \rho^{.57} \cdot w^{2.57} \cdot r^{3.57} \cdot m^{.43} \cdot L}{C^{.43}}$$

r = gap radius
ρ = density
w = angular velocity
m = viscosity
L = core length
C = gap width

Thus, with water in the gap, the power required is increased by approximately 12%. The thruster will operate under these conditions, but the efficiency degradation is unacceptable. To improve efficiency, we have incorporated rotating shaft seals to keep water out of the gap area. Figure 9 shows the position of the BAL seals on the bore of the motor stator. The rubber pieces with garter springs are in the bore rather than on the sleeve because the large diameter and high speed of the rotor would cause unacceptably high centrifugal forces.

The gap area is pressurized with air at 10 psi. The air is supplied by a pressurized bottle located external to the thruster and fed to the gap volume through drilled passages in the top of the housing ends. Similar passages at the bottom of the piece allow water to escape and indicate to the operator when water is present. Theoretically, there should be no need for air replenishment because the seals are capable of zero leakage. The air is pressurized so that, should the seal leak, the air will leak out rather than water in.

The air seals and their supply are added complexities which we would prefer to avoid except for their improvement in efficiency. OSR originally proposed using ferrofluidic seals which would have had no drag on the system. The company which supplies that type of seal studied the idea and concluded that their seals were not

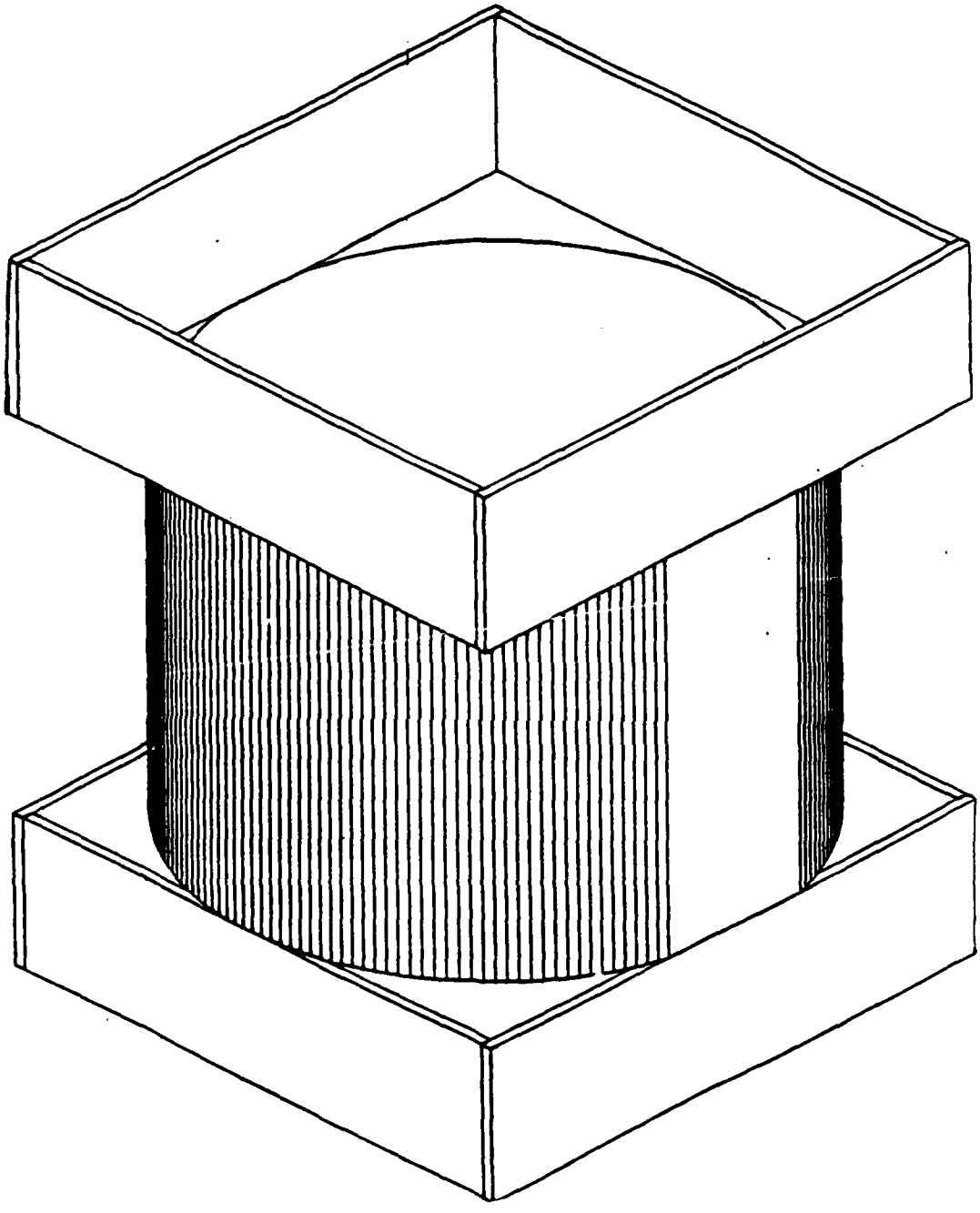

SMAT HOUSING CONCEPT

Figure 7

SMAT

BEARING PADS

Pad Support Posts Tilted in Toward Pad
Tangential Force Causes Pad Deflection
Hydrodynamic Wedge Reduces Friction

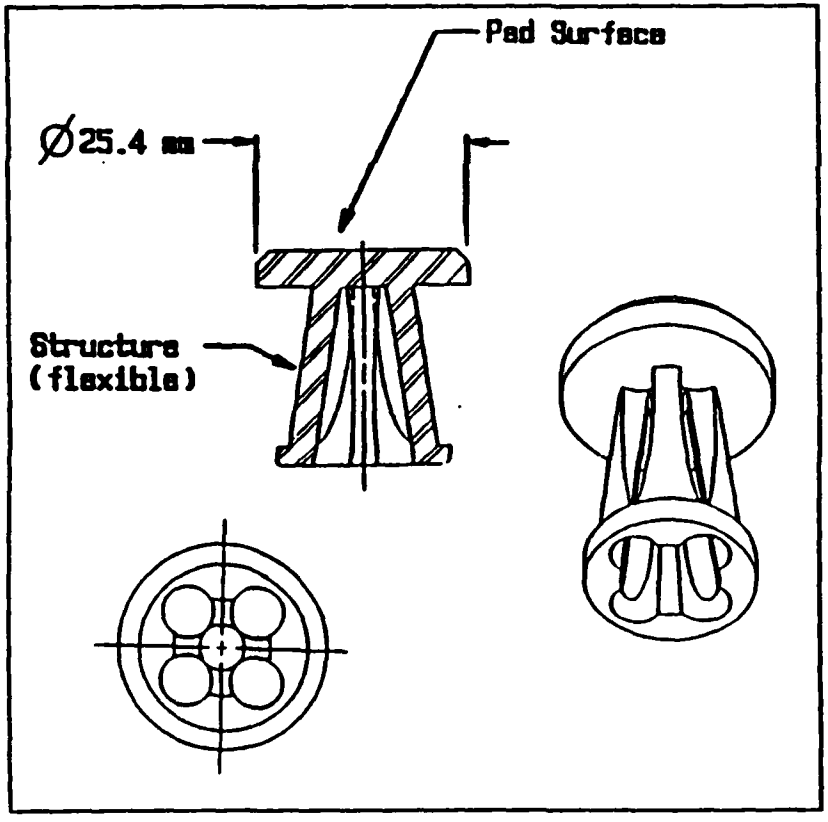

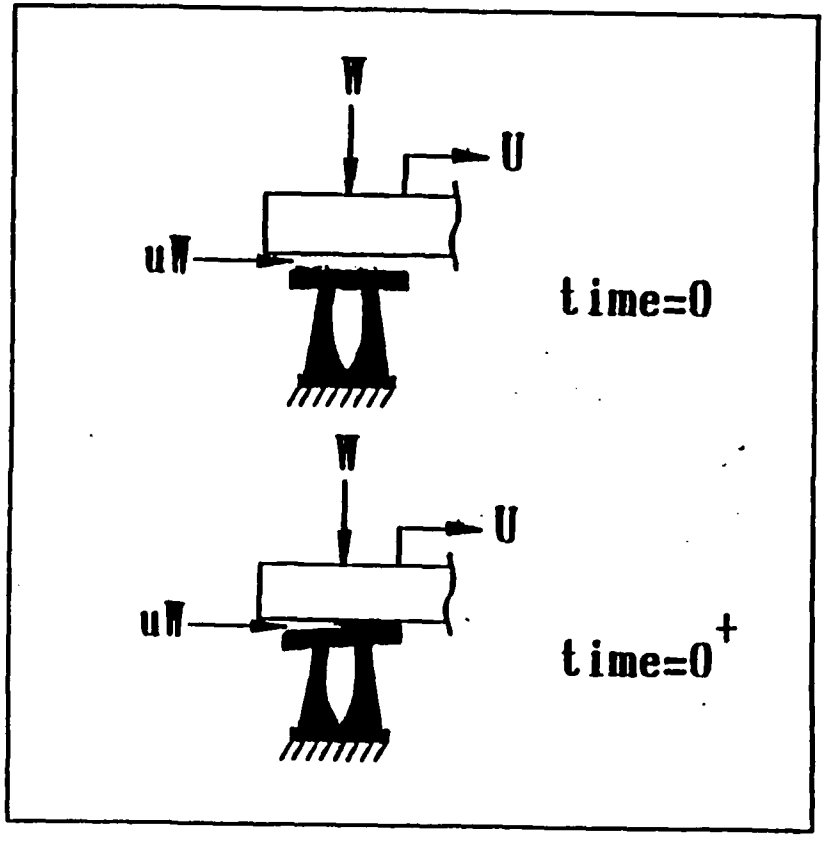

Figure 8

appropriate for this application. The slight drag of the BAL seals is minuscule in comparison to the system power so the effect on efficiency is small.

In case of failure of the air seals, the machine electrical parts must be sealed. For this reason, the rotor is coated with chlorinated polyester applied in a fluidized bed process. See Figure 10. The stator is protected by applying a thin foil of hastelloy metal which is backed by cloth for good adhesion. It is epoxied in place during the vacuum polymer injection of the windings. The windings are encapsulated in polyurethane with a filler to increase its heat transfer characteristics. See figure 11.

3.0 Machinery Comparisons

Figure 12 shows the SMAT arrangement together with that of another contractor. Both have the same power and thrust, and both have the same width and about the same height. Weights of each are estimates based upon the dimensions available. The SMAT is an obvious improvement in length.

TABLE 4
Machine Characteristics

	SMAT	Other
Length	55 inches	76.3 inches
Width	19.25 inches	19.25 inches
Height	20 inches	20.75 inches
Weight	1925 lbs	1990 lbs
Efficiency	91.6%	92% (goal)

The other electric drive used a high speed motor with a speed reducing gearbox. Its goal for efficiency was 92% including all of its machinery from electrical input into the motor through the coupling which drives the impeller. Since it was necessary to add extra cooling and since the motor had to be derated, it seems safe to say that the system did not attain that goal. The goal is reasonable for comparison purposes, however, because it includes the same machinery as the SMAT exclusive of the hydraulic efficiencies of the thruster impeller components.

The power losses in the SMAT are both electrical and mechanical. They are listed in Table 5

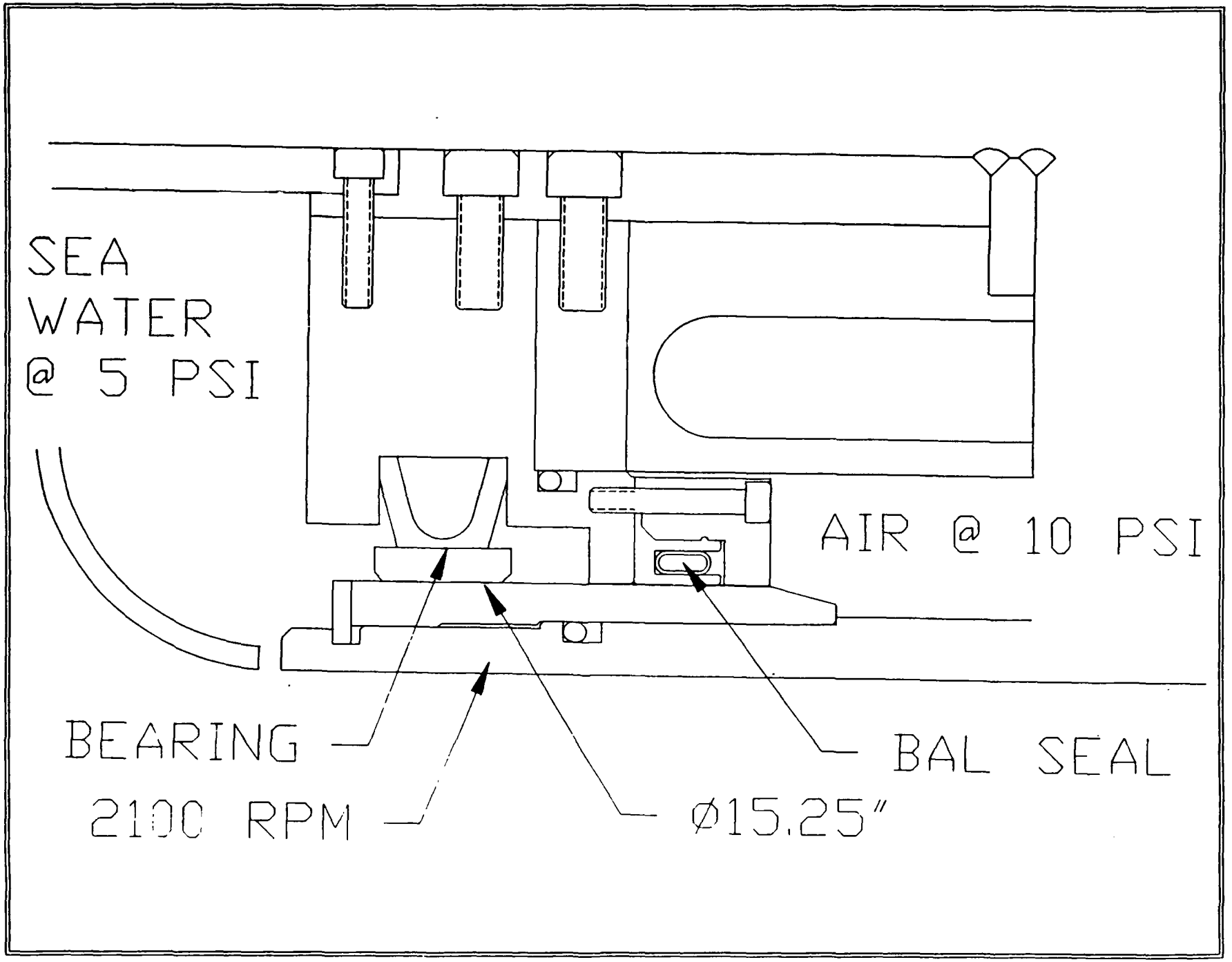

Figure 9

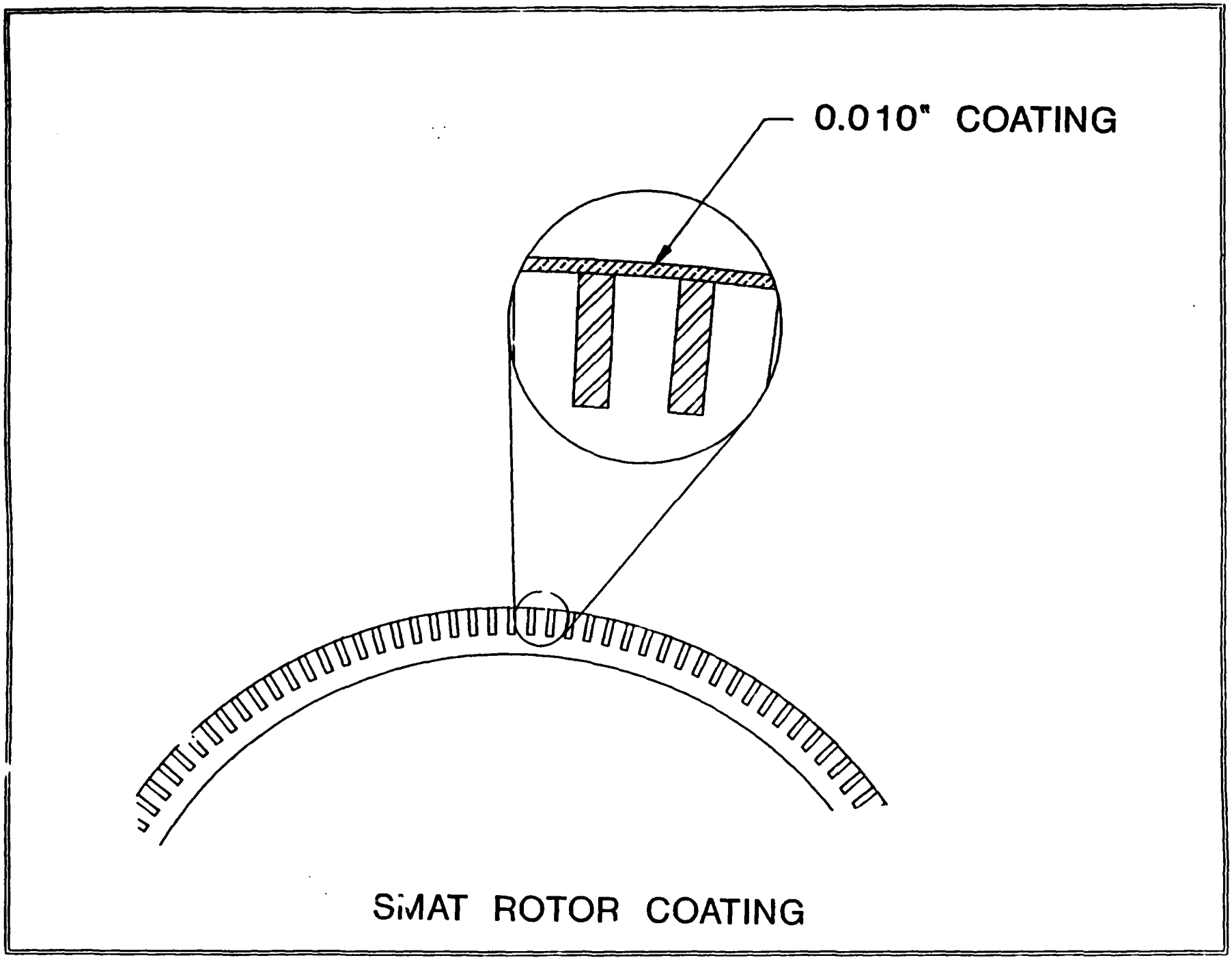

Figure 10

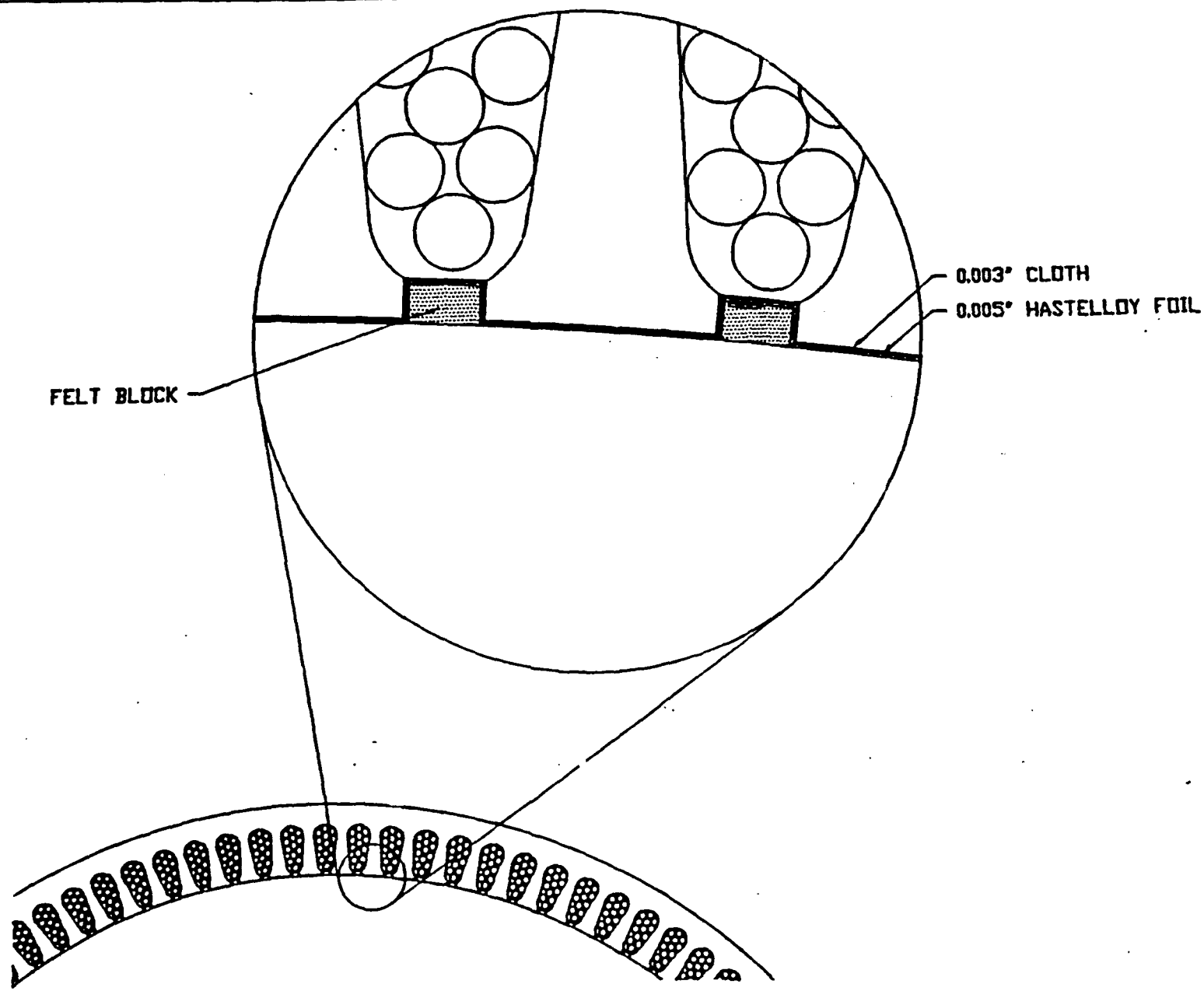

SMAT STATOR CORE SEAL

Figure 11

TABLE 5
SMAT POWER LOSS
(per stage)

ELECTRICAL	
Secondary Copper	- 1153 watts
Primary Copper	- 2477 watts
Core	- 4082 watts
Stray	- 373 watts
MECHANICAL	
Windage	- 550 watts
Radial Bearings	- 1714 watts
Thrust Bearings	- 425 watts
TOTAL	- 10774
EFFICIENCY	- 92.7%

Methods for calculating electrical losses in induction motors are well established, and they should be considered reliable. The loss from the radial deflection pads is estimated based upon an extrapolation of data from reference 6. The thrust bearing loss is calculated using the information reported in reference 4. It should be noted that the core losses are higher than would normally be expected because the dimensional restrictions have limited the amount of back iron which can be accommodated. Also, the radial bearings reported in reference 6 are a first generation design and the manufacturer believes that improvements to efficiency are likely as the development of these kinds of bearings progresses.

4.0 Technical Risk

The OSR Submersible Motor Amphibious Thruster is based upon some technologies which have not been used extensively and are therefore more risky than those which are more mature. The electrical design of the motor is an example. Although the induction motor is well known, the configuration of this motor is new. The back iron in the core of this motor is less than normal because of the overall diameter limitations. Also, since the motor windings are encapsulated in plastic, they have less cooling than other motors even though the plastic is chosen for good heat transfer. These differences have been accounted for in the design. The calculations say it will work. But there are some things about which we can not be sure until we try them.

OSR's In-line Submersible Pump is being tested by Navy personnel at David Taylor Research Center in Annapolis, MD. The stator sealing system for this pump has been subjected to 60 psi water pressure during operation. Unfortunately, the insulation resistance of the motors has been decreasing indicating that the

SMAT
MACHINE CHARACTERISTICS

	SMAT	ALTERNATIVE
LENGTH	55"	76.30
WIDTH	19.25"	19.25
HEIGHT	20"	20.75
WEIGHT	1925 LBS	1990 LBS
MACHINE EFFICIENCY	92.7%	92% GOAL

SMAT

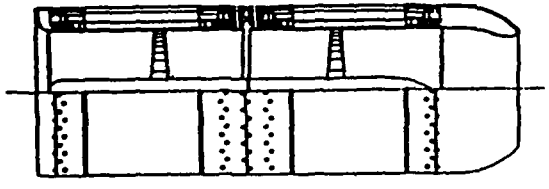

ALTERNATIVE

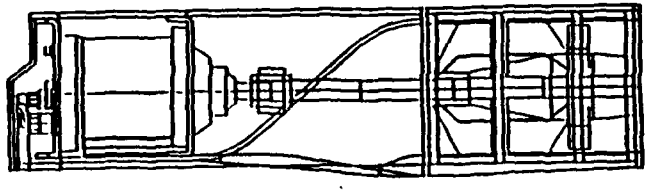

Figure 12

sealing system might have failed. OSR and our subcontractors are investigating the problem and we will propose a solution. The sealing system for the SMAT could have the same problem if the identical sealing system were used for it. In this case, the SMAT will benefit from our efforts with the pump.

The shaft seals are operating at high speed. Fortunately, they are under a relatively low pressure, so that their PV (pressure times velocity, a figure of performance for seals) is still relatively low. The is seal in the bore rather than on the shaft, which helps, but this will be the highest peripheral speed to which these seals have been subjected, according to the manufacturer. The penalty for slight seal leakage is high air use. The penalty for large seal leakage is a 12% reduction in efficiency. The machine will operate without the seals.

All of the risks are mitigated by the fact that OSR has built a similar system before, by the simplicity of the machine, and by the conservative approach taken by the designers.

5.0 Summary

Ocean Systems Research, Inc. has completed a preliminary design of a Submersible Motor Amphibious Thruster. We have conducted hydrodynamic, electrical, and mechanical studies which have shown that the machine as designed should be built. This report documents the design and points out the benefits to be derived from the SMAT system.

6.0 Conclusion

Our initial studies indicate that the SMAT is feasible and desirable. Its configuration is suited to the Advanced Amphibious Assault Vehicle and it is a good way to incorporate electric drive into that vehicle. The SMAT is shorter and more efficient than the alternative electric drive system, and it is far less complicated.

References

1. Witkowski,J., and Triner, J., Amphibious Vehicle Propulsion System Design Report, Westinghouse Oceanic Division, for David Taylor Research Center, July 8, 1988.

2. Eastman, W. and Specht, Steven, Amphibious Vehicle Propulsion System Final Report, Westinghouse Naval Systems Division, for David Taylor Research Center, January 30, 1990.

3. Wilson, D., The Design of High-Efficiency Turbomachinery and Gas Turbines, The MIT Press, 1984.

4. Paquette, D. and Kostrzeewsky, G., Measured Coefficients of Friction for Thrust Bearings with Flexible Support Structures, KMC, Inc. report submitted to: ASME Journal of Tribology, March 1990.

5. Harbage, A., Hydraulic Analysis of a 15-Horsepower, Free Flooding, Submerged Electric Motor; MEL Research and Development Report 109/66, April 1966.

6. Anderson, F., DiNunzio, T., and Taylor, D., In-line Pump Bearing System, Report No. MA-RD-RT0009, for Ocean Systems Research, Inc., January, 1991.

Appendix A

1. Hydrodynamic Design
Approach
The hydrodynamic design of the SMAT pump impellers uses the following sequence:

1. Determine required mass flow and exit velocity to provide 4000 pounds of thrust using the available 400 horse power.

2. Knowing the mass flow and exit velocity, determine the area of the exit nozzle.

3. Determine the shape of the hub.

4. Using the shape of the hub and the maximum diameter of the jet duct, determine the mean radius of the thruster blades.

5. Using the mean radius and thruster RPM, determine the peripheral speed of the blade at the mean radius Um.

6. Using laws of conservation, cross-sectional area of duct, and mass flow, determine axial velocity VXm.

7. Use velocity diagrams to find relative velocities in and out of blade rows.

8. Use Eulers equation to get change in angular fluid velocity across row.

9. Use fluid angles from velocity diagrams to enter carpet plots.

10. Select mid radius blade shapes.

11. Check cavitation index.

12. Use free vortex design $rV_\theta = rmV_{\theta m}$ to repeat for more blade sections.

13. Calculate load coefficient, flow coefficient and reaction for comparison to other designs.

Because both thrust and horsepower are specified, we can solve two equations in two unknowns to find both exit velocity and mass flow.

Thrust = change in momentum in unit time

1. $T = \rho \cdot Vj \cdot Aj\ (Vj - V)/gc$

ρ = density lbm/st^3

Vj = jet velocity ft/sec

V = vehicle velocity ft/sec

Aj = area of nozzle

Note that the efficiency of the jet is given by:

$$\eta = \frac{2V}{Vj + V}$$

This approaches 1 as Vj approaches V. But also note that thrust approaches zero at the same time.

Power = (Total Pressure Loss) x (Mass Flow Rate)

2. $SHP = Hp\ Q\ \rho g/550\eta = 400$

SHP = shaft horsepower

Q = Volume flow rate ft^3/sec

g = 32.2 ft/sec^2

η = pump efficiency (assume $\eta = 0.9$)

Hp = head loss ft

Total head loss = Inlet loss
+ duct loss
+ nozzle head loss
- Ram recovery at inlet
= Hi + Hd + Hn - RR

$$Hi = \frac{Ki\ Q^2}{2g\ A}$$

A = duct area = $\pi D^2/4$

$D = 14.5 \text{ inch} = 1.21 \text{ ft}$

$Ki = 0.05$ for a rounded inlet

$$Hd = \frac{Kd\ Q^2}{2g\ A}$$

$Kd = fL/D$

f = friction factor = 0.005

$L = 38$ inches

$Kd = 0.131$

$$Hn = \frac{Vj^2}{2g}\ (1 + Km)$$

$Km = 1.063$ (ref B)

$$Vj = \frac{Q^2}{Aj}$$

from 1 $\quad T = \rho \cdot Vj \cdot Aj(Vj - V)/gc = 4000$ lbf

$$V + \frac{Tgc}{Q\eta} = \frac{Q}{Aj}$$

Using 18 mph for speed at which 4000 lbf thrust is required, V = 26.4 ft/sec.

$$\frac{Q}{Aj} = \left| 25.4 + \frac{2012.5}{Q} \right|^2$$

Substituting into 2

$$SHP = \left| \frac{.05\ Q^2}{2g\ A^2} + \frac{.0131Q^2}{2gA^2} + \frac{1.063\ Q^2}{2\ Aj^2} \cdot \frac{(26.4)^2}{2g} \right| \frac{Q\rho g}{550\ gc}$$

$$= .024Q^2 + .5315 \left| 26.4 + \frac{201.5}{Q}^{\ 2} \right| - 348.48 \cdot 4x10^{-3}Q = 400$$

This expression must be solved for Q. (We solved it by trial and error using a simple computer program.)

$$Q = 57 \text{ ft/sec}$$

Substitute back into 1 and solve for Vj

$$Vj = 61.,7 \text{ ft/sec}$$

The jet nozzle area is found by Q/Vj. Given that the thruster duct is a constant 14.5 inches, the radius of the hub can be calculated:

$$Aj = Q/Vj = .9238 \text{ ft}^2$$
$$= \pi (R - r_H)^2$$

$$r_H = 3.2 \text{ inches}$$

The shape of the hub at this point is arbitrary except that its radius at the jet exit should be 3.2 inches.

In order to reduce the chances for cavitation at the leading edge of the first stage, the axial velocity there should be as low as possible. That is, the unblocked inlet area should be as large as possible. Therefore the hub radius at the inlet should be zero. One of the advantages of the rim drive impellers is that the root stresses are much lower than they are with cantilevered blades, and there is no center shaft; so the hub area can go to zero at the inlet.

The hub profile can be defined in any numbered of ways. The radius can increase linearly or the duct area can decrease linearly. One good way to define the hub profile is to note that one of the assumptions made for radial equilibrium in free vortex design (which we will use to select blade shapes) is that the radial component of velocity must be constant with radius. By also requiring that it be constant along the axis, a contour can be established as follows:

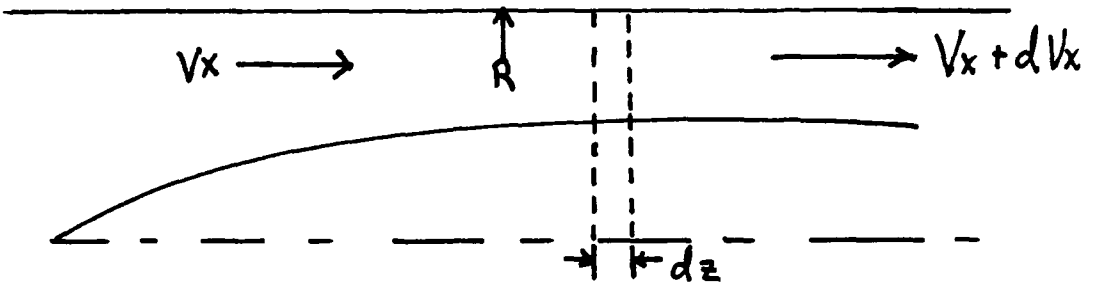

For continuity of flow in the duct as the hub radius increases over the length dz, the contribution to flow from the radial component of velocity must be equal to the increase in flow in the axial direction:

$$(Vx + dVx)(\pi(R^2-r^2)) = Vx(\pi(R^2-r^2)) + Vr \cdot 2\pi r\, dz$$

Where $Vr \cdot 2\pi r\, dz$ is the radial component of velocity times the hub surface area in length dz.

$$dVx = \frac{2 \cdot r \cdot Vr}{R^2 - r^2} dz$$

$$Vx = \frac{Q}{A} = \frac{Q}{\pi (R^2-r^2)}$$

$$dVx = \frac{2Qr}{\pi (R^2-r^2)} dr$$

$$\frac{dr}{dz} = \frac{\pi Vr}{Q} (R^2-r^2)$$

by requiring that Vr be a constant, this first order differential equation can be solved by separation of variables and integration.

$$dz = \frac{Q}{\pi\, Vr} (R^2-r^2)^{-1}\, dr$$

$$z = \frac{Q}{\pi\, Vr} \int \frac{1}{R^2-r^2} dr$$

$$z = \frac{Q}{\pi\, Vr} \cdot \frac{1}{2R} \operatorname{Ln} \left| \frac{R + r}{R - r} \right| + C$$

at z=0, r=0, so c=0

Using 2100 rpm find hub diameter such that $V_{\theta hub} = 0.8\ U_{hub}$

rh = 1.8" (after some iterations)

$$Um = (1.8 + 7.25)/2 \cdot 2\pi \cdot \frac{2100}{60.12} = 82.925$$

$$V_{\theta m} = \frac{180 \cdot 32.2 \cdot 550}{82.925 \cdot 57 \cdot 64} = 10.54 \text{ (Euler's)}$$

$$V_{\theta 2} = \frac{7.25 + 1.8}{2 \cdot 1.8} \cdot 10.54 = 26.496$$

$$U_{hub} = 1.8 \cdot \pi \cdot 2 \cdot 2100/60.12 = 32.987$$

$$V_\theta^2 \approx 0.8\ U_{hub}$$

So the hub radius at the first stage blade exit should be 1.8"

Use velocity diagrams to get flowe angles

ßin = 57.43

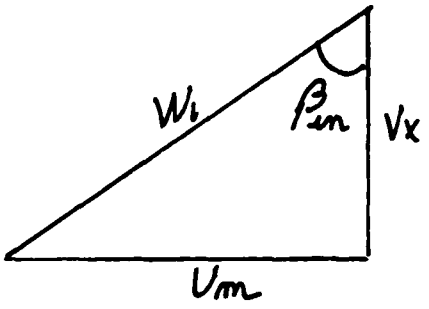

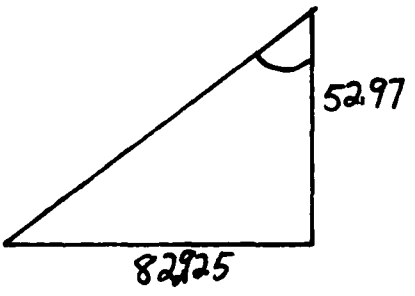

$$Vx = 57/(\pi(7.25^2 - 1.8^2)/144) = 52.97$$

$\beta_{out} = 54.013$

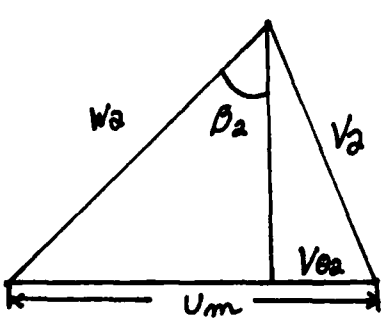

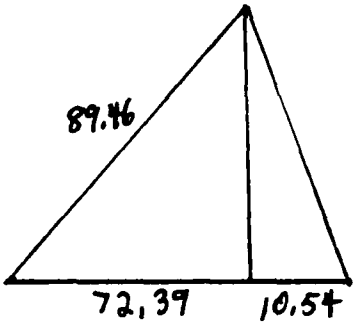

$\beta_{in} - \beta_{out} = 3.42°$

Now enter carpet plots with $\beta_{in} - \beta_{out} = 3.42°$ and $\beta_{in} = 57.43°$

$\epsilon = 3.42$

σ	.75	1.0	1.5
ϵ^*	3.42	11.42	27.42

	0			
σ	0	20	30	40
.75	8°	N	N	N
1.0	68°	N	O	N
1.5	8°	E	N	E

i^*

Select the 0 camber $\sigma = 1.5$ blade for mid radius

At the tip

$$rV_\theta = rm\ V_{\theta m2}$$

$$V_\theta = \frac{7.25 + 1.8}{2} \cdot 10.24/7.25$$

$$= 6.58 \text{ ft/sec}$$

$$U_{tip} = 2 \cdot \pi \cdot 7.25 \cdot \frac{2100}{60.12} = 132.86 \text{ ft/sec}$$

ßin = 68.53

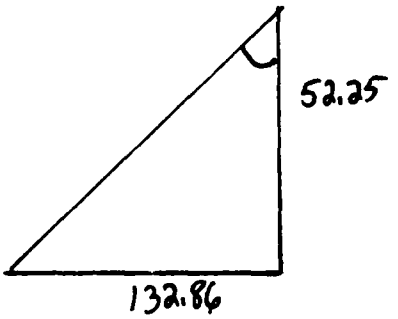

ßout = 67.522

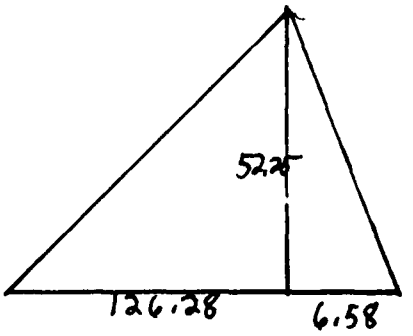

ßin - ßout = 1°

Enter Carpet Plots

σ	.75	1.0	1.5
ϵ*	1.00	9	25

on the 1.5 σ plot 0° camber i* = 5.8

At the hub:

$$V_\theta = \frac{7.25 + 1.8}{2} \cdot 10.54/1.8 = 26.50$$

$$U_{hub} = 2\pi \cdot 1.8 \cdot \frac{2100}{60.12} = 3300$$

ßin = 32.28

ßout = $\tan^{-1} \frac{33}{52.25 - 26.5}$

= 52.035

ßin - ßout = 19.75
for σ = 1.5 ϵ^* = 43.75 40° camber

What U gives 50° inlet angle?

$$\tan 50° = \frac{U}{52.25} \qquad U = 62.26 = 2 \cdot \pi \cdot \lambda \frac{2100}{60.12}$$

r = 3.40

at r = 3.40

$$V_\theta = \frac{7.25 + 1.8}{2} \cdot 10.24/3.4 = 14.03$$

$U_{3.4} = 62.30$

$\beta in = 50°$ $\beta out = 47.27$

$\beta in - \beta out = 2.73$

$i^* = 3.7$

at r = 6"

$V_\theta = \frac{7.25 + 1.8}{2} \cdot 10.54/6 = 7.95$

$U = 109.96$

$\beta in = 64.58$ $\beta out = 62.88$

$\beta in - \beta out = 1.7°$

$i^* = 7°$

Summary

r	i*	σ	0
1.8	3.7	1.5	40
3.4	3.7	1.5	0
4.525	8	1.5	0
6.0	7	1.5	0
7.25	5.8	1.5	0

Find a second order expression which describes chordal incidence as as function of inlet angle

$i^* = a\beta^2 + b\beta + c$

β	i
50	3.7
60	8.2
70	5.5

$3.7 = a\ (50)^2 + b\ (50) + c$
$8.2 = a\ (60)^2 + b\ (60) + c$
$5.5 = a\ (70)^2 + b\ (70) + c$

$i^* = -.036\ \beta^2 + 4.41\ \beta - 126.8$

Complete hub description

Find the length of the blade at r = 1.8" in the arial direction

c= 4.239

γ= blade chord angle to axial direction

= βin - i*

= 32.2545 - 20 = 12.2545° La = 4.239 cos (12.25°)

= 4.14"

for z = 0 at the beginning of the hub inlet
z = 4.18 @ r = 1.8, find K such that

$$z = k \, \text{Ln} \left(\frac{R + r}{R - r} \right)$$

$$4.14 = K \, \text{Ln} \left(\frac{7.25 + 1.8}{7.25 - 1.8} \right) = K \cdot .50715$$

$$K = 8.1633$$

for $0 < z < 4.14$ $z = 8.1633 \, \ell n \left(\frac{7.25 + r}{7.25 - r} \right)$

Find a circular arc which is tangent to r = 3.2 and has the same slope as the log function @ z = 4.14 r = 1.8

$$K = \frac{Q}{\pi V r} \cdot \frac{1}{2R}$$

$$\frac{dr}{dz} = \frac{\pi \, Vr}{Q} (R^2 - r^2)$$

$$= \frac{1}{K \cdot 2R} (R^2 - r^2)$$

$$= \frac{1}{8.1633 \cdot 2 \cdot 7.25} (7.25^2 - 1.8^2)$$

$$= .4167$$

Let R = radius of curviture of arc

$$y^2 + x^2 = R^2$$

$$dy/dx = \frac{-x}{\sqrt{2-x^2}} = .4167 \quad @\ x = -L$$

$$= \frac{1}{\sqrt{2-L^2}} = .4167$$

$$R^2 = L^2 + (R - 1.4)^2$$

$$R^2 = .148^2 + {}^2 - 2.8 + 1.96$$

$$0 = .148^2 - 2.8 + 1.9c$$

$$\frac{L^2}{R^2-L^2} = .1736$$

$$R = \frac{28 \pm \sqrt{2.8^2 - 1.16}}{.296}$$

$$L^2 = .1736\ R^2 - .1736L^2$$

$$R = 18.19",\ .728$$

$$1.1736cL^2 = .1736^2$$

$$L^2 = .148^2$$

$$L = 6.99"$$

Design the second stage blades

Assume:

For free vortex the value of $r \cdot V_\theta$ remains a constant into the second stage

But Vx increases because of continuity of mass

$$Vx = \frac{57 \cdot 144}{\pi\ (7.25^2 - 3.2^2)} = 61.733 \text{ ft/sec}$$

$$V_{\theta m} = 47.7/r_m$$

$$r_m = \frac{7.25 + 3.2}{2} = 5.225$$

$$V_{\theta m} = 9.129$$

$Um = 2\pi rm \frac{2100}{60.12} = 95.753$

$Um + V_{\theta m} = 104.88$

$\beta in = \tan^{-1} \frac{104.88}{61.733} = 59.52°$

$\beta out = \tan^{-1} Um/Vx = 57.19°$

Go to carpet plots

Assume 5 blades

$s = 2\pi rm/5 = 6.57"$

$\varepsilon^* = 2.33 + 32\ (\sigma - .75)$

σ	ε^*	i^*	0
.75	2.33	6	0
1.0	10.33	5.5	0
1.5	26.33	7.8	0

Try thicker blades first

Pick the longer blade ie $\sigma = 1.5$

At the hub

$\beta in = 49.98 \approx 50$ $\beta in - \beta out = 6.47$

σ	ε^*	i^*	0
.75	6.47	5.5	20
1.0	14.47	5	20
1.5	30.47	7	0

again pick the long blade at the tip

$\beta in = 67.05$ $\beta in - \beta out = .97$

σ	ε^*	i^*	0
.75	.97	4.0	0
1.0	8.97	4.5	0
1.5	24.97	5.8	0

Again pick the longer blade

Find a quadratic for i^* vs ßin

$i^* = a\ ßin^2 + b\ ßin + c$

i^*	ß
7.8	60
7	50
5.8	67

a = -.0215
b = 2.447
c = 61.538

The blade shapes are those described by the tables with dimensions defined by this drawing

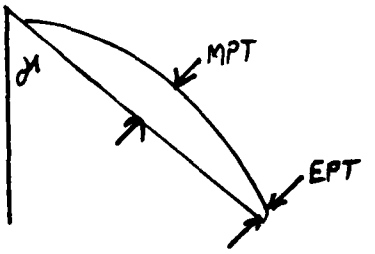

The zero camber blades are symetrical on the other side

The only exception is the first four sections in the first stage which do not have zero camber

Check depression factors, total pressure loss coefficient, cavitation index

First Stage

ßin	r	i	D	W	K
70	7.25	5.8	.08	.04(min)	____
60	4.6	8.35	.03	.028(min)	.05
50	3.4	3.7	.17	.029(min= .025)	1.6

Second Stage

ßin	r	i	D	W	K
67	7.25	5.8737	.09	.04(min)	____
60	5.2	7.95	.13	.028(min)	.5
50	3.2	7.06	.22	.04(min = .025)	.85

```
R=1.8
PRINT USING "&";"      r  ","   chord","    gamma","     ept","      mpt"
RPM=2100
 U=2*3.14*R*RPM/720
IF R>7.25 THEN R=7.25
S=2*3.14*R/4
C=1.5*S
BETIN=ATN(U/52.25)*57.3
VTHET=47.7/R
0 UDIF=U-VTHET
0 BETOUT=ATN(UDIF/52.25)*57.3
0 A=-.036
0 B=4.41
0 ISTAR=(A*BETIN^2)+(B*BETIN)-126.8
0 GAMMA=BETIN-ISTAR
0 IF ISTAR<0 THEN ISTAR=0
1 EDGEPT=.001*C
2 MIDPT=.05*C
0 PRINT USING "####.####";R,C,GAMMA,EDGEPT,MIDPT,ISTAR
0 IF R=7.25 THEN STOP
0 R=R+.4
0 GOTO 40
K

LIST  2RUN  3LOAD" 4SAVE" 5CONT 6,"LPT1 7TRON 8TROFF 9KEY   0SCREEN


0 IF R=7.25 THEN STOP
0 R=R+.4
  GOTO 40
K
RUN
   r     chord    gamma      ept       mpt
1.8000   4.2390  54.2649   0.0042   0.2120   0.0000
2.2000   5.1810  49.4491   0.0052   0.2591   0.0000
2.6000   6.1230  46.9531   0.0061   0.3062   0.0000
3.0000   7.0650  46.0794   0.0071   0.3533   0.3668
3.4000   8.0070  46.3014   0.0080   0.4004   3.7057
3.8000   8.9490  47.2387   0.0089   0.4475   5.8703
4.2000   9.8910  48.6253   0.0099   0.4946   7.1949
4.6000  10.8330  50.2787   0.0108   0.5417   7.9214
5.0000  11.7750  52.0752   0.0118   0.5888   8.2237
5.4000  12.7170  53.9325   0.0127   0.6359   8.2265
5.8000  13.6590  55.7962   0.0137   0.6830   8.0193
6.2000  14.6010  57.6315   0.0146   0.7301   7.6664
6.6000  15.5430  59.4163   0.0155   0.7772   7.2141
7.0000  16.4850  61.1375   0.0165   0.8243   6.6959
7.2500  17.0738  62.7880   0.0171   0.8537   6.1361
eak in 180
K

LIST  2RUN  3LOAD" 4SAVE" 5CONT 6,"LPT1 7TRON 8TROFF 9KEY   0SCREEN
```

```
 10 R=3.2
 25 PRINT USING "&";"   r   ","    chord","    gamma","     ept","     mpt"
 30 RPM=2100
 35    =2*3.14*R*RPM/720
 40 IF R>7.25 THEN R=7.25
 50 S=2*3.14*R/5
 60 C=1.5*S
 70 VTHET=47.7/R
 80 BETIN=ATN((U+VTHET)/61.733)*57.3
 90 UDIF=U-VTHET
 100 BETOUT=ATN(U/61.733)*57.3
 110 A=-.0215
 120 B=2.447
 130 ISTAR=(A*BETIN^2)+(B*BETIN)-61.538
 140 DIFF=BETIN-BETOUT
 150 GAMMA=BETIN-ISTAR
 151 EDGEPT=.001*C
 152 MIDPT=.05*C
 160 PRINT USING "####.####";R,C,GAMMA,EDGEPT,MIDPT
 170 IF R=7.25 THEN STOP
 180 R=R+.4
 190 GOTO 30
Ok

 1LIST   2RUN   3LOAD"  4SAVE"  5CONT  6,"LPT1 7TRON  8TROFF 9KEY    0SCREEN


 RUN
   -       chord     gamma      ept      mpt
     2000    6.0288  42.9269   0.0060   0.3014
    3.6000   6.7824  44.4817   0.0068   0.3391
    4.0000   7.5360  46.1602   0.0075   0.3768
    4.4000   8.2896  47.9092   0.0083   0.4145
    4.8000   9.0432  49.6866   0.0090   0.4522
    5.2000   9.7968  51.4601   0.0098   0.4898
    5.6000  10.5504  53.2064   0.0106   0.5275
    6.0000  11.3040  54.9090   0.0113   0.5652
    6.4000  12.0576  56.5569   0.0121   0.6029
    6.8000  12.8112  58.1434   0.0128   0.6406
    7.2000  13.5648  59.6648   0.0136   0.6782
    7.2500  13.6590  61.1811   0.0137   0.6830
Break in 170
Ok


 1LIST   2RUN   3LOAD"  4SAVE"  5CONT  6,"LPT1 7TRON  8TROFF 9KEY    0SCREEN
```

Appendix B

SMAT PROPULSOR DEVELOPMENT

The external mounting arrangement of the SMAT motors provides an ideal platform for the use of active multistage propulsors, since the rim-driven characteristics of each rotor essentially eliminates the complicated shafting and bearing requirements usually associated with contrarotating configurations. In general, the overall performance of these contrarotating propulsors is superior to that of equivalent size single stage designs or even rotor/stator systems, due to their inherent reductions in individual blade loading, and their ability to cancel swirl over a large portion of the operating range. In addition, the banded propellers associated with this rim-driven arrangement are free from the blade tip gap losses associated with normal propellers operating within a duct.

The improved performance of these contrarotating propulsors can translate to either a reduction in installed power for the same ship speed, a higher ship speed for the same installed power, or a reduction in propulsor size for the same installed power and ship speed. In an effort to quantify these performance characteristics, a preliminary parametric study was conducted on contrarotating propellers designed to operate within a cylindrical duct. For design purposes, the following performance requirements were defined:

Vehicle Speed = 18 MPH
Required Thrust = 4000 lbs/unit

At these conditions, variations in thruster performance were determined as a function of rotor diameter, shaft RPM, and duct induced velocity. During this initial study, all propulsor configurations were designed with an equal power split and an equal RPM split between the forward and aft rotors.

The results of this study are presented in Figures 1-3, where the total required power for each unit is shown as a function of duct inlet velocity ratio (IVR). Figure 1 shows the performance characteristics of 13.0 inch diameter propellers operating at 1700, 2100, and 2500 RPM respectively. The variation in propeller performance with rotation speed involves a trade-off between momentum losses and blade friction losses. Note that for any given mass flow (IVR), Figure 1 shows an overall increase in thruster performance (i.e. a decrease in required SHP) with decreasing RPM, indicating that blade efficiency is still being governed most heavily by frictional losses. In a non-dimensional sense, system performance is increasing with increasing propeller advance coefficient (J), where:

$$J = \frac{Va}{n*D}$$

Va = Axial velocity at the propeller plane (ft/sec)
n = Shaft rotational speed (rev/sec)
D = propeller diameter (ft)

The variation in thruster performance with changes in mass flow (IVR) involves a trade-off between propeller efficiency and duct drag. A duct that accelerates the inflow into the propeller

will also produce a portion of the total fixed system thrust. Both of these actions tend to decrease the rotor's momentum losses and increase efficiency. Unfortunately, increasing the duct internal velocity also increases the duct frictional drag, so that system performance eventually begins to decrease with increasing mass flow.

Superimposed on Figure 1 are lines of constant τ, where τ is defined as the ratio of total propeller thrust to total system thrust (propellers + duct):

$$\tau = \frac{\text{Rotor Thrust}}{\text{Rotor + Duct Thrust}}$$

Ducts designed for large values of τ (low IVR), will actually decelerate the inflow into the propeller, and generate a significant amount of drag. This situation may promote better cavitation performance, but only at the expense of overall system efficiency. As the value of τ decreases, the ducts begin to pick up some loading, and begin to accelerate the inflow into the rotors. As a result, propeller efficiency increases not only from the increased mass flow, but also from a reduction in the rotors' thrust requirement. When τ=1.0, the duct is generating just enough thrust to overcome its own drag. For values of $\tau < 1.0$, the duct is providing additional flow acceleration and is generating a larger portion of the total thrust. Propeller efficiency continues to increase with increasing mass flow, but eventually the duct viscous losses penalize the overall system efficiency. The duct thrust requirements at the higher mass flows may also impose a limit on the minimum allowable value of τ, such that the duct lift coefficients (CL) remain low enough to avoid flow separation.

Figures 2 and 3 show the parametric results for various 14.5 inch and 16.0 inch diameter rotors. Again, for any given IVR, the thruster efficiencies increase with decreasing RPM. The trends associated with changes in mass flow are also similar to those noted in Figure 1. A summary of the optimum thruster efficiency is shown in Figure 4, where minimum power requirements are shown as a function of propeller diameter for the three RPMs considered. As expected, thruster efficiency increases with increasing propeller diameter and decreasing shaft RPM. Unfortunately, these trends are usually opposite to those associated with the motor selection, which would tend to optimize its performance at the smallest diameter propellers and the highest RPMs.

At the onset of these parametric studies, it was recognized that the presence of significant cavitation at the propeller design point could heavily influence the performance characteristics of these thrusters. In an effort to optimize performance under cavitating conditions, the blade area for each rotor considered in this study was selected to maximize the section lift-drag ratios. This optimization involved a trade-off between blade frictional drag and section cavity drag. While blades with large area ratios showed a reduction in section lift coefficients (CL), and a corresponding reduction in cavity drag, they suffered from significant increases in frictional drag. On the other hand, blades with low EAR's showed a reduction in frictional drag, but yielded higher section CL's and higher cavity drags. For the high blade loading associated with the design point operating

conditions, the propellers appeared to yield their maximum performance at expanded area ratios of approximately 0.90.

By accepting the presence of cavitation at the propeller design point, individual blade sections can be designed to operate more efficiently at these conditions. While normal, fully wetted section shapes tend to suffer from thrust breakdown when subjected to increasing amounts of blade surface cavitation, transcavitating and/or supercavitating sections continue to generate lift even when their upper surfaces are entirely engulfed within a cavity. Although the required section shapes necessary to achieve reasonable performance under heavy cavitation often yield large frictional losses when operating fully wetted, their ability to sustain thrust under cavitating conditions results in a marked improvement in overall system performance.

Preliminary results from the motor development analyses indicate that the maximum propeller diameter for the present design is limited to 14.25 inches, and the minimum allowable propeller rotative speed is 2100 RPM. Based on the parametric results presented in Figures 1-4, the optimum IVR (mass flow) for this configuration is approximately 1.86, with a corresponding τ of 0.96. Thus, the optimum duct should be slightly accelerating in nature.

In an attempt to quantify the propulsor performance, a set of contrarotating propellers was developed for the above design point conditions. At this preliminary stage, it was assumed that the inflow into the propulsion unit was uniform, and that the unit itself was not operating at an angle of attack to the flow. In the future, a more detailed wake survey near the entrance to the thruster may reveal a significant wake deficit and/or sheared profile due to the vehicle hull and related boundary layer.

The major propeller design parameters (Diameter, RPM, and EAR) have already been selected from the motor parametric studies and blade surface cavitation criteria. The secondary design parameters (blade number, planform shape, radial load distribution, etc.) have only a minor effect on the hydrodynamic performance of the system, but may effect the acoustic and vibratory modes. Unfortunately, the optimization of these secondary parameters usually requires a detailed knowledge of the flow in the vicinity of each rotor. Since this information is not presently known, typical values for these parameters have been selected for this preliminary design.

Seven blades were selected for the forward propeller, and 9 blades for the aft rotor. This pairing of blade number should help minimize the noise and vibratory response to unsteady forces generated by the propellers. Each propeller was designed with a rectangular planform shape (constant section chord length), and with the radial load distributions shown in Figure 5a. Note that these banded propellers can carry finite loading all the way to the blade tips. The resulting pitch-diameter ratios for the two propellers are presented in Figure 5b. Although a nominal amount of blade skew was incorporated into each propeller, the rake due to skew was removed such that zero total rake was achieved for both designs.

Because the propeller blades associated with any of these rim-driven configurations are supported at both the root and tip, the

overall blade spanwise bending stresses are reduced in comparison to normal, non-banded propellers. As such, these rotors may be attractive candidates for composite material construction, thereby reducing machinery weight. For the present study, the blade thickness requirements for these designs were estimated from curved-beam theory, assuming that the propellers would be constructed from a typical production material such as aluminum or bronze. The recommended thickness-chord ratios for the forward and aft propellers are shown in Figure 6. If composite materials are considered for future manufacturing, then the blade thickness requirements should be re-evaluated. In any event, a finite element stress analysis should be conducted on the final designs.

The geometric and hydrodynamic characteristics of the forward propeller are presented in Table 1, and the projected and side views of the design are shown in Figures 7 and 8 respectively. Table 2 shows the principal characteristics of the aft propeller, while the planform views are presented in Figures 9 and 10. Note that the aft propeller must develop more thrust than the forward propeller in order to attain an equal power split between the two rotors, thus assuring nominal swirl cancellation. The total system thrust produced by the unit is 4000 lbs, with the propellers accounting for 3840.3 lbs, and the duct contributing only 159.7 lbs of thrust.

Typical transcavitating blade section shapes assumed for the propeller designs are shown in Figure 11, superimposed on the expanded outline of the blade. Note that the trailing edge camber incorporated into these section shapes results in improved performance under cavitating conditions, but that the blunt trailing edges will contribute additional drag at low speeds (fully wetted conditions). During this study, every attempt was made to account for the effects of these transcavitating sections on overall performance (including the production of cavity drag), such that the estimates provided in Tables 1 and 2 should be very realistic.

A schematic view of the propellers situated within the thruster unit is shown in Figure 12. For $r = 0.96$, the cylindrical duct will accelerate the inflow into the propeller, and its leading edge shape must be designed for shock free entry. Similarly, the duct trailing edge must diverge at a shallow enough angle to prevent flow separation. While the duct edge shapes shown in Figure 12 are representative of actual geometry, more definitive flow panelization codes (based on detailed wake survey data) should be run to determine the final duct profile.

TABLE 1

SMAT FORWARD PROPELLER CHARACTERISTICS

Diameter	14.25 inches
No. Blades	7
Expanded Area Ratio	0.90
Hub-Diameter Ratio	0.20
Rotation	Right Hand
Vehicle Speed	18.0 MPH
Rotative Speed	2100 RPM
Thrust	1796.6 lbs
Torque	500.2 ft-lbs
Power	200.0 SHP

TABLE 2

SMAT AFT PROPELLER CHARACTERISTICS

Diameter	14.25 inches
No. Blades	9
Expanded Area Ratio	0.90
Hub-Diameter Ratio	0.20
Rotation	Left Hand
Vehicle Speed	18.0 MPH
Rotative Speed	2100 RPM
Thrust	2043.7 lbs
Torque	500.2 ft-lbs
Power	200.0 SHP

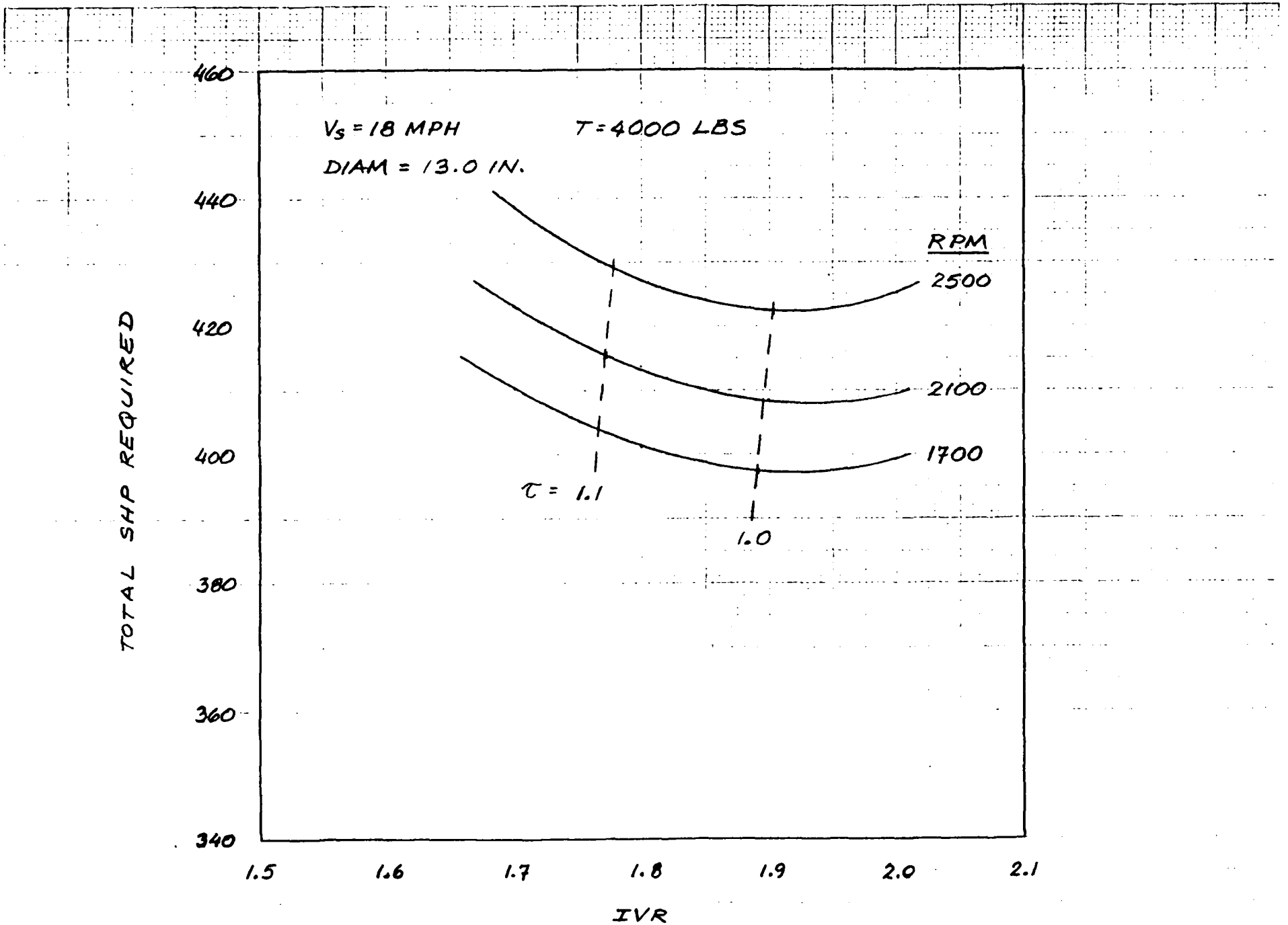

FIG. 1 REQUIRED POWER vs DUCT INLET VELOCITY RATIO (IVR) FOR 13.0 INCH DIAMETER PROPELLERS

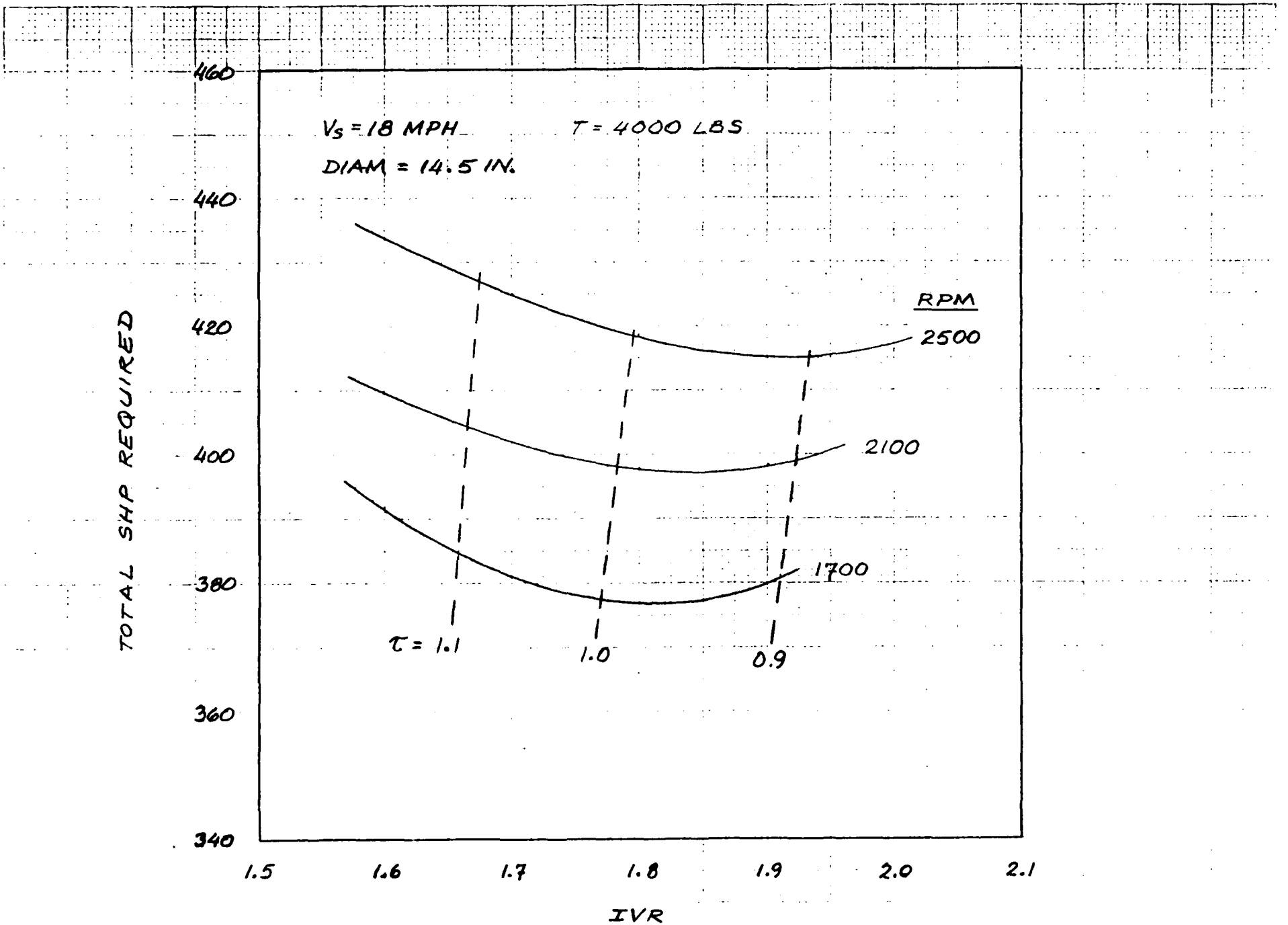

FIG. 2 REQUIRED POWER vs DUCT INLET VELOCITY RATIO (IVR) FOR 14.5 INCH DIAMETER PROPELLERS

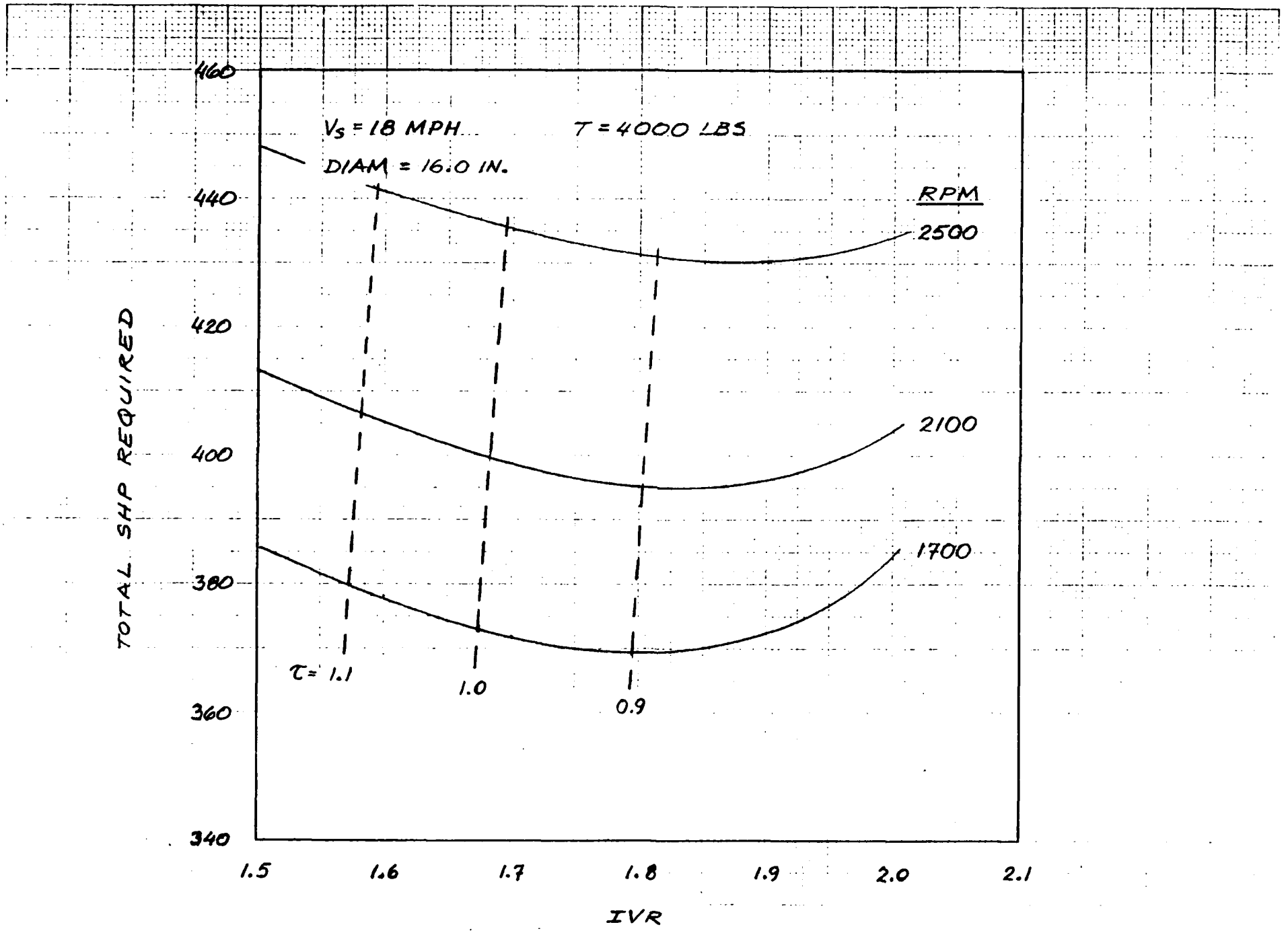

FIG. 3 REQUIRED POWER vs DUCT INLET VELOCITY RATIO (IVR) FOR 16.0 INCH DIAMETER PROPELLERS

FIG. 3

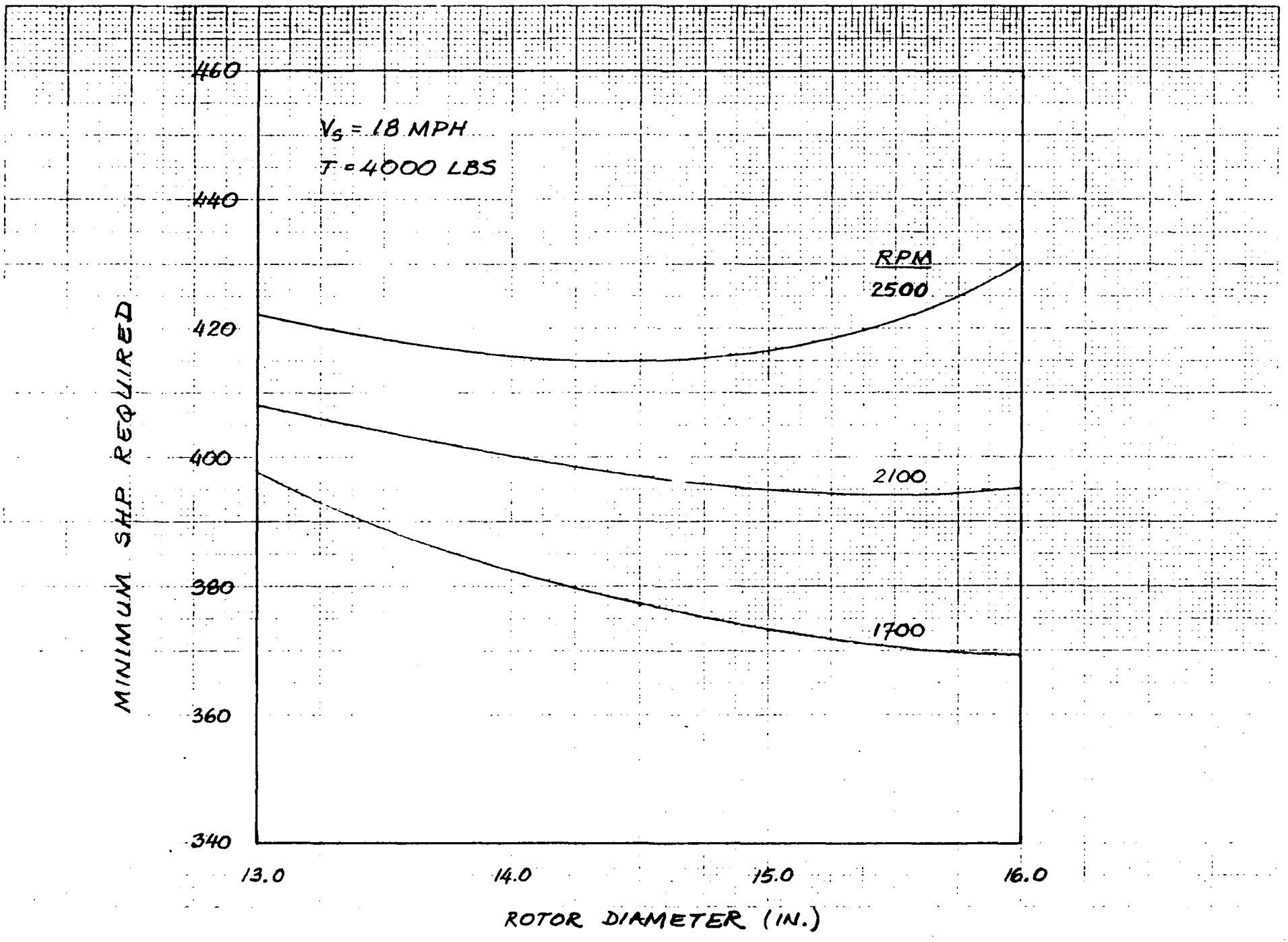

FIG. 4

FIG. 4 MINIMUM POWER REQUIREMENTS vs ROTOR DIAMETER

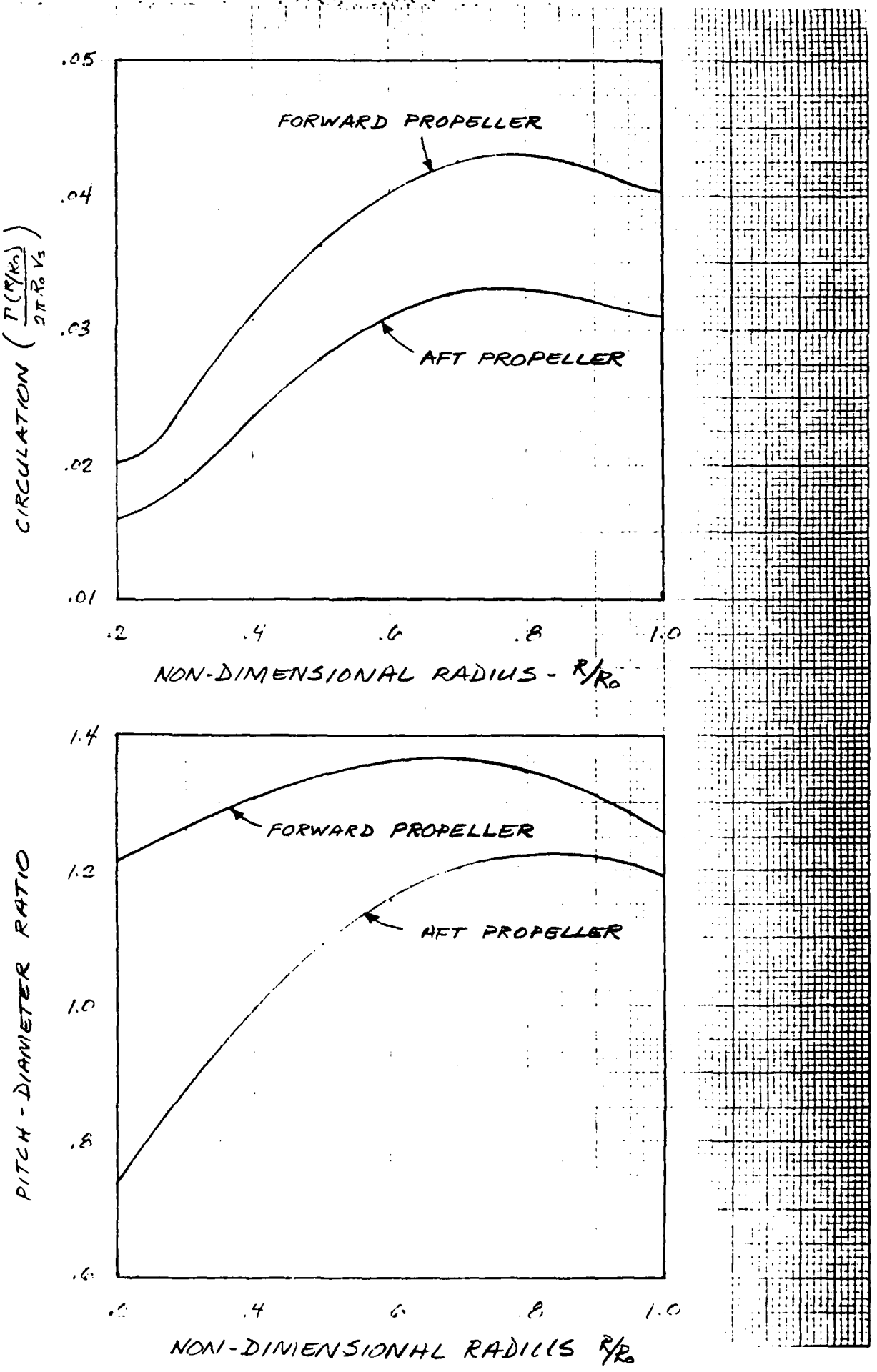

FIG. 5 BLADE LOADING AND PITCH DISTRIBUTIONS vs PROPELLER RADIUS

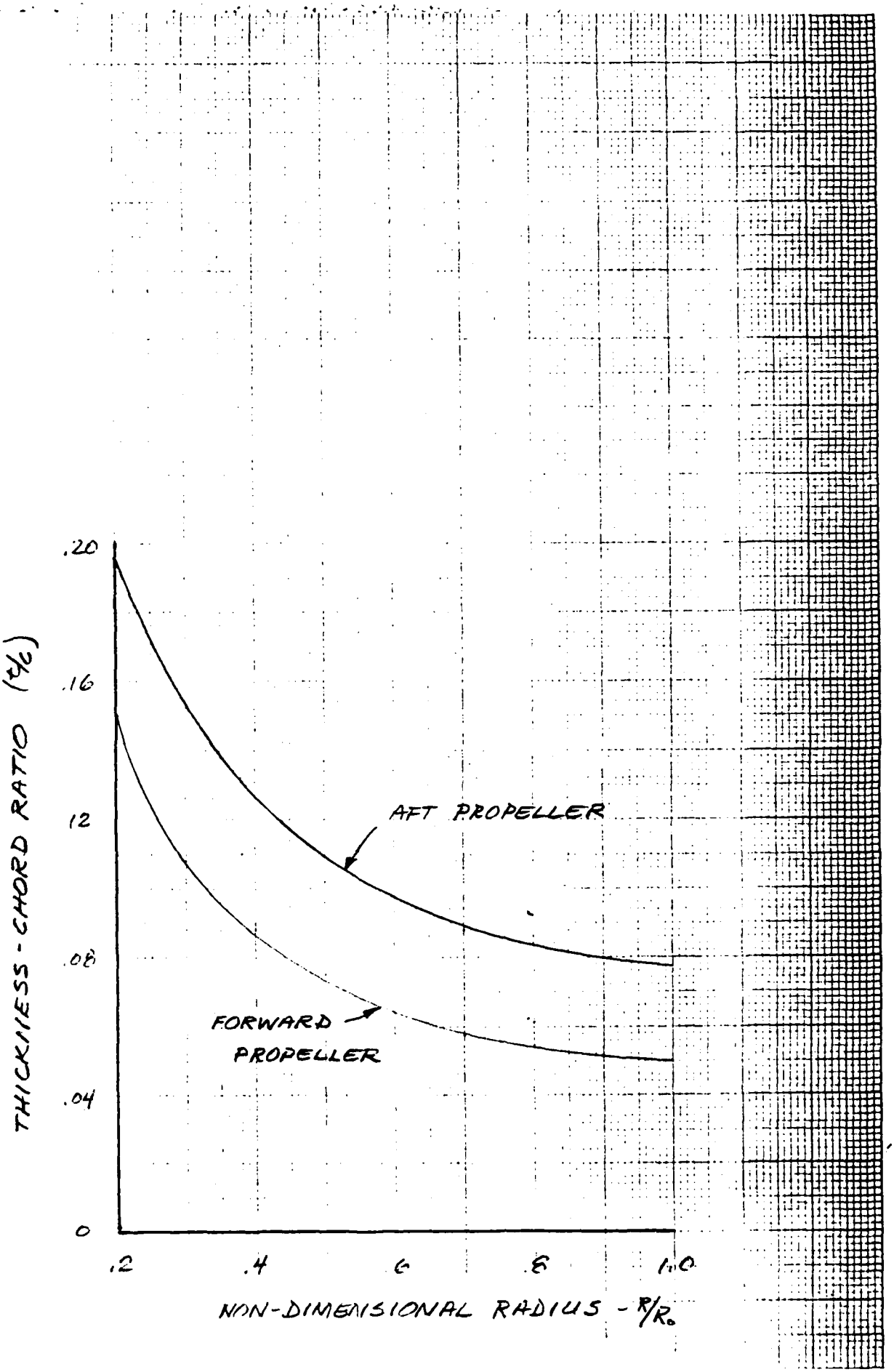

FIG. 6 BLADE THICKNESS DISTRIBUTION vs PROPELLER RADIUS

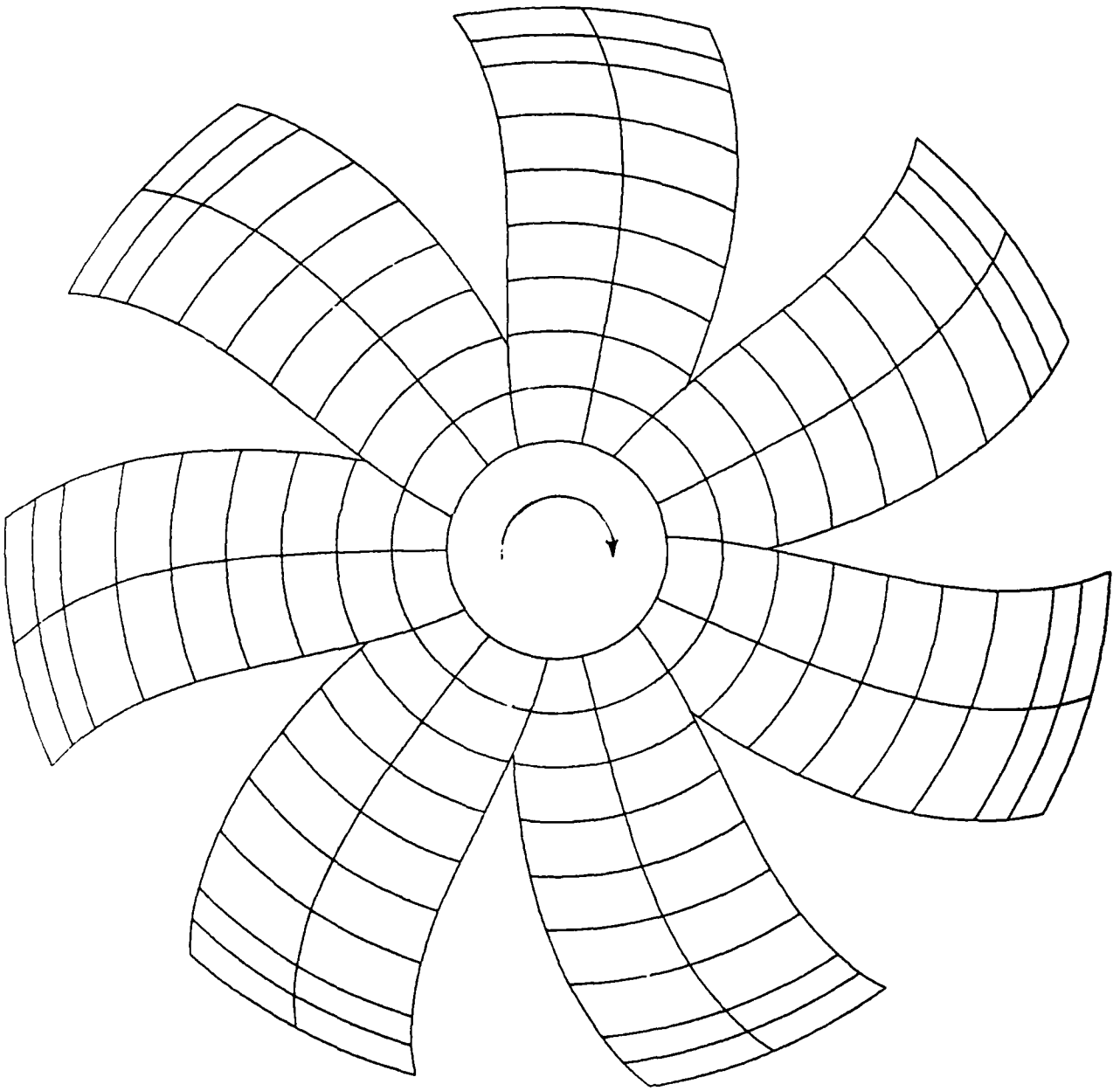

FIG. 7 PROJECTED VIEW OF FORWARD PROPELLER

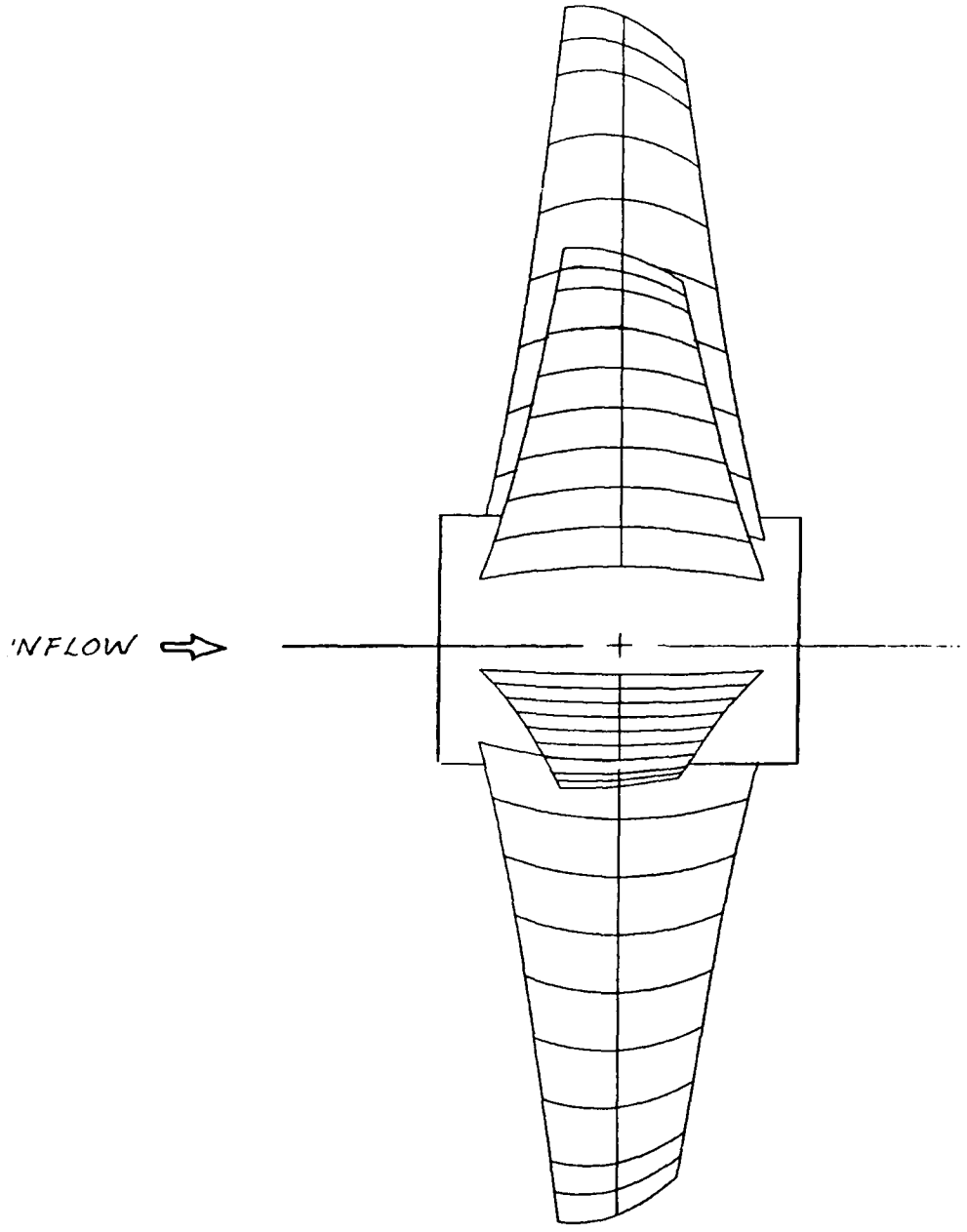

FIG. 8 SIDE VIEW OF FORWARD PROPELLER

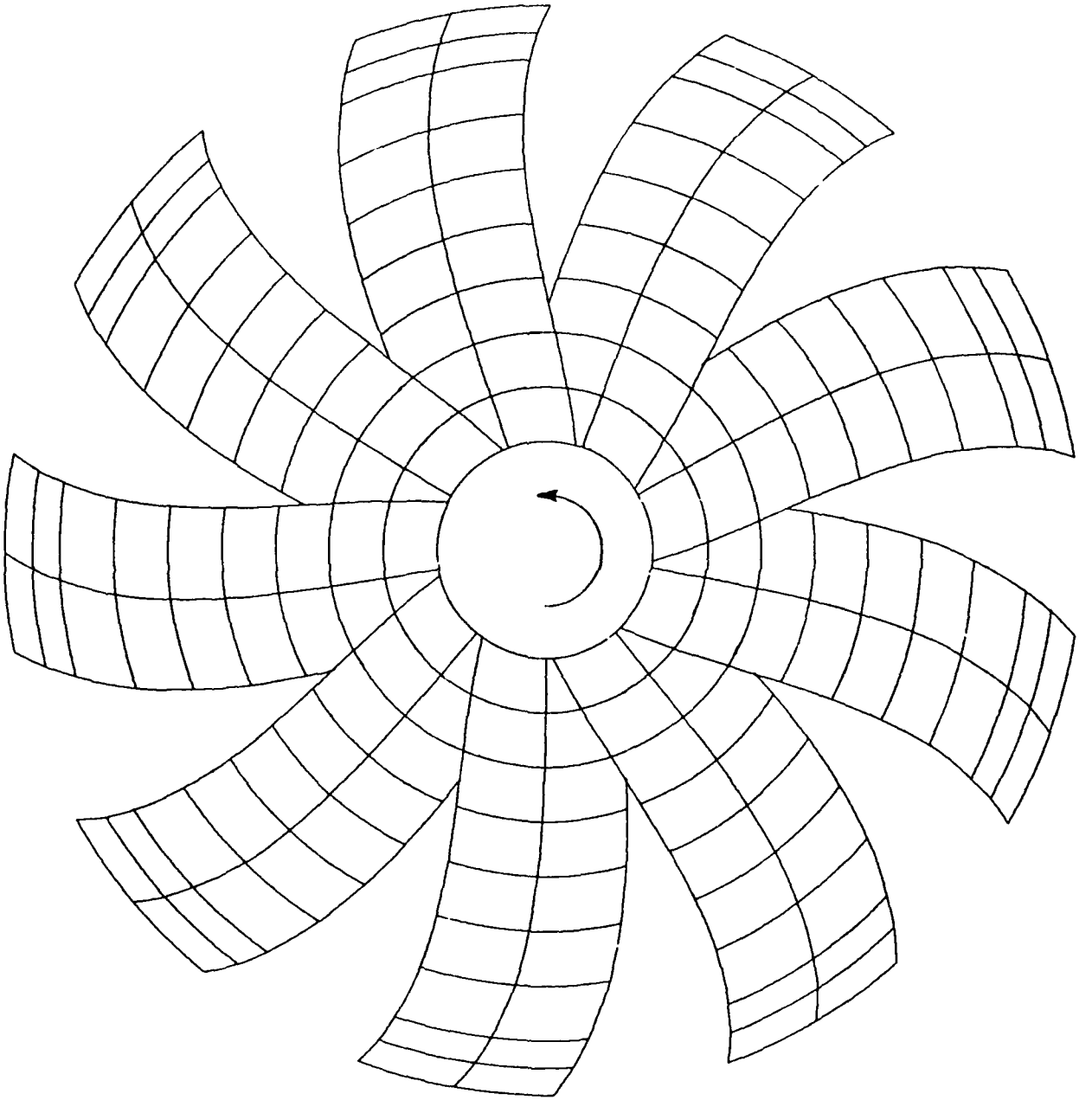

FIG. 9 PROJECTED VIEW OF AFT PROPELLER

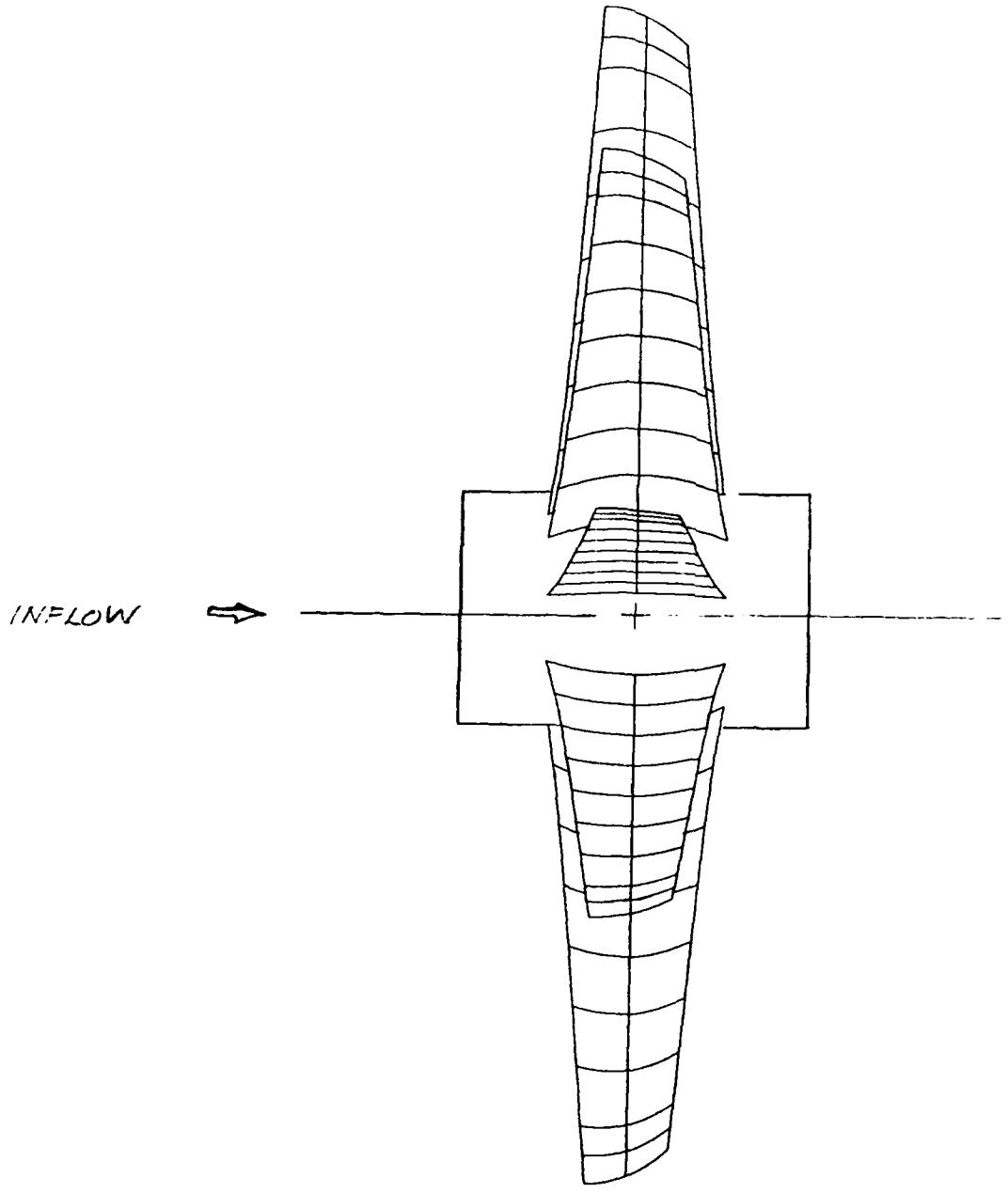

FIG. 10 SIDE VIEW OF AFT PROPELLER

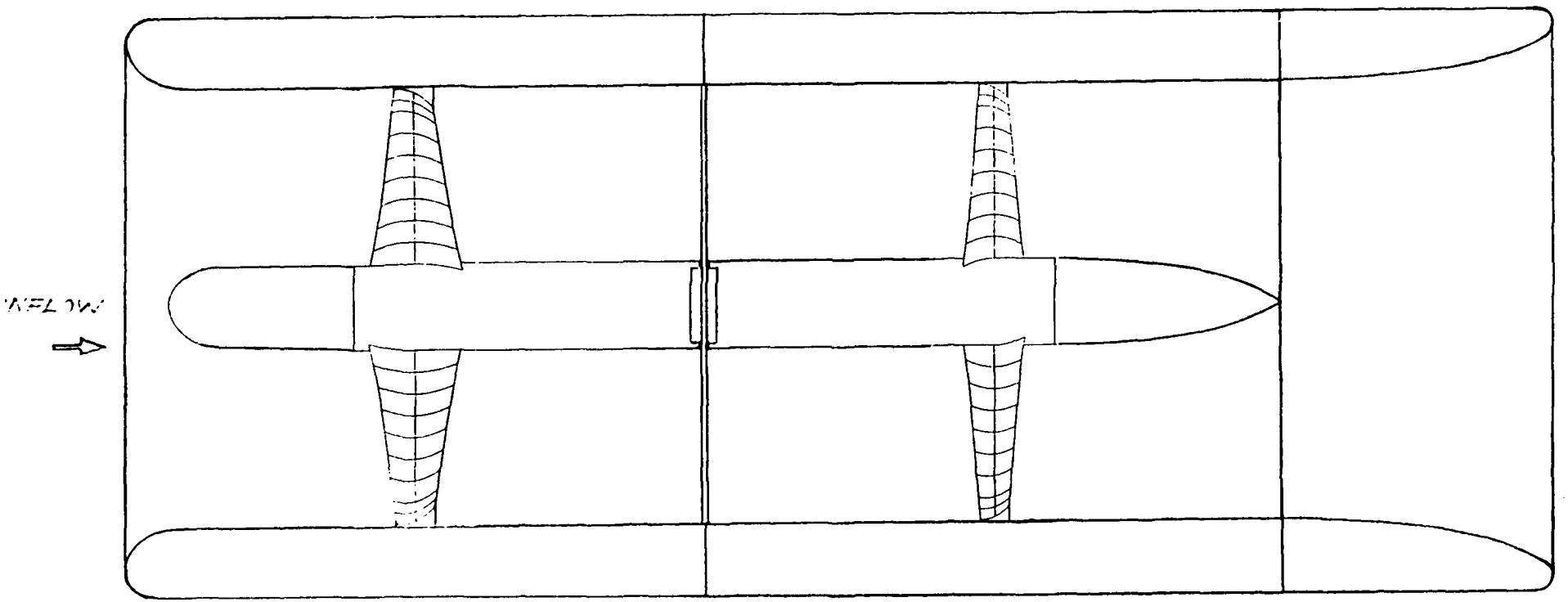

FIG. 11 SCHEMATIC OF THRUSTER UNIT

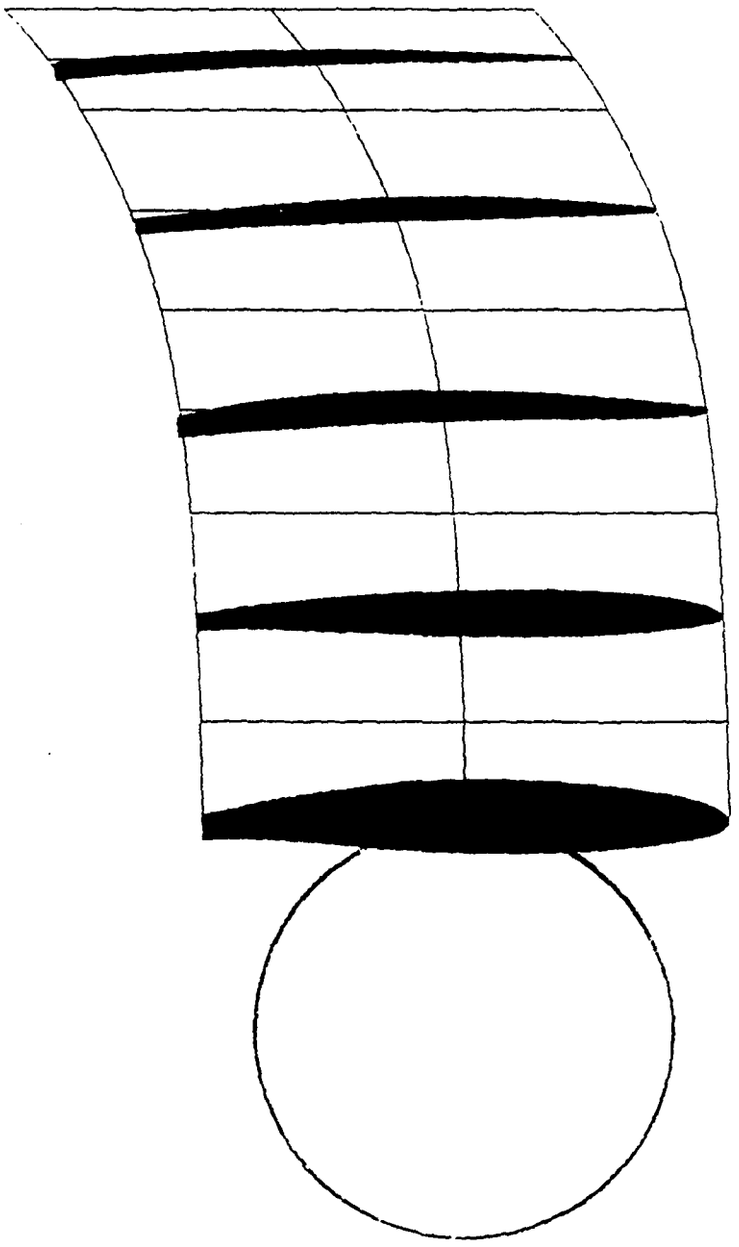

FIG. 12 EXPANDED PROPELLER VIEW SHOWING TYPICAL BLADE SECTION SHAPES

5555 Vantage Point Road
Columbia, Maryland 21044
17 April 1991

Ocean Systems Research
580 Bellerive Drive, Suite 5C
Annapolis, MD 21401

Attention: Mr. James W. White

Dear Jim,

As I mentioned to you on the telephone, I have amended the parametric study figures to reflect "pump" terminology. Basically, my IVR parameter is defined as: IVR = Va/Vo

where
Va = Velocity at the propeller plane
= Q/Ap
Vo = Free stream velocity
Q = Flow rate
= $\dot{m}/\rho$
Ap = Propeller disk area
$\dot{m}$ = Mass rate
ρ = Fluid density

As a result, my definition of IVR = $\dot{m}/(\rho*Ap*Vo)$ = Cm, which is the mass flow coefficient. Unfortunately, "pump" notation gives the following definition for IVR:

IVR = Vi/Vo

where Vi = Velocity at duct entry

Therefore, to be consistent with "pump" notation, I have changed the "IVR" to "Cm" on each graph. In addition, this same quantity (Cm) can be equated to the jet velocity ratio (JVR) by the following relationship:

JVR = 1 + CT/(2*Cm)

where
CT = Thrust coefficient
= Thrust/($\frac{1}{2}\rho*Vo^2*Ap$)

I enclose the same figures based on "JVR" instead of "IVR".

Because the thruster unit can no longer be considered as an isolated duct, the geometry of the diffuser will have to become more "pump-like", resulting in a smaller exit area than originally designed. I have included a schematic of the thruster showing this modified exit, but stress to point out that the propellers will now have to develop additional thrust (at reduced efficiency) to compensate for this new configuration.

Sincerely,

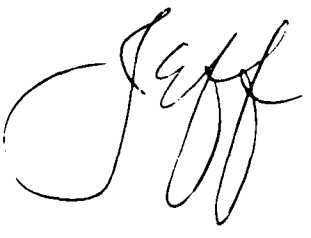

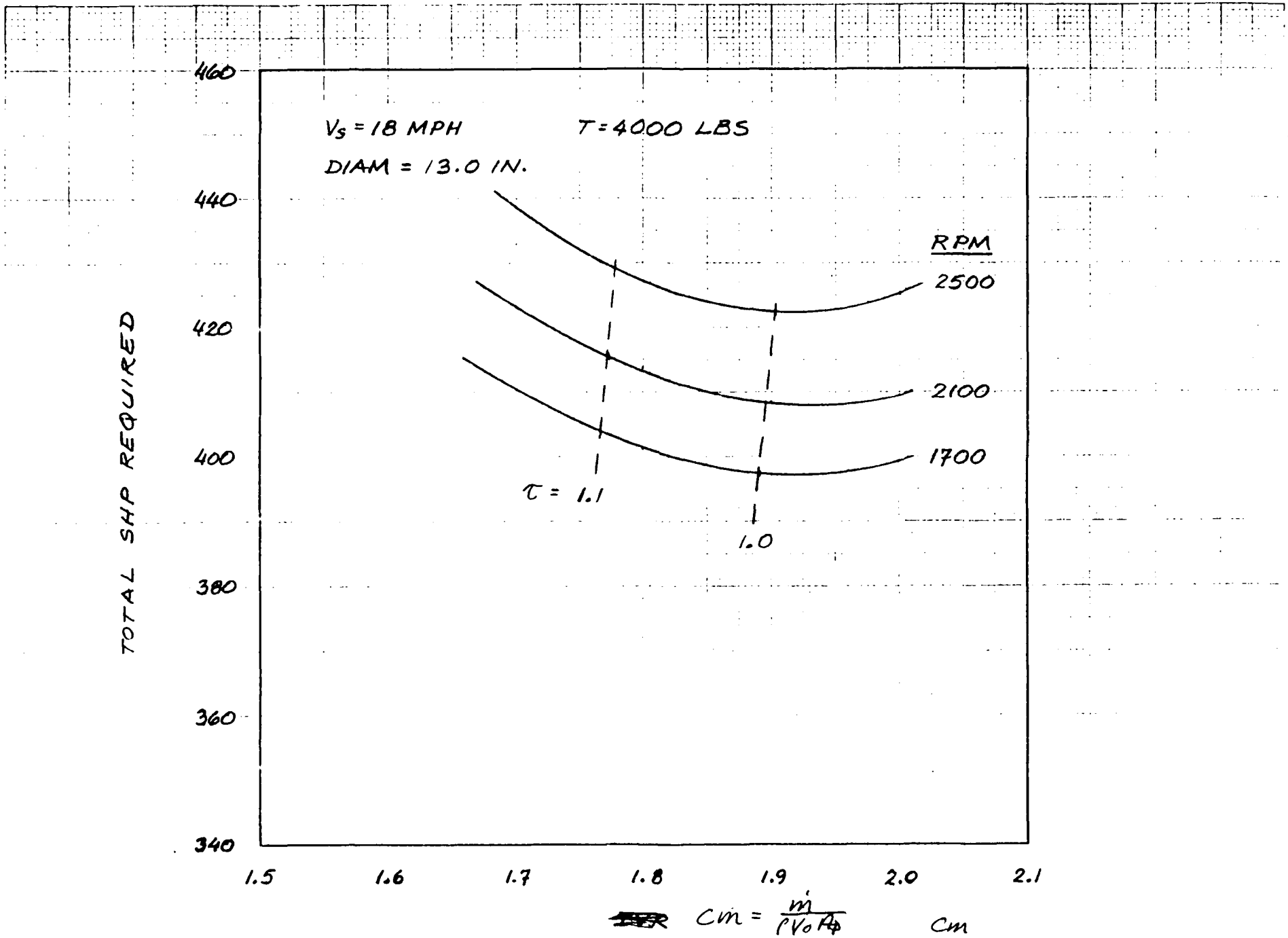

FIG. 1 REQUIRED POWER vs DUCT ~~INLET VELOCITY RATIO~~ (~~ER~~)
FOR 13.0 INCH DIAMETER PROPELLERS ↳ MASS FLOW COEFFICIENT

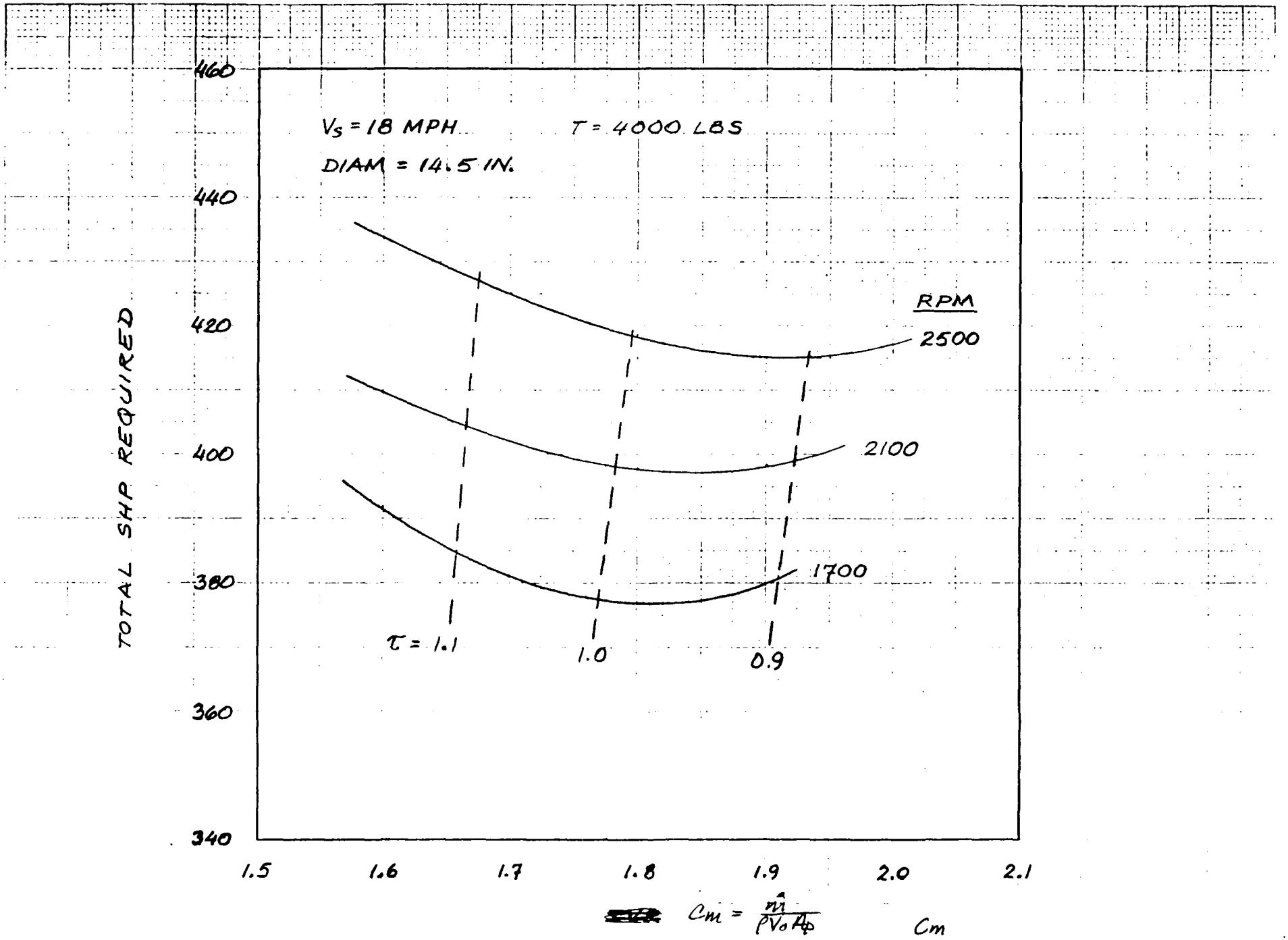

FIG. 2 REQUIRED POWER vs DUCT ~~INLET VELOCITY RATIO~~ ([redacted])
FOR 14.5 INCH DIAMETER PROPELLERS ↖ MASS FLOW COEFFICIENT

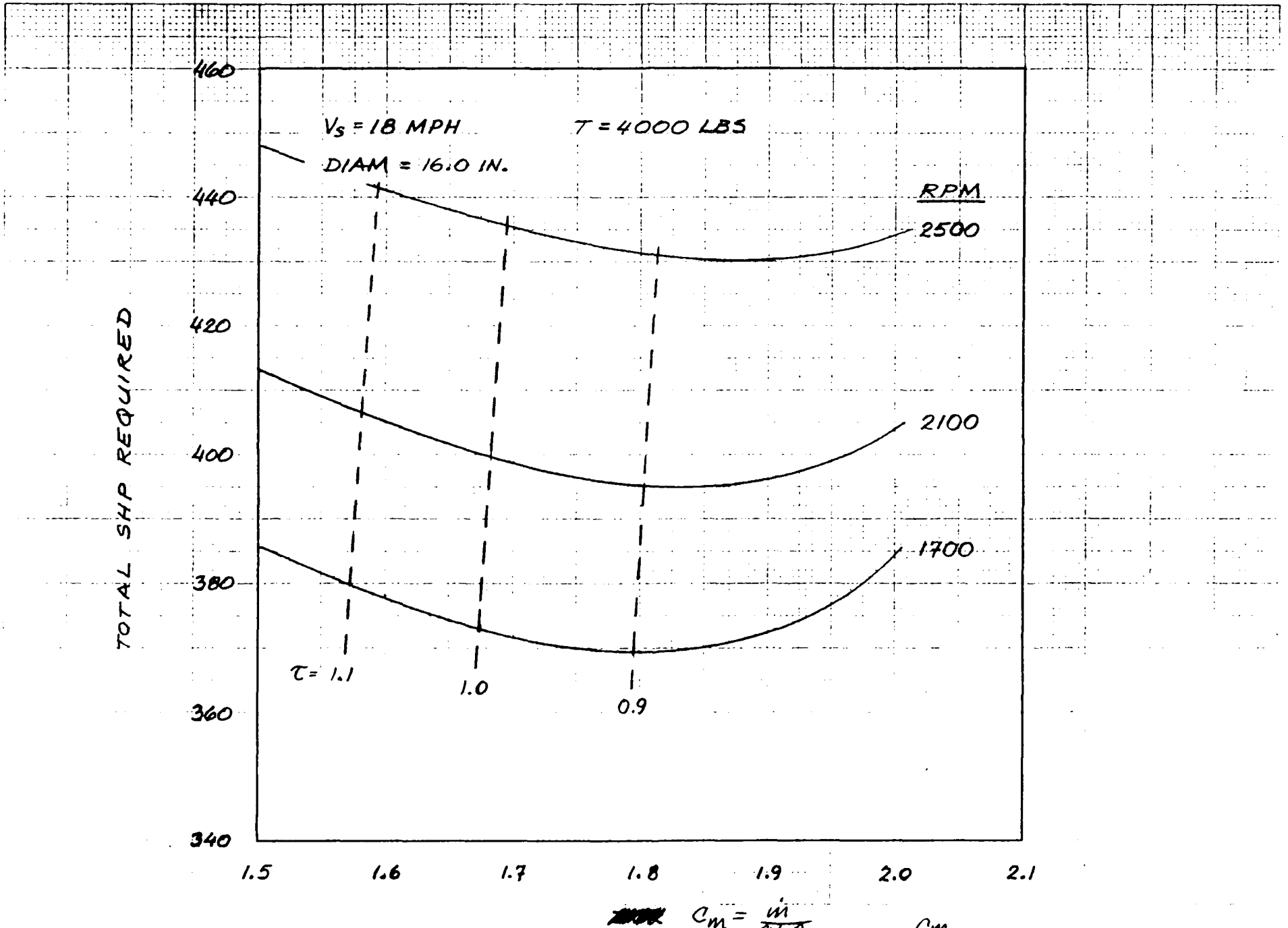

FIG. 3 REQUIRED POWER vs DUCT ~~INLET VELOCITY RATIO~~ (~~IVR~~)
FOR 16.0 INCH DIAMETER PROPELLERS

F16. 3

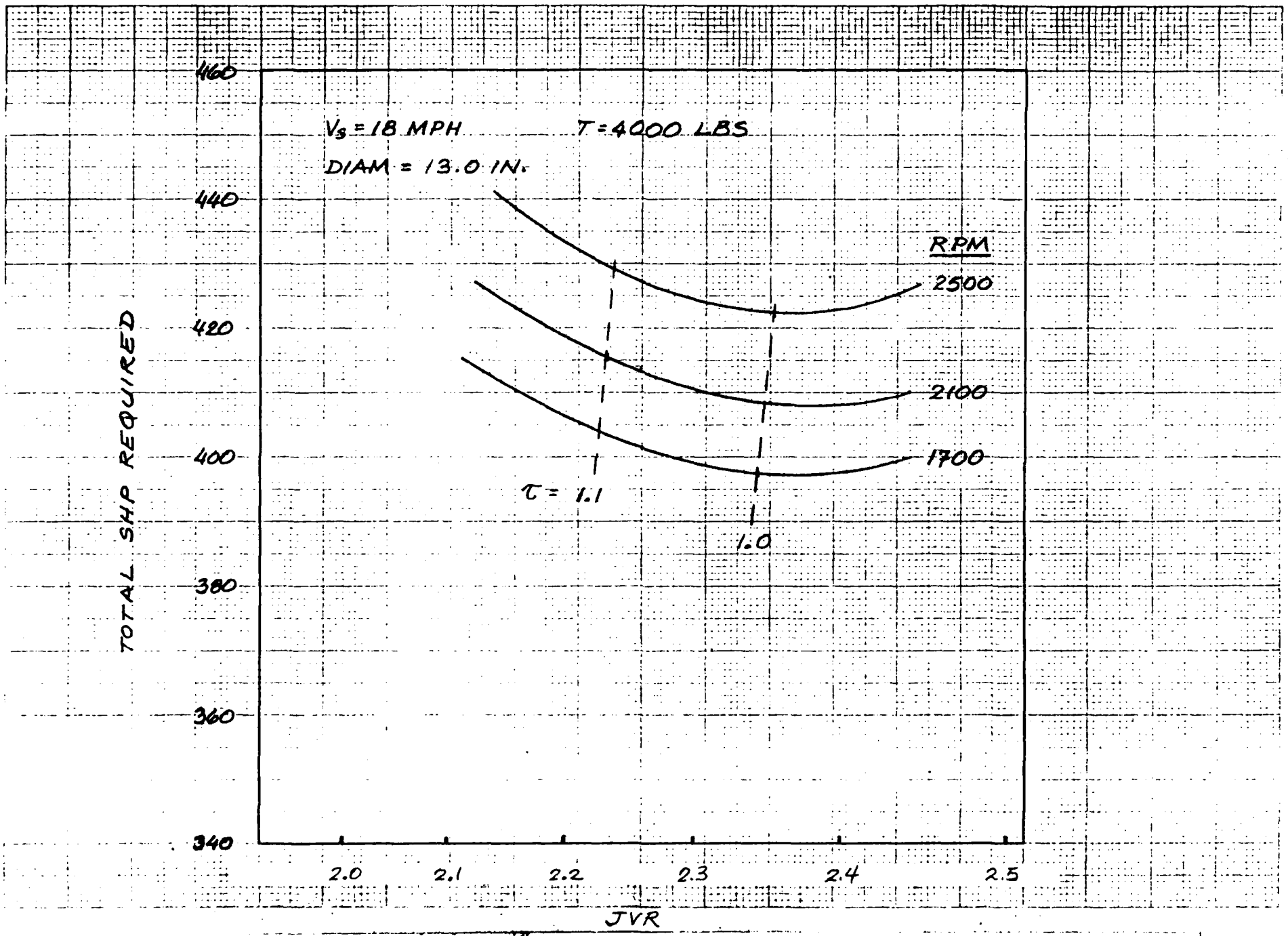

FIG. 1 REQUIRED POWER vs DUCT JET VELOCITY RATIO (JVR)
FOR 13.0 INCH DIAMETER PROPELLERS

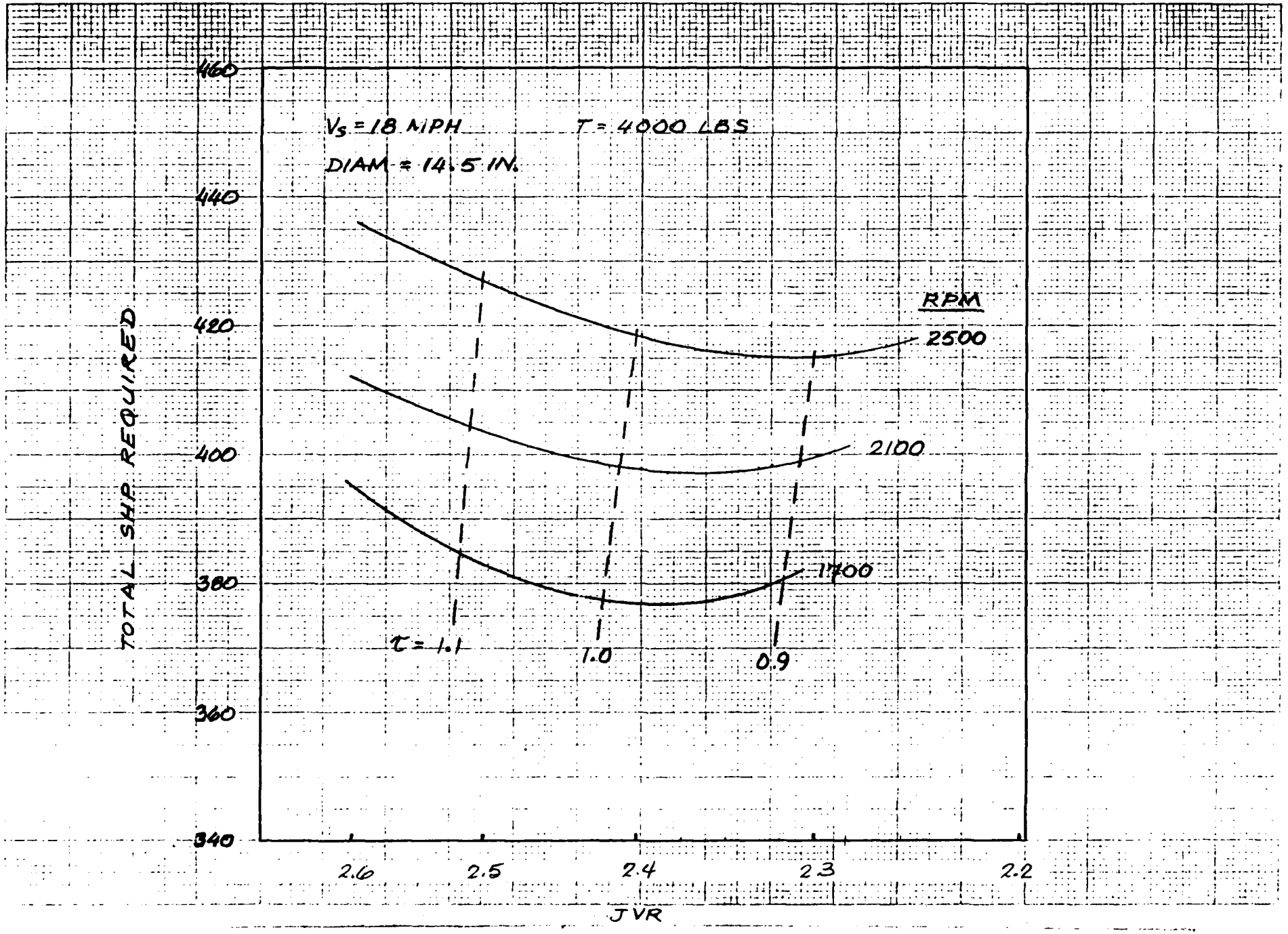

FIG. 2 REQUIRED POWER vs DUCT JET VELOCITY RATIO (JVR) FOR 14.5 INCH DIAMETER PROPELLERS

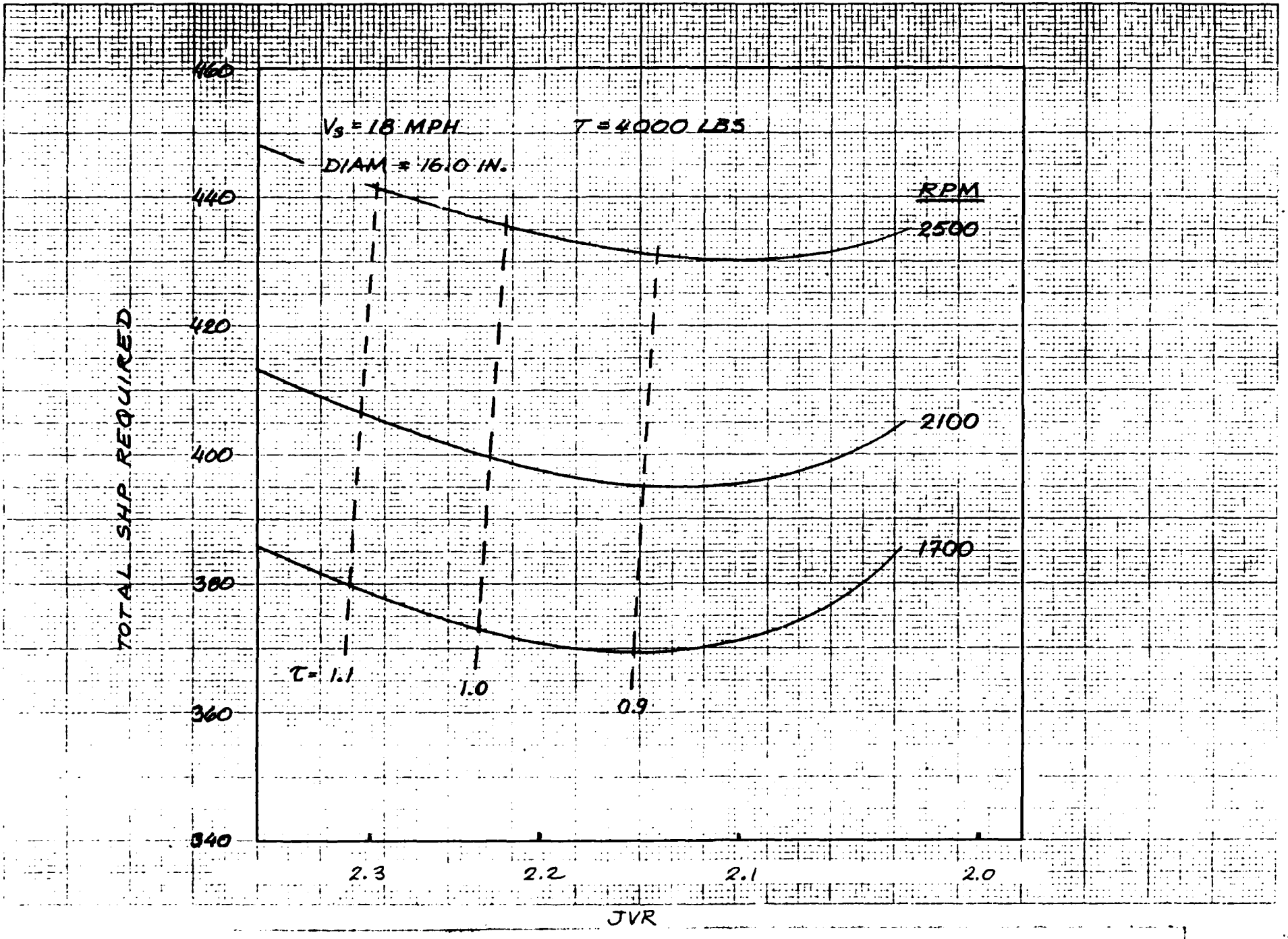

FIG. 3 REQUIRED POWER vs DUCT JET VELOCITY RATIO (JVR) FOR 16.0 INCH DIAMETER PROPELLERS

FIG. 3

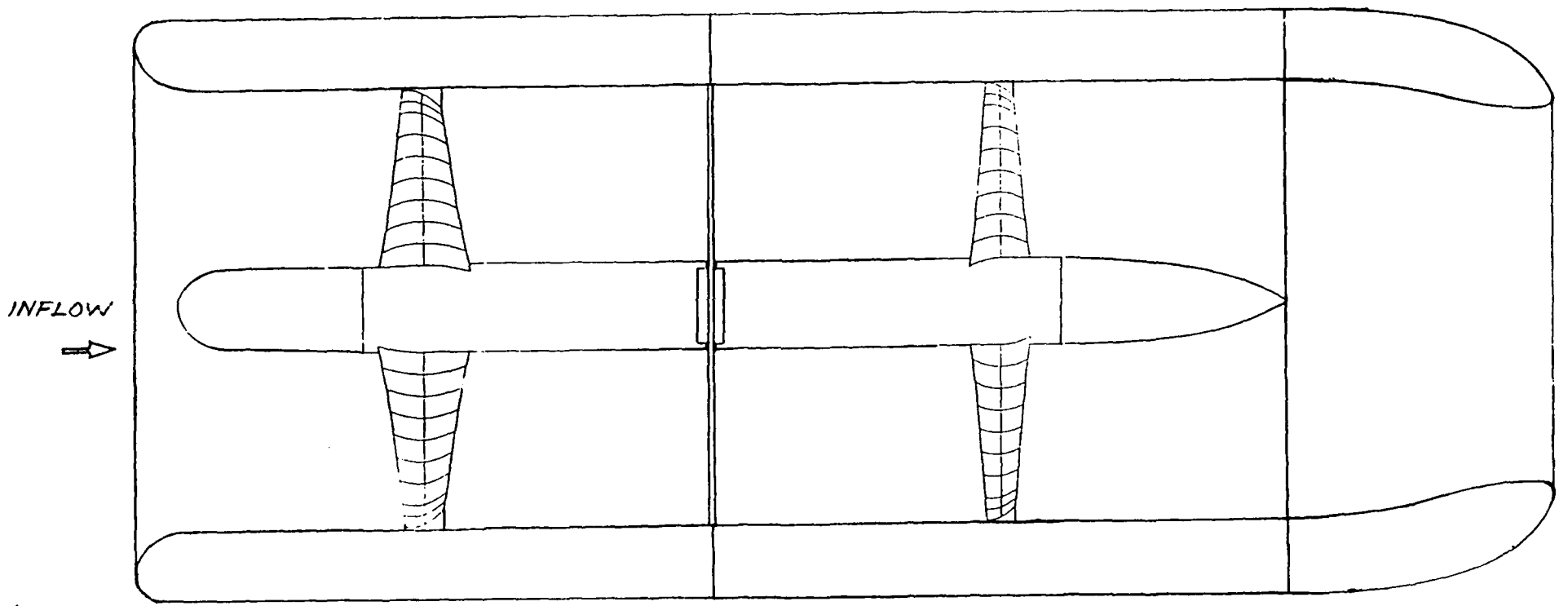

FIG. 11 SCHEMATIC OF THRUSTER UNIT

Appendix C

THRUSTER MOTOR STUDY DISCUSSION

SCOPE:

The work effort specified the following:

a) Determine the motor characteristics which allow for the largest possible stator lamination inside diameter (SID). Choose the optimum number of poles (p) and input frequency (f) by running various motor electrical designs [electrical specification sheets termed (ES)].

b) Provide estimated motor characteristics [(ES) sheets display such information]

c) Provide a discussion (this report) of ED findings including any necessary rationale. Provide verbal assistance as necessary to OSR etc.

BOUNDARY CONDITIONS:

OCR provided ED with preliminary information (both written and verbal) of system and parameter boundaries. Other sub-contractors worked with OCR to define optimum propeller characteristics etc. The sum of the preliminary information provided to ED and which was used as boundary conditions is as follows:

a) The motor outside diameter should be tried to be maintained at a maximum of 19.25" [this was taken to mean the frame outside diameter (FOD) and not the stator lamination outside diameter (SOD)].

b) The power supply frequency is capable of a range between 150 hertz (hz) minimum to 450 (hz) maximum.

c) The general synchronous speed (N_S) range of the motor should be between 1700 to 2500. Subsequently, verbal communication suggested that a motor speed of 2100 (rpm) appeared to be optimum from propeller design and performance aspects.

d) The motor rotor lamination inside diameter (RID) was to be as large as possible. Further, preliminary information provided indicated that the propeller outside diameter appeared to be optimum at about 14.5". Based on this input, ED set the motor rotor lamination inside diameter at 15.0".

e) Each motor rated horsepower (hp) was to be 200.

f) The operational time of the motor was not initially defined. Subsequently, ED was given a time of 30 minutes. The operational duty time is critical information for the losses in the motor and resulting temperature rise are limiting conditions.

g) The power supply "quality" was not defined. ED assumed that the supply waveform was sinusoidal at any frequency in the range specified. It was also assumed that individual harmonic

levels were that of conventional power supplies aboard surface or underwater vessels (or of such a magnitude that additional motor heating associated with high input harmonic levels are not present).

h) The motor "ventilation" was semi-defined. Seawater was delineated to be in contact with parts of the motor exterior (such as the motor frame). No internal motor parts are exposed to seawater. The motor interior was assumed to be "dead air". There is the possibility that the motor interior would be filled with oil. This could help motor cooling by improved heat transfer of associated losses. For purposes of this analysis, we assumed that the motor interior was "dead air". In essence, the ventilation was considered to be similar to that of a conventional totally enclosed, non-ventilated machine (or TENV) with the difference being water contact on the machine's exterior surfaces vs that of ambient air.

i) The intended application is of a nature that the motor design does not have to consider any considerations as to airborne (A/B) and structureborne (S/B) noise levels. Therefore, no inherent low noise design features are incorporated.

j) ED's effort is connected solely with that of a "partial" motor. That is, bearings and propeller considerations are not the responsibility of ED. It is understood that in either future study expansions or when possibly producing prototype hardware, that ED would necessarily have to interface etc with OCR and OCR's bearing and propeller sub-contractors.

RESULTING TYPE OF MOTOR DESIGN APPROACH:

From some of the boundary conditions imposed, the design of the motor would seem to warrant a "pancake" approach (short length, big diameter) when viewed from a (SID)/(RID) perspective. On the other hand, the unusually small radial height of the stator lamination [or a (SOD/(SID) view] would seem to require a design more of the "hot-dog" variety (increased length). In actually, the design might have to be adaptable to both features; length for the small lamination radial height and large (SID) to incorporate the propeller diameter.

In general, motor designs of a large diameter and short core length are more conducive to better overall machine performance versus those of a small diameter, long core variety. The reason for this is that motor output is a function of the diameter squared and length (active core) to the first power (or D^2L). The preliminary designs run are somewhere in between for the reasons mentioned.

GENERAL APPROACH:

Based on a conventional supply frequency of 60 (hz) and assuming a machine of 2 poles, a squirrel cage induction (SCI) motor would have a synchronous speed of 3600 as given by the following equation.

$$(1\text{-}1)\quad N_S = (120)\,(f) / (p)$$

For purposes of this discussion and illustration, assume that these parameters have defined a "base line machine". Now let's consider what increasing supply frequency does as we keep the number of poles (and all other constraints) fixed.

Increasing Supply Frequency With Poles Fixed:

As the supply frequency is increased above 60 hz and keeping the motor poles as 2 or fixed, the motor synchronous speed will rise in proportion to the frequency as given by (1-1).

There are two normal limitations of increasing supply frequency with fixed poles. These are:

a) The mechanical integrity of the rotating motor assembly as the speed is increased (note: this is not a factor for this application)

b) How much the input frequency can be raised before lamination "core" loss becomes so dominant as to restrict the magnitude of this variable. Prior experience with 400 (hz) motors indicates that this also is not a prime consideration in going from 60 to 400 (hz).

Therefore, for the subject application, the higher the input frequency within the given boundary range, the greater should be the machine output and/or the more accommodating to a smaller size.

A second consideration also adds to the benefit of increasing the supply frequency. As (f) is increased for a fixed horsepower and number of poles (with the winding pitch and distribution factors remaining about the same), the number of "effective turns" of the stator winding can be reduced as seen from the equation below:

$$(1\text{-}2)\quad \text{Total machine flux } (\phi) = (V)\,(k) / [(f)\,(N_1)]$$

In the above, (ϕ) is the machine flux, (f) the supply frequency, (N_1) the stator winding effective turns, (V) the per phase line voltage and (k) a constant.

To keep the machine flux about the same, a designer would normally decrease (N_1) in proportion to the increase in (f). Decreasing (N_1) or effective turns allows for more copper to be placed in a given stator slot. More stator per turn copper [for similar (hp) or ampere draw] leads to less stator copper loss and temperature rise and thus the machine output tends to be greater (or the machine size can be reduced for the same output).

Thus, increasing the supply frequency supports greater machine output (or reduced size) from two aspects. Now we'll examine the effect of increasing a machine's number of poles.

Increasing Poles With a Fixed Supply Frequency:

With the supply frequency fixed, increasing poles reduces the (SCI) motor synchronous speed (N_S) and normally lowers the output and/or increases the machine size (if only based on rotational speed ventilation considerations). The primary reason for this is that for a given enclosure or ventilation system, motor output is a function of:

$$(1\text{-}3)\quad \text{Motor HP} = (D)^2\,(L)\,(N_S)\,(B_g)\,(EL)\,(K)$$

where:

D = motor (SOD)

L = motor active core length

N_S = synchronous speed

B_g = air gap flux density

EL = the machine's electric loading (for example, the amps per inch squared or the current density in the stator conductors)

(K) = a variable dependent on machine insulation, ventilation design and capability etc

Since (N_S) will be lower for a fixed frequency as the poles increase, larger poles generally dictate a machine with a reduced output or of increased size and weight for a fixed output.

Thus, increasing both poles and supply frequency tend to be opposite forces which "push" the machine design and capability in divergent directions [the latter (f) reducing size and weight and the former (p) increasing these].

POLES AND FREQUENCY BOUNDARIES:

By using equation (1-1), boundary conditions (b) and (c) give the following range of potential motor poles:

(a) For a speed in the vicinity of 1700 (rpm) at the minimum and maximum input frequencies:

N_S	(f)	(p)
1800	150	10
1800	450	30

(b) For a speed toward the high range end:

N_S	(f)	(p)
2250	150	8
2454.+	450	22

Therefore, for a frequency range of 150 to 400 (hz) and a speed within 1700 to 2500 (rpm), the possible number of poles is 8 minimum and 30 maximum.

With the further guideline that (N_S) should be set at about 2100 (rpm), the poles that could be employed are as follows:

(p)	(f)	(N_S)
8	150	2250 (too far away from 2100)
10	180	2160
12		
14	250	2142.8+
16		
18	321	2140
22	392	2138.+
24	430	2150

In order to get an idea of the potential optimum frequency/pole combination, rough electrical designs were run at pole numbers of 8, 10, 14, 18, and 22 with the supply frequency set to give a (N_S) in the vicinity of 2100 (rpm). Since with 8 poles, the supply frequency at its minimum range yields a speed of 2250 (srpm), only one pass was made. The one design made at 8 poles gave very pessimistic results and therefore no other runs were made at this number of poles.

DESIGN (ES) APPROACH:

A series of rough designs were run at pole values of 10, 14, 18 and 22. Supply frequency was adjusted to give a synchronous speed slightly above the desired operating speed of 2100 (rpm).

Some up-front aspects considered were as follows:

a) Normally, high pole machines are more adaptable to very small lamination radial depth (both stator and rotor). For a given mechanical envelope [such as a frame size with a fixed (SOD)], the machine rotating diameter (ROD) will usually become larger with increasing poles. This comes about for several reasons among which are:

1) Ventilation (larger rotating diameter)
2) Lower air gap flux density
3) Less stator backiron is inherently required to support the stator core flux density
4) In general, improved machine electrical performance

Thus, higher pole machines lend themselves better to the boundaries given.

b) In the absence of noise design considerations, the tendency would be to push the air gap flux density very high (up to 60 to 65 kilolines/inch^2) and thus get "more output" (by lowering turns for the "push" and thus allowing more copper per turn). However, high pole machine power factor (and/or efficiency) tend to decrease markedly with increasing gap density resulting in increased full load current, stator winding copper loss, etc. And the small lamination radial height precludes using a "deeper" stator slot to negate this. Thus, the gap density cannot be optimized (or made as large as would be desirable).

c) High pole machines (as opposed to 2 or 4 pole units) are very sensitive to air gap radial magnitude. Similar to high gap density levels, the air gap radial length can play a large role in determining the machine's full load current. Air gap length and air gap flux density are the two dominant factors that determine the amount of magnetizing current required (normally very close to the so called motor no load current). Increased magnetizing current decreases full load power factor and the progression of more full load current, losses etc results.

Thus, although more poles is conducive to the thin radial lamination necessitated by the boundary conditions, air gap density would probably have to be lower than desired and the machine air gap made as small as mechanically possible to control the magnetizing current and the influence of this component on the full load ampere draw.

A further outcome expected from these two factors is that the machine design would tend to be "magnetically" weak. This means that starting torque, for example, would tend to be lower than that normally expected.

ROUGH ELECTRICAL DESIGNS RUN:

A series of potential 10 pole designs were the first concentrated runs made. As with all other preliminary designs that followed, the following was assumed:

SOD	19.00"
SID	16.75"
RID	15.00"

Air gap, active core length, and air gap flux density (B_g) were varied. Designs are shown in Appendix A. Some "key" values evaluated are:

Air gap per side	g
Air gap flux density	B_g
Net core length	L
Avg. stator teeth density	B_{St}
Avg. Stator core density	B_{sc}
Stator copper loss	I_1^2 (kilowatts)
Starting torque	T_s
Maximum torque	T_{po}
Full load power factor	PF
Full load efficiency	EFF
Stator winding weight	Wt

Subsequently, designs were run at 14, 18, and 22 poles with the air gap initially set as .060". A comparison of the results are indicated in the following tabulation:

poles #	g in	B_g kl/in^2	B_{ts} kl/in^2	B_{cs} kl/in^2	L in	T_s / T_{po} per unit	I_1^2 kw	PF / EFF	Wt lbs	Q_1
10	.060	28.1	115.5	108.7	12.5	.48 / 2.70	3.90	.867/.954	63.2	90
14	.060	35.6	122.5	98.5	12.0	.38 / 2.88	3.43	.745/.960	52.1	84
18	.060	35.6	114.5	109.9	12.0	.31 / 2.74	3.23	.626/.963	62.3	108
22	.060	35.7	114.2	109.8	12.0	.30 / 2.06	3.65	.556/.956	36.7	132

Although none of the designs run were "finalized", the tabulated data enables one to determine a trend. The observations are:

a) In spite of the air gap being maintained at the same value as poles were increased, stator copper loss was the lowest at 18 poles.

b) Full load power factor, as would be expected, decreased with increasing poles. This raised the current and made the stator copper loss higher than it would be if the air gap had been adjusted for different pole numbers.

c) Starting torque (in per unit of full load torque) did not vary appreciably between 14, 18,

and 22 poles and is very low in general.

d) Usually, the stator slot number goes up as the poles increase to keep the number of slots per pole per phase at an acceptable value. We deviated from this approach somewhat. However, note that as the stator slot number increases (with diameters not changing), there is a tendency for the slot to "shrink" in width to accommodate teeth magnetic densities. A point can be reached where the slot width (and height) get reduced to the point that the resulting slot area diminishes appreciably. When this occurs, the room in the slot to accept "ground" insulation becomes disproportionally large in comparison to the room "remaining" to insert the stator conductors. This problem can be alleviated (to some degree) by using fractional slot stator windings in lieu of integral slot windings [$(Q_1) / (3p)$ equals an integer].

Rough ES designs were then repeated except the air gap was now set at .040 and .050". The results of these design runs are:

poles	g	T_s / T_{po}	I_1^2	PF / EFF	g	T_s / T_{po}	I_1^2	PF/EFF
#	in	per unit	kw					
10	No design run was made							
14	.050	.34 / 2.76	3.08	.753/.962	.040	.28 / 2.55	3.12	.750/.961
18	.050	.28 / 2.67	2.80	.670/.965	.040	.24 / 2.54	2.43	.718/.966
22	.050	.28 / 2.05	3.12	.600/.959	.040	.26/ 2.00	2.65	.649/.962

Similar to the .060 air gap runs, the .050 and .040" air gap runs indicated that the optimum stator copper loss condition was at 18 poles.

Preliminary design runs at 14, 18, and 22 poles are contained in Appendix B, C, and D respectively (other runs were also made but are not included).

SPECIFIC COMMENTS:

As was somewhat expected from the earlier comments in this report, the motor performance should tend to improve with increasing frequency. The results turned basically followed this expectation. Thus, increasing frequency overcame the normal decrease in performance expected with increased poles. Increased pole number requires the air gap to be reduced accordingly as the tabulations clearly indicate.

Starting Torque:

As mentioned, starting torque is considered to be very low. This torque is low since:

a) The rotor slot depth and shape cannot (due to the "thin" lamination radial height) incorporate "deep bar" or "skin effect"

b) The air gap flux is lower than desired (weak machine magnetically)

c) As a result, the starting impedance is high and the starting current low

In order to evaluate the ability of a final motor design to accelerate the propeller, a speed versus load torque of the propeller should be made available. Also, any expected "line voltage" drop to the motor must be delineated. Having this information, ED can then determine the "acceleration" capability of any given final design.

We expect that the motor locked rotor torque (for any final pole/frequency combination) can be improved during the finalizing process.

Some knowledge of any variable introduced by the variable frequency generator must also be disclosed. For example, is the "source" preset at the desired frequency and voltage and the motor "thrown across the line" or does the variable frequency source "ramp-up" during the starting process?

Heating:

The temperature rise of the machine is a prime consideration. The present rough designs all have losses which appear to be too high for the motor to be run continuously given the "enclosure" assumed. The losses in conjunction with the ventilation system appear to be too high.

Normally, (TENV) machines are designed with as much surface area as possible (ribs added to outside surfaces) and the electric loading (EL) made as low as possible (usually no higher than 1.0 and more toward .5). All the designs run indicate (EL) values of about 3 or higher.

Therefore, there is little doubt that even the most optimum of the rough designs generated have losses that are too high to be able to rate the machine for continuous duty. The question is how long the machine can run under rated load with a class B (70 °C) or F (95 °C) temperature rise not being exceeded.

One way to establish this is to do a thermal heat transfer analysis. The contract funds did not allow for such a labor intensive study to be performed. And the designs, being of a rough and preliminary nature, do not warrant such an elaborate analysis at this time.

We briefly looked at the temperature rise of the 18 pole design with .040" air gap. In so doing, we used the approach normally used when estimating a machine's time capability under locked rotor conditions. In so doing, adiabatic (or no heat transfer conditions) are assumed and the

time capability is estimated as:

$$(1\text{-}4)\quad t = (^{\circ}C \text{ rise})\,(Wt) / [(5.65)\,(kw \text{ loss})]$$

where (°C rise) is a maximum rise assumed to be allowable, (Wt) the weight of the stator copper, (kw) the stator copper loss in kilowatts (without resistance compounding considerations) and (t) the time in seconds.

Design (C) in Appendix C gives:

$$t = (95)\,(62.3) / (2.43)\,(5.65) = 431 \text{ seconds} = 7.2 \text{ minutes}$$

As stated, this is a very conservative and "rough" analysis and not truely applicable to steady state conditions.

However, we can get a better feel for what the estimated (no heat transfer) 7 minutes might mean in real life by looking at the design and test of some (TENV) units rated for continuous duty. Some units designed and tested gave the following:

Unit	kw loss	Wt lbs	Calculated (t) for 95 °C rise	Rise on test after (x) hours	Final Data
25 (hp) @ 900	.328	170	145 minutes	20 °C (2.5 hrs)	37 °C rise (7.5 hrs)
30 (hp) @ 1200	.211	310	411 minutes	40 °C (7 hrs)	40 °C (9 hrs)
"	"	"	"	30 °C (2.5 hrs)	"

Both reference designs had a large amount of stator copper weight and used a 21.473" (SOD) with a (SID) of 13.20". From the above tabulation, one can get an appreciation of the extreme difference in estimated time to reach 95 °C for the rough 18 pole design versus some actual (TENV) units that were tested etc. As such, it appears that the 7.2 minutes calculated for one of the preliminary designs might translate to an actual time of 17 to about 80 minutes (to reach 95 °C rise) depending on which of the above references are used.

Thus, temperature rise versus 1 hour duty time appears to be at best marginal if (TENV) type of ventilation is assumed.

End Turn Lengths:

As the poles increase for approximately the same coil throw (pitch), coil end turn length gets smaller. As a result, the end turn length per side is about 2.25" for the 18 pole design and 3.5" for the 10 pole. This also suggests, that for the anticipated ventilation system, that the prime thermal heat transfer path will be from the coils embedded in the core slots radially to the steel backiron, to the frame, and then out to the surrounding seawater.

Backiron:

The backiron is relatively small to accommodate the total flux (about .325" for the 18 pole design with .040" air gap). Thus leaves an extremely limited amount of room available for any clearance between the stator coils outside diameter (and connections) and the frame inside diameter. The coils will have to be perfectly straight to be able to fit such a geometry situation.

Frame Thickness:

As roughed out, the (SOD) is 19.0 inches. Therefore, the 19.25" (FOD) cannot be satisfied. Even if the frame could be made to a radial thickness of .25" per side, this would leave the (FOD) at a minimum of 19.5". It does not look feasible to maintain a 19.25" diameter (FOD) unless the propeller diameter can be made smaller [while demanding no more than 200 (hp)] and/or the length of the machine can be increased. Both appear to be necessary. The frame thickness must be sufficient to support the stator core laminations and to accommodate screws necessary for attachment to motor housings etc. Also, the frame inside diameter must be sufficiently large to clear the stator coil outside diameter, winding connections and outgoing "cable".

The geometry boundaries appear to be such that they limit the design to such an extent that the 19.25" (FOD) cannot be met.

Core Loss:

It should be noted that the computer program used to estimate machine performance uses 60 (hz) core loss curves. Therefore, the core loss and machine efficiencies estimated are optimistic. Any final design would need to be re-evaluated for these effects by the use of another program with 400 (hz) type core loss "curves".

Lamination Radial Thickness:

The total lamination radial thickness dictated by the boundaries [(.5) (19.0 - 15.0) = 2.0"] is a major limitation and problem. For a stator and rotor backiron of .5" (to carry the flux and limit the core densities to acceptable values), the slot depths are limited to .5 " each. These are very small depth values; particularly for that of the stator slot. As a result. slot area is very small and the

necessary room to accommodate sufficient copper for 200 (hp) operation is severely restricted.

SUMMARY:

a) The optimum pole number seems to be at about 18 with associated frequency to obtain a speed slightly higher than 2100 (srpm). However, none of the preliminary 18 pole designs run are considered satisfactory.

b) The (FOD) of 19.25" cannot be maintained with an propeller (OD) of 14.5" and a (RID) of 15.0". The propeller (OD) must be somewhat smaller and the machine length increased.

c) Heating appears to be very marginal even for 1 hour operation at 200 (hp).

d) Room for stator coil connections and outgoing cable is very limited.

Both funded dollars and time did not allow us to proceed further with our evaluation. It should be obvious that much more study needs to be done to determine if a viable design can be obtained and that some boundary conditions relaxed in order to achieve the required output in a 19.25" (FOD). At this time, it does not appear that a viable design can be made to fit the boundary conditions given. The problem stems from 3 factors:

the envelope restictions
the rating of the motor
the ventilation (cooling) available

APPENDIX A

PRELIMINARY AND ROUGH 10 POLE DESIGNS

FORM-621

GENERAL DYNAMICS/ELECTRO DYNAMIC

A.C. INDUCTION MOTOR
DESIGN & ELEC. SPEC. SHEET

ENCL	H.P.	VOLTS	AMPS	SYN. R.P.M.	F.L. R.P.M.	PH.	CYC.	°C RISE	INS. CL.	DUTY	M/P # TYPE	DES.	CODE
	200.00	440		2160		3	180	70					

ROTOR VOLTS	ROTOR AMPS	BRUSHES PER SET & GRADE	ENGR.	APP'D	DATE	CUSTOMER	ORDER #
1.00 SF							200UCEAJ

	BLANK #	O.D.	I.D.	# SLOTS	SLOT-DIE ESA	SLOT SETTING	GROSS CORE	VENTS 3/8	NET CORE	CARTER FACTOR	GRADE STL.#24	AIR GAP
STATOR		19.700	16.750	90	1001 0		12.000	0	12.000	1.045	M-19	.0600
ROTOR		16.630	15.000	130	1028 25		12.000	0	12.000	1.026	M-19	

COIL WDG. DWG. #	TURNS PER COIL	WIRE SIZE	WIRE WT.	WIRE SIZE	WIRE WT.	WIRE AREA (IN²)	COILS PER GROUP	NET SLOT AREA	FULLNESS	PITCH	MLT	COIL DIMENSIONS ST	SPD	LOOP
STATOR	6	3 #14	75.5	0 # 0	0.0	.00766	3.0	0.214	77	8	44.2	14.0	3.9	20.2
ROTOR														

CONNECTION & CABLE

INS. SPEC #	CONN.	INTERNAL CONN DWG	EXTERNAL CONN DWG.	CABLES #	CABLES SIZE	LEADS #	LEADS VOLTS	R. LINE @25°C
								0.0460

NO. OF CORE PLATES: STATOR= 480 ROTOR= 480
ST. CORE STL WT= 123.5 LBS ROT CORE STL WT= 110.5 LBS

4750 / 5063 / 70

REMARKS-
~~VT1= 7.1 VC1= 42.3~~
BAR WT= 30.72 LB
ER(2)WT= 47.26 LB

ROTOR CAGE	BAR SIZE AREA	LENGTH	MATERIAL	END RING THICK	RAD. HT	MATERIAL	TRICKEY FACTOR	SKEW O.D.	ARBOR	FIXTURE	FABRICATED BAR DIMENSIONS (ACTUAL)	FAN #
	0.0585	12.00		0.5625	2.700		1.05				x x	

REFERRAL FACTORS	CONN	CKT	Nt	Kp	Kd	K damp	Φ fv MEGALINES	Bg fv KILOLINES	K1	K2	K3	Rer μ ohms	Rb μ ohms	Kr	Kx
		5	36	.940	.960	.63	0.98	24.4	0.075	0.563	97	6	142	1.11	.970

	λ OF ROT NECK OR BRIDGE	λ js	λ sr	HARMONIC LEAKAGE FACTORS	λ b	λ e	Btg fv (KILOLINES/in²)	Bw fv (KILOLINES/in²)	Bc fv (KILOLINES/in²)	AMPS per in²	A COND per in	ELEC LOADING (X10⁻³)	RING DENSITY
STATOR	—	—	0.903	.00903	0.428	0.687	114.5	113.9	109.8	4897	971	4.76	—
ROTOR	0.50	1.209	2.231	.00727	0.784	0.189	47.0	51.2	130.4	5647			813

PERFORMANCE	R1 ph @25°C	R2'r @25°C	R2'L @80°C	X1	X2'r	X2'L	Xm	Io	FL SLIP	PO SLIP	FLT lb. ft	°C RISE FL. THER	RXR
CALCULATED	0.0230	0.014	0.016	0.151	0.135	0.092	3.9	63.34	.0161	.0662	494.5		
TEST													

	EFFICIENCY 1/2	3/4	FL	1 1/4	1 1/2	POWER FACTOR 1/2	3/4	FL	1 1/4	1 1/2	LRA	LRPF	LRT (pu)	POT (pu)	PUT
CALCULATED	0.960	.955	.946	.939	.953	.808	.863	.876	.873	.616	1044	.157	0.33	1.92	1.18
GUARANTEE															
TEST															

FULL LOAD LOSSES	V AIR GAP	F. L. AMPS	SEC. CU @ °C	PRI. CU @ °C	F & W	CORE	STRAY	TOTAL
CALCULATED	292.7	236.52	2463	4750	550	515	373	8651
TEST								

TEST S.O. #
TEST
DATE

COMMERCIAL-

NO LOAD TEST

VOLTS	AMPS	WATTS

SURGE RING DWG-

10P

ROTOR ASSEMBLY-
ROTOR PLATE- 98

NAVY-
STATOR PLATE- 99

RING & FAN ASSEMBLY

LRT-BAR= 19.3 ST= 22 ER= 718

FRAME	CORE	TYPE	WDG.		POLES		REV

SHEET OF

P=10

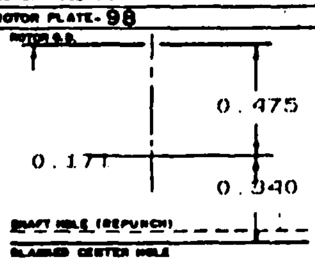

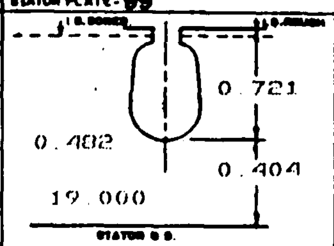

G.L. 131
C.L. 227
T.L. 158

FORM-621

GENERAL DYNAMICS/ELECTRO DYNAMIC

A.C. INDUCTION MOTOR DESIGN & ELEC. SPEC SHEET

ENCL.	HP	VOLTS	AMPS	SYN. R.P.M.	F.L. R.P.M.	PH.	CYC.	°C RISE	INS. CL.	DUTY	TYPE	DES.	CODE
	200.00	440		2160		3	180	70					

M/P #

ROTOR VOLTS	ROTOR AMPS	BRUSHES PER SET & GRADE	ENGR.	APP'D	DATE	CUSTOMER	ORDER #
1.00 SF							2000CEAR

	BLANK #	O.D.	I.D.	# SLOTS	SLOT-DIE E&A	SLOT SETTING	GROSS CORE	VENTS 3/8	NET CORE	CARTER FACTOR	GRADE STL. #24	AIR GAP
STATOR		17.000	16.750	90	1001 0		12.500	0	12.500	1.045	19	.0600
ROTOR		16.630	15.000	130	1028 25		12.500	0	12.500	1.026	19	

COIL WDG. DWG. #	TURNS PER COIL	WIRE SIZE	WT.	SIZE	WT.	WIRE AREA (IN²)	COILS PER GROUP	NET SLOT AREA	FULL-NESS	PITCH	MLT	COIL DIMENSIONS ST	SPD	LOOP
STATOR	4	2 13	40.2	0 0	0.0	00814	3.0	0.120	78	8	41.9	14.5	3.9	10.8
ROTOR														

CONNECTION & CABLE

INS. SPEC #	CONN	INTERNAL CONN DWG.	EXTERNAL CONN DWG.	CABLES #	SIZE	LEADS #	VOLTS	R. LINE @25°C
								0.0345

$\frac{4059}{40.2} = 100.97$

NO. OF CORE PLATES STATOR= 500 ROTOR= 500

ST CORE STL WT= 166.6 LBS ROT CORE STL WT= 115.1 LBS

REMARKS-

~~VT1= 10.6 VE1= 42.3~~

BAR WT= 31.94 LB

ER(2)WT= 47.26 LB

ROTOR CAGE	BAR SIZE AREA	LENGTH	MATERIAL	END RING THICK	RAD. HT	MATERIAL	TRICKEY FACTOR	SKEW O.D.	ARBOR	FIXTURE	FABRICATED BAR DIMENSIONS (ACTUAL)	FAN #
	0.0585	12.50		0.625	2.700		1.05				x x	

REFERRAL FACTORS	CONN	CKT	Kt	Kp	Kd	K damp	Φ fv MEGALINES	Bg fv KILOLINES	K1	K2	K3	R er p ohms	R b p ohms	Kr	Ks
	1	5	24	.940	.960	.63	1.47	35.1	0.035	0.563	43	6	140	1.11	.970

	λ OF ROT NECK OR BRIDGE	λ sL	λ sr	HARMONIC LEAKAGE FACTORS	λ h	λ e	Bfg fv	Btr fv	Bc fv	AMPS per in²	A COND per in.	ELEC LOADING (x 10⁻⁶)	RING DENSITY
STATOR	—	—	0.831	.00903	0.420	0.539	114.3	114.9	109.9	6203	691	4.29	—
ROTOR	0.50	1.209	2.231	.00727	0.786	0.182	67.7	73.7	187.8	3587			516

(Bfg, Btr, Bc in KILOLINES/in²)

PERFORMANCE	R1 ph @25°C	R2'r @25°C	R2'L @25°C	X1	X2'r	X2'L	Xm	Io	FL SLIP	PO SLIP	FLT ft lb	°C RISE FL THER	RKR
CALCULATED	0.0172	0.007	0.007	0.062	0.062	0.042	1.9	30.34	0063	0696	490.3		
TEST													

	EFFICIENCY 1/2	3/4	FL	1 1/4	1 1/2	POWER FACTOR 1/2	3/4	FL	1 1/4	1 1/2	LRA	LRPF	LRT (pu)	POT (pu)	PUT
CALCULATED	0.955	.958	.957	.955	.933	.611	.742	.812	.838	.877	2387	.228	0.80	4.10	1.11
GUARANTEE															
TEST															

FULL LOAD LOSSES	V AIR GAP	F.L. AMPS	SEC. CU @ °C	PRI. CU @ °C	F&W	CORE	STRAY	TOTAL
CALCULATED	240.7	252.47	1033	4059	550	812	373	6826
TEST								

TEST S.O. #

TEST

DATE

COMMERCIAL-

NAVY-

NO LOAD TEST

VOLTS	AMPS	WATTS

SURGE RING DWG-

10P

LRT-BAR= 7.3 ST= 3 ER= 394

ROTOR ASSEMBLY-

ROTOR PLATE- 98

STATOR PLATE- 99

RING & FAN ASSEMBLY

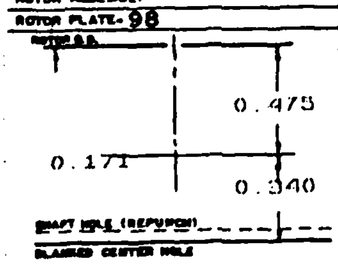

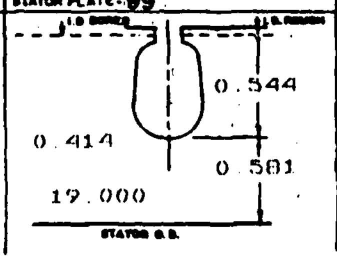

S.L. 316

C.L. 337

T.L. 158

FRAME	CORE	TYPE	WDG.			POLES	REV.

SHEET OF

P=10

FORM-621

GENERAL DYNAMICS/ELECTRO DYNAMIC
A.C. INDUCTION MOTOR
DESIGN & ELEC. SPEC. SHEET

M/P #

ENCL.	H.P	VOLTS	AMPS	SYN. R.P.M.	F.L. R.P.M.	PH.	CYC.	°C RISE	INS. CL.	DUTY	TYPE	DES.	CODE
A	200.00	440		2160		3	180	70					

ROTOR VOLTS	ROTOR AMPS	BRUSHES PER SET & GRADE	ENGR.	APP'D	DATE	CUSTOMER	ORDER #
1.00 SF							2000CEAC

	BLANK #	O.D.	I.D.	# SLOTS	SLOT-DIE ESA	SLOT SETTING	GROSS CORE	VENTS 3/8	NET CORE	CARTER FACTOR	GRADE STL. #24	AIR GAP
STATOR		12.000	16.750	90	1001 0		12.500	0	12.500	1.045	M-19	.0600
ROTOR		16.630	15.000	130	1028 25		12.500	0	12.500	1.026	M-19	

COIL WDG. DWG. #	TURNS PER COIL	WIRE SIZE	WIRE WT.	SIZE	WT.	WIRE AREA (in²)	COILS PER GROUP	NET SLOT AREA	FULLNESS	PITCH	MLT	COIL DIMENSIONS ST	SPD	LOOP
STATOR	1	12 #3	63.2	0 # 0	0.0	04884	3.0	0.177	79+	8	43.2	14.5	3.9	19.2
ROTOR														

INS. SPEC. #	CONNECTION & CABLE: CONN.	INTERNAL CONN DWG	EXTERNAL CONN DWG.	CABLES #	CABLES SIZE	LEADS #	LEADS VOLTS	R LINE @25°C
								0.0376

3900 / 63.2 = 61.7

10 Poles

NO. OF CORE PLATES STATOR= 500 ROTOR= 500

ST CORE STL. WT= 183.0 LBS ROT CORE STL. WT= 115.1 LBS

REMARKS-

VT1= 0.5 VC1= 0.5

BAR WT= 31.24 LB

ER(2)WT= 47.26 LB

ROTOR CASE	BAR SIZE AREA	BAR SIZE LENGTH	BAR SIZE MATERIAL	END RING THICK	END RING RAD. HT	END RING MATERIAL	TRICKEY FACTOR	SKEW O.D.	SKEW ARBOR	SKEW FIXTURE	FABRICATED BAR DIMENSIONS (ACTUAL)	FAN #
	0.0585	12.50		0.625	2.700		1.05				X X	

REFERRAL FACTORS	CONN	CKT	N1	Kp	Kd	K damp	Φ fv MEGALINES	BG1 fv KILOLINES/in²	K1	K2	K3	R ar μ ohms	R b μ ohms	Kr	Ks
	1	1	30	.940	.960	.63	1.18	28.1	0.054	0.563	68	6	148	1.11	.970

	λ OF ROT NECK OR BRIDGE	λ sl	λ sr	HARMONIC LEAKAGE FACTORS	λ h	λ e	Bfg fv	Bw fv	Bs fv	AMPS per in²	A. COND. per in.	ELEC LOADING (X 10⁻⁹)	RING DENSITY
							KILOLINES/in²						
STATOR	—	—	0.888	.00903	0.428	0.612	115.4	115.7	108.7	4850	811	3.93	—
ROTOR	.50	1.209	0.231	.00729	0.786	0.182	54.1	59.0	150.3	4565			657

PERFORMANCE	R1 ph @25°C	R2'r @25°C	R2'L @25°C	X1	X2'r	X2'L	Xm	Io	FL SLIP	PO SLIP	FLT lb ft	°C RISE F.L. THER	°C RISE F.L. RTR
CALCULATED	0.0188	0.010	0.011	0.104	0.097	0.066	2.9	85.45	.0110	0676	492.1		
TEST													

	EFFICIENCY 1/2	3/4	FL	1 1/4	1 1/2	POWER FACTOR 1/2	3/4	FL	1 1/4	1 1/2	LRA	LRPF	LRT (pu)	POT (pu)	PUT
CALCULATED	0.960	.959	.954	.951	.946	.748	.831	.867	.877	.514	1402	.174	0.48	2.70	1.15
GUARANTEE															
TEST															

FULL LOAD LOSSES	V AIR GAP	F.L. AMPS	SEC. CU @ °C	PRI. CU @ °C	F & W	CORE	STRAY	TOTAL
CALCULATED	237.7	236.89	1673	3900	550	745	373	7241
TEST								

TEST SQ. #

TEST

DATE

COMMERCIAL-

NO LOAD TEST: VOLTS | AMPS | WATTS

SURGE RING DWG

ROTOR ASSEMBLY-

ROTOR PLATE- 98

NAVY-

STATOR PLATE- 99

RING & FAN ASSEMBLY

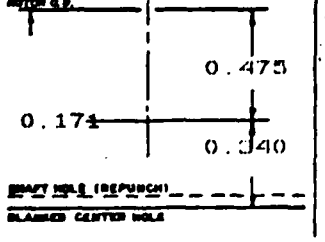

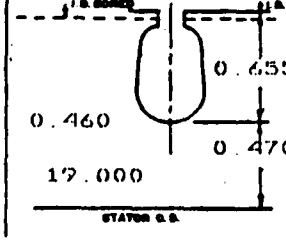

C.L.: 189
C.L.: 266
C.L.: 290

LRT-BAR= 14.0 ST= 11 ER= 655

FRAME	CORE	TYPE	WDG.	POLES	REV

SHEET OF

P=10

APPENDIX B

PRELIMINARY AND ROUGH 14 POLE DESIGNS

Form-631

GENERAL DYNAMICS/ELECTRO DYNAMIC
A.C. INDUCTION MOTOR
DESIGN & ELEC. SPEC. SHEET

M/P #

ENCL.	H.P.	VOLTS	AMPS	SYN. R.P.M.	F.L. R.P.M.	PH.	CYC.	°C RISE	INS. CL.	DUTY	TYPE	DES.	CODE
	200.00	440		2143		3	250	70					

MOTOR VOLTS	ROTOR AMPS	BRUSHES PER SET & GRADE	ENGR.	APP'D	DATE	CUSTOMER	ORDER #
1.00 5D							2000CEAE

	BLANK #	O.D.	I.D.	# SLOTS	SLOT-DIE ESA	SLOT SETTING	GROSS CORE	VENTS 3/8	NET CORE	CARTER FACTOR	GRADE STL #24	AIR GAP
STATOR		19.000	16.750	84	1001	0	12.000	0	12.000	1.056	M- 19	.0400
ROTOR		16.670	15.000	126	1028	25	12.000	0	12.000	1.034	M- 19	

COIL WDG. DWG. #	TURNS PER COIL	WIRE SIZE	WIRE WT.	WIRE SIZE	WIRE WT.	WIRE AREA (in²)	COILS PER GROUP	NET SLOT AREA	FULL-NESS	PITCH	MLT	COIL DIMENSIONS ST	SPD	LOOP
STATOR	6	2 #13	52.1	0 # 0	0.0	.00814	2.0	0.177	7/9	6	38.8	14.0	2.7	17.8
ROTOR														

CONNECTION & CABLE

INS. SPEC. #	CONN.	INTERNAL CONN DWG.	EXTERNAL CONN DWG.	CABLES #	CABLES SIZE	LEADS #	LEADS VOLTS	R LINE @25°C
								0.0228

REMARKS-
VTL=10.6 VCL= 63.5
BAR WT= 29.78 LB
ER(2)WT= 15.00 LB

NO. OF CORE PLATES STATOR= 480 ROTOR= 480
ST CORE STL WT= 178.1 LBS ROT CORE STL WT= 114.8 LBS

ROTOR CAGE

BAR SIZE AREA	BAR SIZE LENGTH	BAR SIZE MATERIAL	END RING THICK	END RING RAD. HT	END RING MATERIAL	TRICKEY FACTOR	SKEW O.D.	SKEW ARBOR	SKEW FIXTURE	FABRICATED BAR DIMENSIONS (ACTUAL)	FAN #
0.0585	12.00		0.625	0.750		1.12				X X	

REFERRAL FACTORS

CONN	CKT	Ns	Kp	Kd	K damp	W/V MEGALINES	SS in POLE PIECE	Xr	Xs	Xm	Rst	Rs	Kr	Ks
1	7	24	.966	.966	.92	1.02	35.6	0.049	0.580	48	11	142	1.11	.970

	λ OF ROT NECK OR BRIDGE	λ ss	λ sr	HARMONIC LEAKAGE FACTORS	λ b	λ e	Bg fr	Bw fr	Bd fr	AMPS per in²	A COND per in	ELEC LOADING (X10-6)	RING DENSITY
							KILOLINES/in²						
STATOR	—	—	0.925	.02050	0.994	0.383	122.7	122.4	98.5	4776	745	3.56	—
ROTOR	0.50	1.209	2.231	.01526	1.201	0.107	67.0	72.8	128.6	3996			1.437

PERFORMANCE	Ri pu @25°C	Re'r @25°C	Re'L @90°C	Xs	Xe'r	Xe'b	Xm	Io	FL SLIP	PO SLIP	FLT lb ft	°C RISE F.L. THEA	°C RISE F.L. ARA
CALCULATED	0.0114	0.007	0.008	0.114	0.101	0.072	1.7	143.54	.0082	.0464	495.6		
TEST													

	EFFICIENCY 1/2	3/4	FL	1 1/4	1 1/2	POWER FACTOR 1/2	3/4	FL	1 1/4	1 1/2	LRA	LRPF	LRT (pu)	POT (pu)	PUT
CALCULATED	0.957	.962	.961	.959	.935	.560	.685	.750	.773	.341	1383	.102	0.28	2.55	1.36
GUARANTEE															
TEST															

FULL LOAD LOSSES	V AIR GAP	F.L. AMPS	SEL. CU @ °C	FRI. CU @ °C	F & W	CORE	STRAY	TOTAL
CALCULATED	231.7	272.12	1298	3119	550	1030	373	6310
TEST								

TEST S.O. #
TEST
DATE

COMMERCIAL-
NAVY-

NO LOAD TEST

VOLTS	AMPS	WATTS

RING & FAN ASSEMBLY

SURGE RING DWG-

LRT-BAR= 22.3 ST= 18 ER= 194

ROTOR ASSEMBLY-
ROTOR PLATE- 98

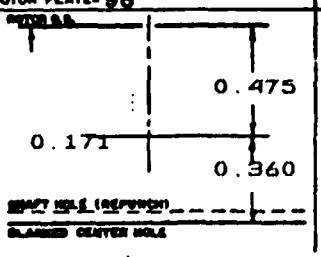

STATOR PLATE- 99

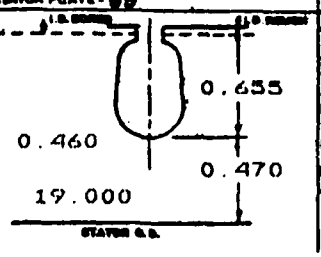

G.L.: 491
C.L.: 196
T.L.: 343

FRAME	CORE	TYPE	WDG.				REV.
				POLES			

SHEET OF P=14

FORM-621

GENERAL DYNAMICS/ELECTRO DYNAMIC
A.C. INDUCTION MOTOR
DESIGN & ELEC. SPEC. SHEET

M/P #

ENCL	H.P.	VOLTS	AMPS	SYN. R.P.M.	F.L. R.P.M.	PH.	CYC.	°C RISE	INS. CL.	DUTY	TYPE	DES.	CODE
	200.00	440		2143		3	250	70					

TOR VOLTS	ROTOR AMPS	BRUSHES PER SET & GRADE	ENGR.	APP'D	DATE	CUSTOMER	ORDER #
1.00 SF							2000CEAE

	BLANK #	O.D.	I.D.	# SLOTS	SLOT-DIE ESA	SLOT SKEWING	GROSS CORE	VENTS (I/D)	NET CORE	CARTER FACTOR	GRADE STL. # 24	AIR GAP
STATOR		17.000	16.750	84	1001 0		12.000	0	12.000	1.040	M-19	.0500
ROTOR		16.650	15.000	126	1028 25		12.000	0	12.000	1.029	M-19	

COIL WDG. DWG. #	TURNS PER COIL	WIRE SIZE	WIRE WT.	SIZE	WT.	WIRE AREA (IN²)	COILS PER GROUP	NET SLOT AREA	FULLNESS	PITCH	MLT	COIL DIMENSIONS ST	SPC	LOOP
STATOR	6	2 #3	52.1	0 # 0	0.0	00814	2.0	0.177	79	1-6	38.8	14.0	2.7	17.8
ROTOR														

INS. SPEC. #	CONNECTION & CABLE: CONN.	INTERNAL CONN DWG.	EXTERNAL CONN. DWG.	CABLES #	CABLES SIZE	LEADS #	LEADS VOLTS	R LINE @ 25°C
								.0.0228

REMARKS-
VT1=10.6 VC1= 69.5
BAR WT= 29.78 LB
ER(2)WT= 14.99 LB

NO. OF CORE PLATES STATOR= 480 ROTOR= 480
ST CORE STL. WT= 178.1 LBS ROT CORE STL. WT= 113.0 LBS

ROTOR CAGE	BAR SIZE AREA	BAR SIZE LENGTH	BAR SIZE MATERIAL	END RING THICK	END RING RAD. HT.	END RING MATERIAL	TRICKEY FACTOR	SKEW O.D.	SKEW ARBOR	SKEW FIXTURE	FABRICATED BAR DIMENSIONS (ACTUAL)	FAN #
	0.0585	12.00		0.625	0.750		1.12				X X	

REFERRAL FACTORS	CONN	CKT	R_1	K_p	K_d	K_{damp}	@ fr MEGALINES	@ fr KILOLINES	K_1	K_2	K_3	R_{qr} μ ohms	R_b μ ohms	X_r	K_s
	1	7	24	.966	.966	.92	1.02	35.6	0.049	0.580	48	11	142	1.11	.970

	λ OF ROT NECK OR BRIDGE	λ_{sl}	λ_{sr}	HARMONIC LEAKAGE FACTORS	λ_s	λ_o	B_{fg} fr	B_{tv} fr	B_{tc} fr	AMPS per in²	A COND per in	ELEC LOADING (X10⁻⁶)	RING DENSITY
							KILOLINES/in²						
STATOR	—	—	0.925	.02050	0.805	0.989	122.7	122.4	98.5	4747	741	3.52	—
ROTOR	0.50	1.209	2.231	.01526	0.972	0.107	67.0	72.9	132.3	3959			1423

PERFORMANCE	R_1 pb @ 25°C	$R_2'r$ @ 25°C	$R_2'L$ @ 25°C	X_1	$X_2'r$	$X_2'L$	X_m	I_o	FL SLIP	PO SLIP	FLT lb. ft	°C RISE F.L. THER	°C RISE F.L. RXN
CALCULATED	0.0114	0.007	0.008	0.104	0.095	0.066	1.6	145.06	.0080	0488	494.5		
TEST													

	EFFICIENCY 1/2	EFFICIENCY 3/4	EFFICIENCY FL	EFFICIENCY 1 1/4	EFFICIENCY 1 1/2	POWER FACTOR 1/2	POWER FACTOR 3/4	POWER FACTOR FL	POWER FACTOR 1 1/4	POWER FACTOR 1 1/2	LRA	LRPF	LRT (pu)	POT (pu)	PUT
CALCULATED	0.959	.962	.962	.960	.937	.556	.685	.753	.778	.838	1503	.112	0 34	2.76	1.11
GUARANTEE															
TEST															

FULL LOAD LOSSES	V AIR GAP	F.L. AMPS	SEC. CU @ 90°C	PRI. CU @ 95°C	F & W	CORE	STRAY	TOTAL
CALCULATED	233.4	270.51	1215	3082	550	913	373	6133
TEST								

TEST S.O. #
TEST
DATE

COMMERCIAL-
NAVY-
ROTOR ASSEMBLY-
ROTOR PLATE- 98
STATOR PLATE- 99

NO LOAD TEST

VOLTS	AMPS	WATTS

RING & FAN ASSEMBLY

SURGE RING DWG -

RT-BAR= 18 7 ST= 15 ER= 154

FRAME	CORE	TYPE	WDG.	POLES	REV.

SHEET OF P=14

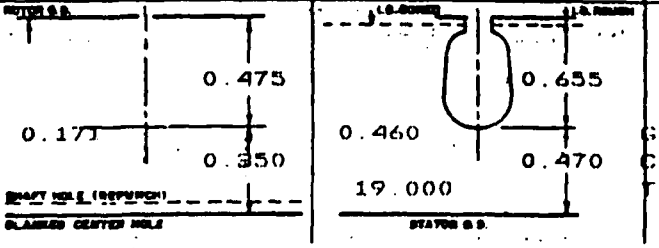

G.L: 374
C.L: 196
T.L: 343

FORM-621

GENERAL DYNAMICS/ELECTRO DYNAMIC
A.C. INDUCTION MOTOR
DESIGN & ELEC. SPEC. SHEET

M/P #

ENCL.	H.P.	VOLTS	AMPS	SYN. R.P.M.	F.L. R.P.M.	PH.	CYC.	°C RISE	INS. CL.	DUTY	TYPE	DES.	CODE
	200.00	440		2143		3	250	70					

ROTOR VOLTS	ROTOR AMPS	BRUSHES PER SET & GRADE	ENGR.	APP'D	DATE	CUSTOMER	ORDER #
1.00 SE							2000CEAE

	BLANK #	O.D.	I.D.	# SLOTS	SLOT-DIE ESA	SLOT SETTING	GROSS CORE	VENTS 3/8	NET CORE	CARTER FACTOR	GRADE STL. # 24	AIR GAP
STATOR		19.000	16.750	84	1001 0		12.000	0	12.000	1.042	M-19	0600
ROTOR		16.630	15.000	126	1028 25		12.000	0	12.000	1.025	M-19	

COIL WDG. DWG. #	TURNS PER COIL	WIRE SIZE	WIRE WT.	WIRE SIZE	WIRE WT.	WIRE AREA (IN²)	COILS PER GROUP	NET SLOT AREA	FILLNESS	PITCH	MLT	COIL DIMENSIONS ST	SPD	LOOP
STATOR	6	2 #13	52.1	0 # 0	0.0	00814	2.0	0.177	72%	6	38.8	14.0	2.7	17.3
ROTOR														

INS. SPEC. #	CONNECTION & CABLE: CONN.	INTERNAL CONN DWG	EXTERNAL CONN DWG.	CABLES #	CABLES SIZE	LEADS #	LEADS VOLTS	R LINE @25°C
								0.0228

REMARKS-
WT=10.6 WC1= 6.75
BAR WT= 22.78 LB
ER(2)WT= 14.97 LB

NO. OF CORE PLATES STATOR= 480 ROTOR= 480
ST CORE STL WT= 173.1 LBS ROT CORE STL WT= 111.3 LBS

ROTOR CAGE	BAR SIZE AREA	BAR SIZE LENGTH	BAR SIZE MATERIAL	END RING THICK	END RING RAD HT	END RING MATERIAL	TRICKEY FACTOR	SKEW O.D	SKEW ARBOR	SKEW FIXTURE	FABRICATED BAR DIMENSIONS (ACTUAL)	FAN #
	0.0585	12.00		0.625	0.750		1.12				X X	

REFERRAL FACTORS	CONN	CKT	Ni	Kp	Kd	K damp	Bfv MEGALINES	Bg fv KILOLINES/in²	Ki	Kz	Ks	Rar μ ohms	Rb μ ohms	Kr	Ks
		7	24	.966	.966	.92	1.07	35.6	0.042	0.500	46	11	142	1.11	270

	λ OF ROT NECK OR BRIDGE	λ sl	λ ar	HARMONIC LEAKAGE FACTORS	λ b	λ e	Bg fv	Bt fv	Bc fv	AMPS per in²	A COND per in.	ELEC LOADING (X10⁻⁹)	RING DENSITY
							KILOLINES/in²						
STATOR	—	—	0.923	.02050	0.676	0.383	122.7	122.4	98.5	5008	781	3.91	—
ROTOR	0.50	1.209	2.231	.01526	0.817	0.107	67.1	79.0	136.8	3970			1430

PERFORMANCE	R1 @25°C	R2' @25°C	R2 L @90°C	X1	X2'r	X2'L	Xm	Io	FL SLIP	PO SLIP	FLT lb ft	TORQUE FL TIER	TORQUE FL RYR
CALCULATED	0.0114	0.007	0.008	0.098	0.090	0.061	1.4	168.72	0081	0525	494.4		
TEST													

	EFFICIENCY 1/2	3/4	FL	1 1/4	1 1/2	POWER FACTOR 1/2	3/4	FL	1 1/4	1 1/2	LRA	LRPF	LRT (pu)	POT (pu)	PUT
CALCULATED	0.955	.960	.960	.958	.931	.505	.688	.716	.745	.297	1610	.119	0.30	2.38	1.09
GUARANTEE															
TEST															

FULL LOAD LOSSES	V AIR GAP	F.L. AMPS	SEC CU @ °C	PRI. CU @ °C	F&W	CORE	STRAY	TOTAL
CALCULATED	232.9	285.99	1227	3430	550	830	373	6417
TEST								

TEST S.O. #
TEST
DATE

COMMERCIAL-
NAVY-

NO LOAD TEST VOLTS	AMPS	WATTS

SURGE RING DWG

ROTOR ASSEMBLY-
ROTOR PLATE- 98
STATOR PLATE- 99
RING & FAN ASSEMBLY

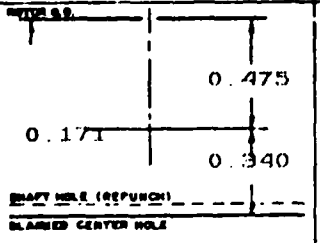

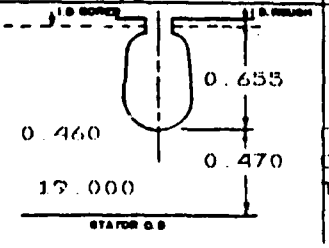

C.L. 229
C.L. 196
T.L. 340

LRT-BAR= 16.6 ST= 13 CB= 136

FRAME	CORE	TYPE	WDG	POLES	REV

SHEET OF

P=14 P=14

APPENDIX C

PRELIMINARY AND ROUGH 18 POLE DESIGNS

FORM-621

GENERAL DYNAMICS/ELECTRO DYNAMIC

A.C. INDUCTION MOTOR DESIGN & ELEC. SPEC. SHEET

M/P #

ENCL.	H.P.	VOLTS	AMPS	SYN. R.P.M.	F.L. R.P.M.	PH.	CYC.	°C RISE	INS. CL.	DUTY	TYPE	DES.	CODE
	200.00	440		2140		3	321	70					

STATOR VOLTS	ROTOR AMPS	BRUSHES PER SET & GRADE	ENGR.	APPD	DATE	CUSTOMER	ORDER #
.00 SF							200DCEAG

	BLANK #	O.D.	I.D.	# SLOTS	SLOT-DIE ESA	SLOT SETTING	GROSS CORE	VENTS 3/8	NET CORE	CARTER FACTOR	GRADE STL. #24	AIR GAP
STATOR		19.000	16.750	108	1001 0		12.000	0	12.000	1.054	M-19	.0600
ROTOR		16.630	15.000	144	1028 25		12.000	0	12.000	1.028	M-19	

COIL WDG. DWG. #	TURNS PER COIL	WIRE SIZE	WIRE WT.	WIRE SIZE	WIRE WT.	WIRE AREA (in²)	COILS PER GROUP	NET SLOT AREA	FULL-NESS	PITCH	MLT	COIL DIMENSIONS ST	COIL DIMENSIONS SPD.	COIL DIMENSIONS LOOP
STATOR	4	3 #3	62.3	0 # 0	0.0	.01221	2.0	0.173	78	1-6	36.1	14.0	2.3	16.5
ROTOR														

INS. SPEC. #	CONNECTION & CABLE: CONN.	INTERNAL CONN DWG	EXTERNAL CONN DWG.	CABLES #	CABLES SIZE	LEADS #	LEADS VOLTS	R. LINE @25°C
								0.0165

NO. OF CORE PLATES - STATOR= 480 ROTOR= 480

STATOR CORE STL. WT= 125.5 LBS ROTOR CORE STL. WT= 107.8 LBS

REMARKS:
VT1=10.6 VC1= 47.3
BAR WT= 34.03 LB
ER(2)WT= 14.97 LB

18 Poles

ROTOR CAGE	BAR SIZE AREA	LENGTH	MATERIAL	END RING THICK	END RING RAD. WT.	MATERIAL	TRICKEY FACTOR	SKEW O.D.	SKEW ARBOR	SKEW FIXTURE	FABRICATED BAR DIMENSIONS (ACTUAL)	FAN #
	0.0585	12.00		0.0685	0.750		1.17				X X	

REFERRAL FACTORS	CONN	CKT	Ns	Kp	Kd	K demp	Bfr MEGALINES	Bg fr KILOLINES/in²	Xl	X2	X3	Rqr μ ohms	Rb μ ohms	Kr	Ks
	1	6	24	.966	.966	.92	0.80	35.6	0.049	0.653	42	8	142	1.11	270

	λ OF ROT NECK OR BRIDGE	λ sl	λ er	HARMONIC LEAKAGE FACTORS	λ b	λ e	Bfg fr	Bfr fr	Bs fr KILOLINES/in²	AMPS per in²	A COND per in	ELEC LOADING (X10-6)	RING DENSITY
TATOR	—	—	1.156	.02050	0.519	0.321	114.7	114.4	109.9	4442	891	0.96	—
ROTOR	0.50	1.209	2.291	.01935	0.705	0.074	74.8	82.2	106.0	3554			1137

PERFORMANCE	Rs ph @25°C	Rs'r @25°C	Rs'L @80°C	Xs	Xs'r	Xs'L	Xm	Io	FL SLIP	PO SLIP	FLT lb. ft	°C RISE FL THER	°C RISE FL RXR
CALCULATED	0.0082	0.006	0.007	0.098	0.097	0.064	1.1	220.62	.0072	.0440	495.2		
TEST													

	EFFICIENCY 1/2	3/4	FL	1 1/4	1 1/2	POWER FACTOR 1/2	3/4	FL	1 1/4	1 1/2	LRA	LRPF	LRT (pu)	POT (pu)	PUT
CALCULATED	0.955	.962	.963	.962	.925	.411	.540	.626	.662	.293	1593	.090	0.31	2.74	1.12
GUARANTEE															
TEST															

FULL LOAD LOSSES	V AIR GAP	F. L. AMPS	SEC. CU @ °C	PRI. CU @ °C	F&W	CORE	STRAY	TOTAL
CALCULATED	227.7	325.45	1096	3224	550	722	373	5965
TEST								

TEST SQ #
TEST
DATE

SURGE RING DWG=

COMMERCIAL-
NAVY-
STATOR ASSEMBLY-
STATOR PLATE- 98
STATOR PLATE- 99
NO LOAD TEST: VOLTS | AMPS | WATTS
RING & FAN ASSEMBLY

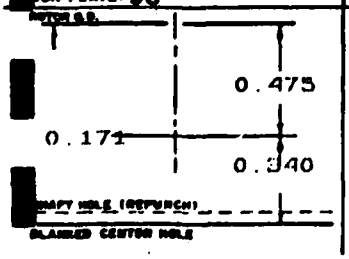

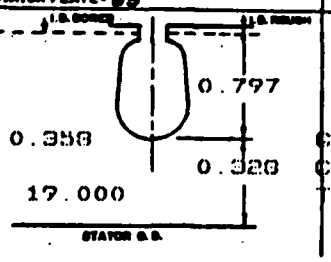

C.L: 340
C.L: 185
C.L: 197

LRT-BAR= 22.6 ST= 22 ER= 226

FRAME	CORE	TYPE	WDG.			POLES		REV.

SHEET OF

P=18

FoRM-621

GENERAL DYNAMICS/ELECTRO DYNAMIC
A.C. INDUCTION MOTOR
DESIGN & ELEC. SPEC. SHEET

ENCL.	H.P.	VOLTS	AMPS	SYN. R.P.M.	F.L. R.P.M.	PH.	CYC.	°C RISE	INS. CL.	DUTY	TYPE	DES.	CODE
	200.00	440		2140		3	321	70					

ROTOR VOLTS	ROTOR AMPS	BRUSHES PER SET & GRADE	ENGR.	APP'D	DATE	CUSTOMER	ORDER #
1.00 SF							200DCEAG

N/P #

	BLANK #	O.D.	I.D.	# SLOTS	SLOT-DIE EQA	SLOT SETTING	GROSS CORE	VENTS 3/8	NET CORE	CARTER FACTOR	GRADE STL.#24	AIR GAP
STATOR		19.000	16.750	108	1001 0		12.000	0	12.000	1.062	M-19	.0500
ROTOR		16.650	15.000	144	1028 25		12.000	0	12.000	1.033	M-19	

COIL WDG. DWG. #	TURNS PER COIL	WIRE SIZE	WIRE WT.	WIRE SIZE	WIRE WT.	WIRE AREA (IN²)	COILS PER GROUP	NET SLOT AREA	FULLNESS	PITCH	MLT	COIL DIMENSIONS ST	SPD	LOOP
STATOR	4	3 #13	62.3	0 # 0	0.0	.01221	2.0	0.179	78	1-6	36.1	14.0	2.3	16.5
ROTOR														

CONNECTION & CABLE

INS. SPEC. #	CONN.	INTERNAL CONN DWG.	EXTERNAL CONN. DWG.	CABLES #	CABLES SIZE	LEADS #	LEADS VOLTS	R LINE @25°C
								0.0165

NO. OF CORE PLATES STATOR= 480 ROTOR= 480
ST CORE STL WT= 123.5 LBS ROT CORE STL WT= 109.5 LBS

REMARKS-
~~VT1=10.6 VE1= 42.9~~
BAR WT= 34.03 LB
ER(2)WT= 14.99 LB

ROTOR CAGE	BAR SIZE AREA	LENG. in	MATERIAL	END RING THICK	RAD. HT	MATERIAL	TRICKEY FACTOR	SKEW O.D.	ARBOR	FIXTURE	FABRICATED BAR DIMENSIONS (ACTUAL)	FAN #
	0.0585	12.00		0.625	0.750		1.17				x x	

REFERRAL FACTORS	CONN	CKT	N₁	Kp	Kd	K damp	Φ fv MEGALINES	Bg₁ fv KILO LINES	K₁	K2	K3	R₀₁ μ ohms	Rb μ ohms	Kr	Kx
	1	6	24	.966	.966	.92	0.80	35.6	0.049	0.653	42	8	142	1.11	.970

	λ OF ROT NECK OR BRIDGE	λ sl	λ ar	HARMONIC LEAKAGE FACTORS	λ b	λ e	Bfg fv (KILOLINES/in²)	Bt fv (KILOLINES/in²)	Bc fv (KILOLINES/in²)	AMPS per in²	A COND per in	ELEC LOADING (X 10⁻⁶)	RING DENSITY
STATOR	—	—	1.156	.02050	0.614	0.321	114.7	114.4	109.9	4137	830	3.43	—
ROTOR	0.50	1.209	2.231	.01935	0.837	0.074	74.8	82.1	103.0	3521			1127

PERFORMANCE	R₁ ph @25°C	R2'r @25°C	R2'L @25°C	X1	X2'r	X2'L	Xm	Io	FL SLIP	PO SLIP	FLT lb ft	°C RISE FL THER	RXR
CALCULATED	0.0082	0.006	0.007	0.103	0.101	0.068	1.2	190.28	.0071	.0421	494.5		
TEST													

	EFFICIENCY 1/2	3/4	FL	1 1/4	1 1/2	POWER FACTOR 1/2	3/4	FL	1 1/4	1 1/2	LRA	LRPF	LRT(pu)	POT (pu)	PUT
CALCULATED	0.959	.965	.965	.964	.935	.459	.590	.670	.702	.264	1500	.086	0.28	2.67	1.13
GUARANTEE															
TEST															

FULL LOAD LOSSES	V AIR GAP	F.L. AMPS	SEC. CU @ °C	PRI. CU @ °C	F & W	CORE	STRAY	TOTAL
CALCULATED	229.5	303.10	1075	2797	550	806	373	5601
TEST								

TEST S.O. #
TEST DATE

COMMERCIAL-
NAVY-

NO LOAD TEST

VOLTS	AMPS	WATTS

SURGE RING DWG-

ROTOR ASSEMBLY-
ROTOR PLATE- 98
STATOR PLATE- 99

RING & FAN ASSEMBLY

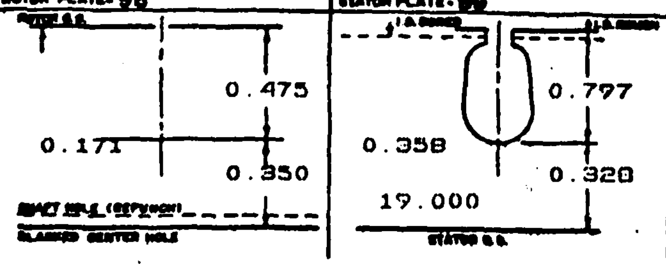

C.L: 424
C.L: 185
T.L: 197

LRT-BAR= 24.9 ST= 25 ER= 251

FRAME	CORE	TYPE	WDG.		POLES		REV

SHEET OF

P= 18

ORM-621

GENERAL DYNAMICS/ELECTRO DYNAMIC
A.C. INDUCTION MOTOR
DESIGN & ELEC. SPEC SHEET

H.P	VOLTS	AMPS	SYN. R.P.M.	F.L. R.P.M.	PH.	CYC.	°C RISE	INS. CL.	DUTY	TYPE	SER.	CODE
200.00	440		2140		3	321	70					

M/P #

? VOLTS	ROTOR AMPS	BRUSHES PER SET & GRADE	ENGR.	APP'D	DATE	CUSTOMER	ORDER #
L.00 SF							2000CEAG

	BLANK #	O.D.	I.D.	# SLOTS	SLOT-DIE ESA	SLOT SETTING	GROSS CORE	VENTS 3/8	NET CORE	CARTER FACTOR	GRADE STL. #24	AIR GAP
STATOR		19.000	16.750	108	1001 0		12.000	0	12.000	1.073	M-19	.0400
ROTOR		16.670	15.000	144	1028 25		12.000	0	12.000	1.040	M-19	

WDG. DWG. #	TURNS PER COIL	WIRE SIZE	WIRE WT.	WIRE SIZE	WIRE WT.	WIRE AREA (IN²)	COILS PER GROUP	NET SLOT AREA	FULLNESS	PITCH	MLT	COIL DIMENSIONS ST	SPG	LOOP
STATOR	4	3 13	62.3	0 # 0	0.0	.01221	2.0	0.179	78	1- 6	36.1	14.0	2.3	16.5
ROTOR														

CONNECTION & CABLE

AL. SPEC. #	CONN.	INTERNAL CONN DWG.	EXTERNAL CONN DWG.	CABLES #	CABLES SIZE	LEADS #	LEADS VOLTS	R. LINE @25°C
								0.0165

~~NO. OF CORE PLATES STATOR= 480 ROTOR= 480~~

ST CORE STL WT= 125.5 LBS ROT CORE STL WT= 111.3 LBS

REMARKS-
~~VT1=10.6 VB1= 42.3~~
BAR WT= 34.03 LB
ER(2)WT= 15.00 LB

ROTOR CAGE	BAR SIZE AREA	LENGTH	MATERIAL	END RING THICK	RAD. HT	MATERIAL	TRICKEY FACTOR	SKEW O.D.	ARBOR	FIXTURE	FABRICATED BAR DIMENSIONS (ACTUAL)	FAN #
	0.0585	12.00		0.625	0.750		1.17				X X	

REFERRAL FACTORS	CONN	CKT	N1	Kp	Kd	N damp	Φ fv MEGALINES	BG1 fv KILOLINES	K1	K2	K3	R ar μ ohms	Rb μ ohms	Kr	Ks
	1	6	24	.966	.966	.92	0.80	35.6	0.049	0.653	42	8	142	1.11	.970

	λ OF ROT NECK OR BRIDGE	λ sb	λ er	HARMONIC LEAKAGE FACTORS	λ h	λ e	Bfg fv	Bt fv	Bc fv (KILOLINES/IN²)	AMPS per in²	A COND per in	ELEC LOADING (X10⁻⁶)	RING DENSITY
STATOR	—	—	1.156	.02050	0.757	0.321	114.7	114.4	109.9	3860	774	2.99	—
ROTOR	0.50	1.209	2.231	.01935	1.031	0.074	174.7	82.0	100.1	3501			1120

PERFORMANCE	R1 ph @25°C	R2' @25°C	R2'L @25°C	X1	X2'r	X2'L	Xm	Io	FL SLIP	PO SLIP	FLT lb. ft	°C RISE FL THER	RXR
CALCULATED	0.0082	0.006	0.007	0.110	0.107	0.074	1.5	159.40	.0070	.0388	495.1		
TEST													

	EFFICIENCY 1/2	3/4	FL	1 1/4	1 1/2	POWER FACTOR 1/2	3/4	FL	1 1/4	1 1/2	LRA	LRPF	LRT(pu)	POT (pu)	PUT
CALCULATED	0.962	.967	.966	.965	.940	.51?	.647	.718	.743	.810	1398	.080	0.24	2.54	1.16
GUARANTEE															
TEST															

FL LOAD LOSSES	V AIR GAP	F.L. AMPS	SEC. CU @ °C	PRI. CU @ °C	F & W	CORE	STRAY	TOTAL
CALCULATED	231.2	282.75	1064	2434	550	939	373	5357
TEST								

TEST S.O. #
TEST
DATE

COMMERCIAL-

NAVY-

NO LOAD TEST VOLTS	AMPS	WATTS

SURGE RING DWG-

ROTOR ASSEMBLY-
ROTOR PLATE- 98
ROTOR O.D.

STATOR PLATE- 99

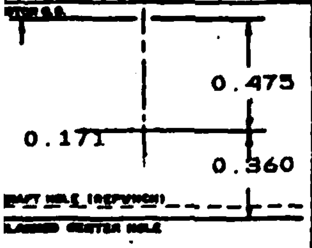

SHAFT HOLE (KEYWAY)
PLANNED CENTER HOLE

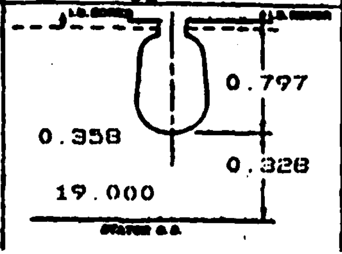

STATOR O.D.

RING & FAN ASSEMBLY

G.L: 557
C.L: 185
T.L: 197

LRT-BAR= 28.6 ST= 29 ER= 289

FRAME	CORE	TYPE	WDG.				
				POLES			REV.

SHEET 1 OF

P=18

APPENDIX D

PRELIMINARY AND ROUGH 22 POLE DESIGNS

FORM-621

GENERAL DYNAMICS/ELECTRO DYNAMIC
A.C. INDUCTION MOTOR
DESIGN & ELEC. SPEC. SHEET

ENCL.	H.P.	VOLTS	AMPS	SYN. R.P.M.	F.L. R.P.M.	PH	CYC.	°C RISE	INS. CL.	DUTY	M/P # TYPE	DES.	CODE
	200.00	440		2138		3	392	70					

ROTOR VOLTS	ROTOR AMPS	BRUSHES PER SET & GRADE	ENGR.	APP'D	DATE	CUSTOMER	ORDER #
1.00 SF							2000CEAR

	BLANK #	O.D.	I.D.	# SLOTS	SLOT-DIE ESA	SLOT SETTING	GROSS CORE	VENTS 3/8	NET CORE	CARTER FACTOR	GRADE STL. #24	AIR GAP
STATOR		19.000	16.750	132	1001 .0		12.000	0	12.000	1.067	M-19	.0600
ROTOR		16.630	15.000	98	1028 25		12.000	0	12.000	1.019	M-19	

COIL WDG. DWG. #	TURNS PER COIL	WIRE SIZE	WIRE WT.	SIZE	WT.	WIRE AREA (IN²)	COILS PER GROUP	NET SLOT AREA	FULL-NESS	PITCH	MLT	COIL DIMENSIONS ST	SPD	LOOP
STATOR	6	1 #3	36.7	1 #14	29.1	.00729	2 0	0.158	80	6	34.8	14.0	2.0	16.2
ROTOR														

INS. SPEC #	CONNECTION & CABLE: CONN.	INTERNAL CONN DWG	EXTERNAL CONN DWG	CABLES #	CABLES SIZE	LEADS #	LEADS VOLTS	R. LINE @25°C
								0.0145

REMARKS:
VT1=10.6 VC1= 63.5
BAR WT= 29.16 LB
ER(2)WT= 14.97 LB

NO. OF CORE PLATES: STATOR= 480 ROTOR= 480

ST CORE STL WT= 116.0 LBS ROT CORE STL WT= 116.8 LBS

ROTOR CAGE	BAR SIZE AREA	LENGTH	MATERIAL	END RING THICK	RAD. HT.	MATERIAL	TRICKEY FACTOR	SKEW O.D.	ARBOR	FIXTURE	FABRICATED BAR DIMENSIONS (ACTUAL)	FAN #
	.10585	12.00		0.625	0.750		1.17				X X	

REFERRAL FACTORS	CORR	CKT	Ns	Kp	Kd	Kd comp	Φ fv MEGALINES	Φg fv KILOLINES	Ki	K2	K3	Rar μ ohms	Rb μ ohms	Kr	Kx
	1	11	24	.966	.966	.92	0.65	35.7	0.049	1.172	61	4	142	1.11	.270

	λ OF ROT NECK OR BRIDGE	λ st	λ sr	HARMONIC LEAKAGE FACTORS	λ b	λ e	Φg fv	Φr fv	Φs fv	AMPS per in²	A. COND. per in	ELEC LOADING (X10⁻⁸)	RING DENSITY
							KILOLINES/in²						
STATOR	—	—	1.358	.02050	0.423	0.300	115.0	113.5	109.8	4596	1009	4.64	—
ROTOR	0.50	1.209	2.231	.01935	0.320	0.094	58.0	62.3	86.8	5427			981

PERFORMANCE	Rs pb @25°C	Rs'r @25°C	Rr'L @25°C	X1	Xs'r	Xr'L	Xm	Io	FL SLIP	PO SLIP	FLT lb ft	°C RISE F.L. THER	RXR
CALCULATED	0.0073	0.009	0.010	0.103	0.149	0.090	0.9	259.02	.0111	.0483	497.2		
TEST													

	EFFICIENCY 1/2	3/4	FL	1 1/4	1 1/2	POWER FACTOR 1/2	3/4	FL	1 1/4	1 1/2	LRA	LRPF	LRT (pu)	POT (pu)	PUT
CALCULATED	0.950	.956	.956	.955	.921	.359	.476	.556	.588	.200	1372	.083	0.30	2.06	1.09
GUARANTEE															
TEST															

FULL LOAD LOSSES	V AIR GAP	F. L. AMPS	SEC. CU @ °C	FRI. @ °C	F & W	CORE	STRAY	TOTAL
CALCULATED	221.5	368.55	1686	3647	550	729	373	6986
TEST								

TEST SQ #
TEST
DATE

COMMERCIAL-
NAVY-

NO LOAD TEST VOLTS	AMPS	WATTS

RING & FAN ASSEMBLY

SURGE RING DWG-

LRT-BAR= 15.2 ST= 36 CR= 490

ROTOR ASSEMBLY-
ROTOR PLATE- 98
STATOR PLATE- 99

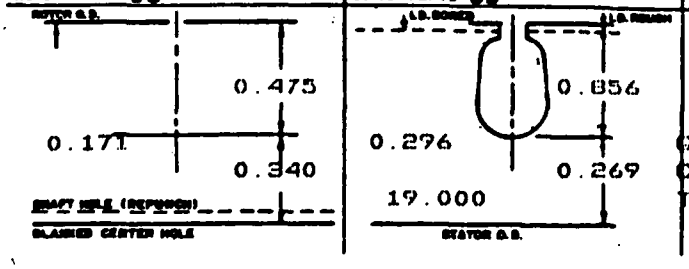

C.L: 376
C.L: 152
T.L: 202

FRAME	CORE	TYPE	WDG			POLES		REV.

SHEET OF

P=22

FORM-621

GENERAL DYNAMICS/ELECTRO DYNAMIC
A.C. INDUCTION MOTOR
DESIGN & ELEC. SPEC. SHEET

ENCL.	H.P.	VOLTS	AMPS	SYN. R.P.M.	F.L. R.P.M.	PH.	CYC.	°C RISE	INS. CL.	DUTY	TYPE	DES.	CODE
	200.00	440		2198		3	392	70					

ROTOR VOLTS	ROTOR AMPS	BRUSHES PER SET & GRADE	ENGR.	APP'D	DATE	CUSTOMER	ORDER #
1.00 SF							200DCERK

M/P #

	BLANK #	O.D.	I.D.	# SLOTS	SLOT-DIE ESA	SLOT SETTING	GROSS CORE	VENTS 3/8	NET CORE	CARTER FACTOR	GRADE STL.#24	AIR GAP
STATOR		19.000	16.750	192	1001 0		12.000	0	12.000	1.077	M-19	.0500
ROTOR		16.650	15.000	98	1028 25		12.000	0	12.000	1.022	M-19	

COIL WDG. DWG. #	TURNS PER COIL	WIRE SIZE	WIRE WT.	WIRE SIZE	WIRE WT.	WIRE AREA (IN²)	COILS PER GROUP	NET SLOT AREA	FULLNESS	PITCH	MLT	COIL DIMENSIONS ST	SPD	LOOP
STATOR	6	1 #13	36.7	1 #14	29.1	.00729	2.0	0.158	80	1-6	34.8	14.0	2.0	16.2
ROTOR														

CONNECTION & CABLE

INS. SPEC. #	CONN.	INTERNAL CONN DWG.	EXTERNAL CONN DWG.	CABLES #	CABLES SIZE	LEADS #	LEADS VOLTS	R. LINE @25°C
								0.0145

NO. OF CORE PLATES STATOR= 480 ROTOR= 480

ST CORE STL WT= 116.0 LBS ROT CORE STL WT= 118.5 LBS

REMARKS-
~~VT1=10.6 VG1= 63.5~~
BAR WT= 23.16 LB
ER(2)WT= 14.99 LB

ROTOR CAGE	BAR SIZE AREA	BAR SIZE LENGTH	BAR SIZE MATERIAL	END RING THICK	END RING RAD. HT.	END RING MATERIAL	TRICKEY FACTOR	SKEW O.D.	SKEW ARBOR	SKEW FIXTURE	FABRICATED BAR DIMENSIONS (ACTUAL)	FAN #
	0.0585	12.00		0.625	0.750		1.17				x x	

REFERRAL FACTORS	CONN.	CKT	N1	Kp	Kd	K damp	Φ fv MEGALINES	BG1 fv KILOLINES/IN²	K1	K2	K3	R er	R b	Kr	Ks
	1	11	24	.966	.966	.92	0.65	35.7	0.049	1.172	61	4	142	1.11	.970

	λ OF ROT NECK OR BRIDGE	λ sL	λ er	HARMONIC LEAKAGE FACTORS	λ b	λ e	Btg fv	Bt fv	Bc fv	AMPS per in²	A.COND. per in	ELEC LOADING (X10⁻⁶)	RING DENSITY
							KILOLINES/in²						
STATOR	—	—	1.358	.02050	0.502	0.300	115.0	113.5	109.8	4249	933	3.96	—
ROTOR	0.50	1.209	2.231	.01985	0.380	0.084	58.0	62.3	84.4	5364			970

PERFORMANCE	R1 pb @25°C	R2'r @25°C	R2'L @ °C	X1	X2'r	X2'L	Xm	Ie	FL SLIP	PO SLIP	FLT lb. ft	°C RISE FL THER	°C RISE FL RXR
CALCULATED	0.0073	0.009	0.010	0.106	0.153	0.094	1.0	224.38	.0109	.0470	497.1		
TEST													

	EFFICIENCY 1/2	3/4	FL	1 1/4	1 1/2	POWER FACTOR 1/2	3/4	FL	1 1/4	1 1/2	LRA	LRPF	LRT(pu)	POT(pu)	PUT
CALCULATED	0.955	.960	.959	.958	.929	.401	.522	.600	.629	.227	1316	.081	0.28	2.05	1.11
GUARANTEE															
TEST															

FULL LOAD LOSSES	V AIR GAP	F.L. AMPS	SEC. CU @ °C	PRI. CU @ °C	F&W	CORE	STRAY	TOTAL
CALCULATED	224.0	340.76	1649	3118	550	823	373	6513
TEST								

TEST S.O. #
TEST DATE

COMMERCIAL-

NO LOAD TEST

VOLTS	AMPS	WATTS

SURGE RING DWG-

ROTOR ASSEMBLY-
ROTOR PLATE- 98

NAVY-
STATOR PLATE- 99

RING & FAN ASSEMBLY

LRT-BAR= 16.2 ST= 39 ER= 523

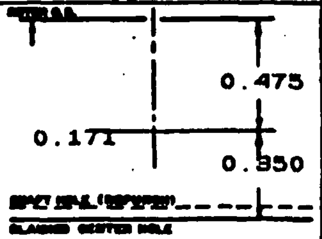

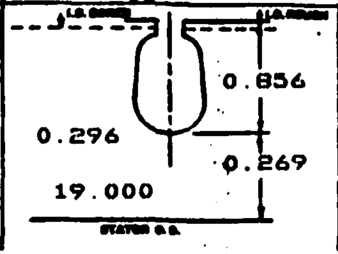

G.L: 469
C.L: 152
T.L: 202

FRAME	CORE	TYPE	WDG.	POLES		REV.

SHEET OF

P=22

FL24 & 21

GENERAL DYNAMICS/ELECTRO DYNAMIC

A.C. INDUCTION MOTOR

DESIGN & ELEC. SPEC. SHEET

M/P #

ENCL.	H.P.	VOLTS	AMPS	SYN. R.P.M.	FL. R.P.M.	PH.	CYC.	°C RISE	INS. CL.	DUTY	TYPE	DES.	CODE
	200.00	.440		2138		3	392	70					

FOR VOLTS	ROTOR AMPS	BRUSHES PER SET & GRADE	ENGR.	APP'D	DATE	CUSTOMER	ORDER #
1.00 SF							2000CEAK

	BLANK #	O.D.	I.D.	# SLOTS	SLOT-DIM. ESA	SLOT SETTING	GROSS CORE	VENTS I/D	NET CORE	CARTER FACTOR	GRADE STL. #29	AIR GAP
STATOR		19.000	16.750	132	1001 0		12.000	.0	12.000	1.091	.19	.0400
ROTOR		16.670	15.000	98	1028.25	—	12.000	0	12.000	1.027	.19	

COIL MOD. DWG. #	TURNS PER COIL	WIRE SIZE	WIRE WT.	WIRE SIZE	WIRE WT.	WIRE AREA (IN²)	COILS PER GROUP	NET SLOT AREA	FULL-NESS	PITCH	MLT	COIL DIMENSIONS ST	COIL DIMENSIONS SPG	COIL DIMENSIONS LOOP
STATOR	6	1 #23	36.7	1 #14	29.1	.00729	2.0	0.156	80	6	34.8	14.0	2.0	16.2
ROTOR														

INS. SPEC. #	CONNECTION & CABLE: CONN.	INTERNAL CONN. DWG.	EXTERNAL CONN. DWG.	CABLES #	CABLES SIZE	LEADS #	LEADS VOLTS	R LINE @ 25°C
								0.0145

NO. OF CORE PLATES STATOR= 480 ROTOR= 480

ST CORE STL WT= 116.0 LBS ROT CORE STL WT= 120.3 LBS

REMARKS: UT1=10.4 UC1= 62.5

BAR WT= 23.16 LB

ER(2)WT= 15.00 LB

.5/1.5

ROTOR CAGE	BAR SIZE AREA	BAR SIZE LENGTH	BAR SIZE MATERIAL	END RING THICK	END RING RAD. HT	END RING MATERIAL	TRICKEY FACTOR	SHEW O.D.	SHEW ARBOR	SHEW FIXTURE	FABRICATED BAR DIMENSIONS (ACTUAL)	FAN #
	0.0585	12.00		0.625	0.750		1.17				X X	

REFERRAL FACTORS	CONN.	CKT	Ki	Kp	Kd	K damp	Φ fr MEGALINES	Φg fr KILOLINES	Ki	Kz	Ks	R ϕ ohms	R b ϕ ohms	Kr	Kx
	1	11	24	.966	.966	.92	0.65	35.7	0.049	1.172	61	4	142	1.11	.970

	λ OF ROT NECK OR BRIDGE	λ ss	λ sr	HARMONIC LEAKAGE FACTORS	λ b	λ e	Bfg fr KILOLINES/in²	Bsw fr	Bc fr	AMPS per in²	A. COND. per in.	ELEC. LOADING (X10-6)	RING DENSITY
STATOR	—	—	1.358	.02050	0.617	0.300	115.0	118.5	109.8	3915	860	3.97	—
ROTOR	0.50	1.209	2.231	.01935	0.466	0.094	58.0	62.3	82.0	5300			960

PERFORMANCE	R' ss @ 25°C	R s'r @ 25°C	R s'L @ 25°C	Xi	Xs'r	Xs'L	Xm	Io	FL SLIP	PO SLIP	PLT lb. ft.	°C RISE FL THEA	°C RISE FL RTD
CALCULATED	0.0073	0.009	0.010	0.112	0.158	0.099	1.2	188.65	.0106	.0453	497.0		
TEST													

	EFFICIENCY 1/2	3/4	FL	1 1/4	1 1/2	POWER FACTOR 1/2	3/4	FL	1 1/4	1 1/2	LRA	LRPF	LRT (pu)	PGT (pu)	PUT
CALCULATED	0.958	.963	.962	.960	.935	.455	.579	.649	.674	.265	.1244	.077	0.26	2.00	1.19
GUARANTEE															
TEST															

FULL LOAD LOSSES	V AIR GAP	F.L. AMPS	SEC. CU @ °C	FRL CU @ °C	F & W	CORE	STRAY	TOTAL
CALCULATED	226.4	313.97	1615	2647	550	969	373	6155
TEST								

TEST S.O. #

TEST

DATE

SURGE RING DWG-

COMMERCIAL-

NAVY-

NO LOAD TEST: VOLTS | AMPS | WATTS

ROTOR ASSEMBLY-

ROTOR PLATE- 98

STATOR PLATE- 99

RING & FAN ASSEMBLY

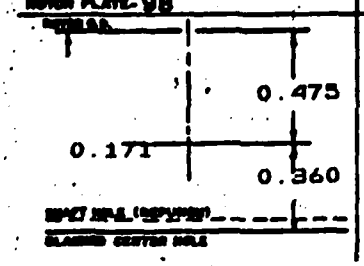

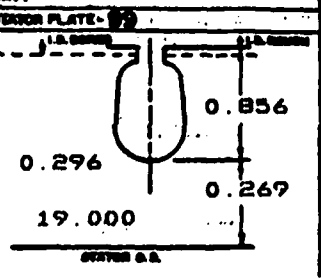

G.L: 616

C.L: 152

T.L: 202

LAT-BAR= 17.8 ST= 44 ER= 575

FRAME	CORE	TYPE	WDG.			POLES		REV.

SHEET OF

P = 22